

**SIMPLIFIED METHOD FOR DESIGN OF
MOMENT END-PLATE CONNECTIONS**

by

Jeffrey T. Borgsmiller

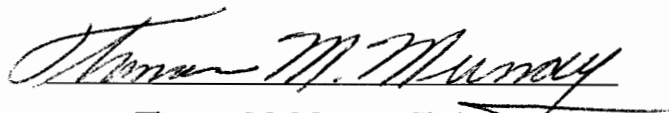
Thesis submitted to the faculty of the
Virginia Polytechnic Institute and State University
in partial fulfillment of the requirements for the degree of

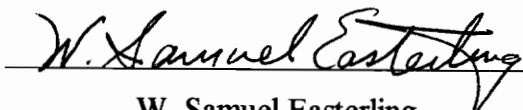
MASTER OF SCIENCE

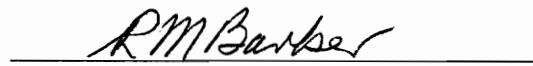
in

CIVIL ENGINEERING

APPROVED:


Thomas M. Murray, Chairman


W. Samuel Easterling


Richard M. Barker

March, 1995
Blacksburg, Virginia

2

LD
8655
V855
1995
B674
C.2

SIMPLIFIED METHOD FOR DESIGN OF MOMENT END-PLATE CONNECTIONS

by

Jeffrey T. Borgsmiller

**Thomas M. Murray, Chairman
Civil Engineering**

(ABSTRACT)

Bolted moment end-plate connections are extremely popular in the metal building industry due to economics and construction ease, yet have proven to be quite complicated from the analysis and design standpoint. Past research has shown that the design of these connections is controlled by either the strength of the end-plate, determined by yield-line analysis, or the strength of the bolts, determined by the semi-empirical Kennedy method. The calculations involved in the Kennedy bolt analysis incorporate prying action, yet are complex and extensive.

This study presents a simplified method for determining the ultimate strength of moment end-plate connections. Classic yield-line analysis is used to determine the connection capacity based on end-plate strength, and a simplified version of the Kennedy method is used to predict the connection capacity based on bolt strength with prying action. Assumptions are made that substantially reduce the calculations involved in the bolt analysis. The simplified design procedure is verified by comparison with the results of 52 previously conducted full-scale connection tests. Design recommendations are made and examples presented.

ACKNOWLEDGMENTS

The author wishes to express his sincere gratitude to his advisor, Dr. Thomas M. Murray, for his guidance and support throughout the development of this thesis. His effort and generosity will not be forgotten. Thanks also to Dr. W. Samuel Easterling and Dr. Richard M. Barker for their advice and influence as committee members.

Emmett Sumner, Pete Allen, Dennis Huffman, and Brett Farmer all helped tremendously in building and running the laboratory tests. The author wishes to thank them and his other fellow lab workers for their kindness and assistance: Brad Davis, David Gibbings, Karl Larson, Ron Meng, Bruce Shue, Rod Simon, and Budi Widjaja. The laboratory test specimens were provided by Steelox Systems Inc. under the sponsorship of Kawada Industries; great thanks goes to Hiro Matsuzaki from Kawada Industries.

Finally, the author wishes to give warm regards to his family. It has been their love, support, and encouragement throughout the years that have made everything possible.

TABLE OF CONTENTS

	<u>Page</u>
ABSTRACT.....	ii
ACKNOWLEDGMENTS	iii
TABLE OF CONTENTS	iv
LIST OF FIGURES.....	vii
LIST OF TABLES.....	x
CHAPTER I. INTRODUCTION.....	1
1.1 Background	1
1.2 Literature Review.....	7
1.3 Scope of Research.....	18
CHAPTER II. CONNECTION STRENGTH USING YIELD-LINE THEORY.....	29
2.1 General	29
2.2 Application to Flush Moment End-Plates.....	34
2.2.1 Two-Bolt Flush Unstiffened Moment End-Plates	34
2.2.2 Four-Bolt Flush Unstiffened Moment End-Plates	36
2.2.3 Four-Bolt Flush Stiffened Moment End-Plates	38
2.2.4 Six-Bolt Flush Unstiffened Moment End-Plates	41
2.3 Application to Extended Moment End-Plates	44
2.3.1 Four-Bolt Extended Unstiffened Moment End-Plates.....	44
2.3.2 Four-Bolt Extended Stiffened Moment End-Plates.....	47
2.3.3 Multiple Row Extended Unstiffened 1/2 Moment End-Plates	49
2.3.4 Multiple Row Extended Unstiffened 1/3 Moment End-Plates	52
2.3.5 Multiple Row Extended Stiffened 1/3 Moment End-Plates.....	55
CHAPTER III. CONNECTION STRENGTH USING SIMPLIFIED BOLT ANALYSIS.....	61
3.1 General	61

3.2	Application to Flush Moment End-Plates.....	71
3.2.1	Two-Bolt Flush Unstiffened Moment End-Plates	72
3.2.2	Four-Bolt Flush Unstiffened Moment End-Plates	72
3.2.3	Four-Bolt Flush Stiffened Moment End-Plates.....	74
3.2.4	Six-Bolt Flush Unstiffened Moment End-Plates	75
3.3	Application to Extended Moment End-Plates	77
3.3.1	Four-Bolt Extended Unstiffened Moment End-Plates.....	77
3.3.2	Four-Bolt Extended Stiffened Moment End-Plates.....	79
3.3.3	Multiple Row Extended Unstiffened 1/2 Moment End-Plates.....	80
3.3.4	Multiple Row Extended Unstiffened 1/3 Moment End-Plates.....	82
3.3.5	Multiple Row Extended Stiffened 1/3 Moment End-Plates.....	84
CHAPTER IV. COMPARISON OF EXPERIMENTAL RESULTS AND PREDICTIONS		86
4.1	Previous Experimental Results.....	86
4.2	Determination of the Predicted Connection Strength	92
4.3	Flush Moment End-Plate Comparisons.....	95
4.4	Extended Moment End-Plate Comparisons.....	98
CHAPTER V. SUMMARY, CONCLUSIONS AND RECOMMENDATIONS.....		102
5.1	Summary.....	102
5.2	Conclusions.....	120
5.3	Design Recommendations	121
5.4	Design Examples.....	124
5.4.1	Two-Bolt Flush Unstiffened Moment End-Plate Connection	124
5.4.2	Multiple Row Extended Unstiffened 1/3 Moment End-Plate Connection	130
REFERENCES.....		141
APPENDIX A. NOMENCLATURE.....		143
APPENDIX B. TWO-BOLT FLUSH UNSTIFFENED MOMENT END-PLATE TEST CALCULATIONS.....		149
APPENDIX C. FOUR-BOLT FLUSH UNSTIFFENED MOMENT END-PLATE TEST CALCULATIONS.....		155
APPENDIX D. FOUR-BOLT FLUSH STIFFENED MOMENT END-PLATE TEST CALCULATIONS.....		160

APPENDIX E. SIX-BOLT FLUSH UNSTIFFENED MOMENT END-PLATE TEST CALCULATIONS.....	166
APPENDIX F. FOUR-BOLT EXTENDED UNSTIFFENED MOMENT END-PLATE TEST CALCULATIONS.....	171
APPENDIX G. FOUR-BOLT EXTENDED STIFFENED MOMENT END-PLATE TEST CALCULATIONS.....	176
APPENDIX H. MULTIPLE ROW EXTENDED UNSTIFFENED 1/2 MOMENT END-PLATE TEST CALCULATIONS.....	181
APPENDIX I. MULTIPLE ROW EXTENDED UNSTIFFENED 1/3 MOMENT END-PLATE TEST CALCULATIONS.....	185
APPENDIX J. MULTIPLE ROW EXTENDED STIFFENED 1/3 MOMENT END-PLATE TEST CALCULATIONS.....	193
VITA.....	198

LIST OF FIGURES

<u>Figure</u>	<u>Page</u>
1.1 Typical Uses of Moment End-Plate Connections	2
1.2 Example of a Flush End-Plate Configuration	3
1.3 Example of an Extended End-Plate Configuration	3
1.4 Flush End-Plate Configurations in Unification Study.....	5
1.5 Extended End-Plate Configurations in Unification Study	6
1.6 Kennedy Split-Tee Analogy.....	8
1.7 Kennedy Split-Tee Behavior.....	10
1.8 Extended End-Plate Configurations with Large Inner Pitch Distances Used in this Study.....	17
1.9 Limits of Geometric Parameters for the Two-Bolt Flush Unstiffened Moment End-Plate Connection Tests in the Unification Study	20
1.10 Limits of Geometric Parameters for the Four-Bolt Flush Unstiffened Moment End-Plate Connection Tests in the Unification Study	21
1.11 Limits of Geometric Parameters for the Four-Bolt Flush Stiffened Moment End-Plate Connection Tests in the Unification Study	22
1.12 Limits of Geometric Parameters for the Six-Bolt Flush Unstiffened Moment End-Plate Connection Tests in the Unification Study	23
1.13 Limits of Geometric Parameters for the Four-Bolt Extended Unstiffened Moment End-Plate Connection Tests in the Unification Study	24
1.14 Limits of Geometric Parameters for the Four-Bolt Extended Stiffened Moment End-Plate Connection Tests in the Unification Study	25

1.15	Limits of Geometric Parameters for the Multiple Row Extended Unstiffened 1/2 Moment End-Plate Connection Tests in the Unification Study	26
1.16	Limits of Geometric Parameters for the Multiple Row Extended Unstiffened 1/3 Moment End-Plate Connection Tests in the Unification Study	27
1.17	Limits of Geometric Parameters for the Multiple Row Extended Stiffened 1/3 Moment End-Plate Connection Tests in the Unification Study	28
2.1	Virtual Displacements in a Two-Bolt Flush Unstiffened End-Plate Configuration.....	33
2.2	Yield-Line Mechanism for Two-Bolt Flush Unstiffened Moment End-Plate.....	35
2.3	Yield-Line Mechanism for Four-Bolt Flush Unstiffened Moment End-Plate.....	37
2.4	Yield-Line Mechanisms for Four-Bolt Flush Stiffened Moment End-Plate	40
2.5	Yield-Line Mechanisms for Six-Bolt Flush Unstiffened Moment End-Plate.....	42
2.6	Yield-Line Mechanism for Four-Bolt Extended Unstiffened Moment End-Plate.....	46
2.7	Yield-Line Mechanisms for Four-Bolt Extended Stiffened Moment End-Plate	48
2.8	Yield-Line Mechanisms for Multiple Row Extended Unstiffened 1/2 Moment End-Plate.....	50
2.9	Yield-Line Mechanisms for Multiple Row Extended Unstiffened 1/3 Moment End-Plate.....	53
2.10	Yield-Line Mechanism I for Multiple Row Extended Stiffened 1/3 Moment End-Plate.....	56
2.11	Yield-Line Mechanism II for Multiple Row Extended Stiffened 1/3 Moment End-Plate.....	57
3.1	Prying Forces as a Result of Plate Bending	62
3.2	Sample Applied Moment vs. Bolt Force Plots.....	64

3.3	Bolt Analysis for Two-Bolt Flush Unstiffened Moment End-Plates.....	67
3.4	Simplified Bolt Force Model for Two-Bolt Flush Unstiffened Moment End-Plates.....	67
3.5	Effects of Bolt Pretension.....	69
3.6	Simplified Bolt Force Model for Four-Bolt Flush Unstiffened and Stiffened Moment End-Plates.....	73
3.7	Simplified Bolt Force Model for Six-Bolt Flush Unstiffened Moment End-Plates.....	76
3.8	Deformed Shape of Multiple Row End-Plates.....	76
3.9	Simplified Bolt Force Model for Four-Bolt Extended Unstiffened and Stiffened Moment End-Plates.....	78
3.10	Simplified Bolt Force Model for Multiple Row Extended Unstiffened 1/2 Moment End-Plates.....	81
3.11	Simplified Bolt Force Model for Multiple Row Extended Unstiffened and Stiffened 1/3 Moment End-Plates.....	83
4.1	Longitudinal Elevation of Laboratory Test Setup.....	88
4.2	Cross-section of Laboratory Test Setup.....	89
4.3	Sample of Applied Moment vs. End-Plate Separation Plots.....	91
4.4	Determination of Experimental Yield Moment.....	91
5.1	Design Example--Two-Bolt Flush Unstiffened Moment End-Plate Connection.....	125
5.2	Design Example--Multiple Row Extended Unstiffened 1/3 Moment End-Plate Connection.....	131

LIST OF TABLES

<u>Table</u>		<u>Page</u>
4.1	Flush Moment End-Plate Predicted and Experimental Results.....	96
4.2	Extended Moment End-Plate Predicted and Experimental Results	99
5.1	Summary of Bolt Equations.....	104
5.2	Summary of Two-Bolt Flush Unstiffened Moment End-Plate Analysis.....	105
5.3	Summary of Four-Bolt Flush Unstiffened Moment End-Plate Analysis.....	106
5.4	Summary of Four-Bolt Flush Stiffened Moment End-Plate Analysis-- Stiffened Between the Tension Bolt Rows.....	107
5.5	Summary of Four-Bolt Flush Stiffened Moment End-Plate Analysis-- Stiffened Outside the Tension Bolt Rows	108
5.6	Summary of Six-Bolt Flush Unstiffened Moment End-Plate Analysis.....	109
5.7	Summary of Four-Bolt Extended Unstiffened Moment End-Plate Analysis	111
5.8	Summary of Four-Bolt Extended Stiffened Moment End-Plate Analysis	112
5.9	Summary of Multiple Row Extended Unstiffened 1/2 Moment End-Plate Analysis	114
5.10	Summary of Multiple Row Extended Unstiffened 1/3 Moment End-Plate Analysis	116
5.11	Summary of Multiple Row Extended Stiffened 1/3 Moment End-Plate Analysis	118

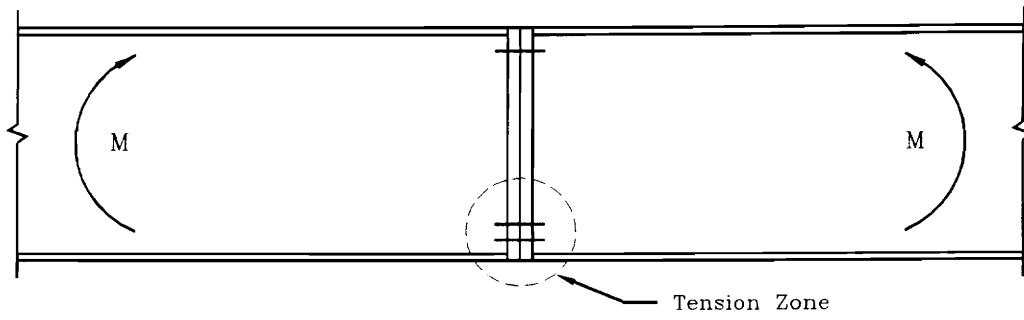
CHAPTER I

INTRODUCTION

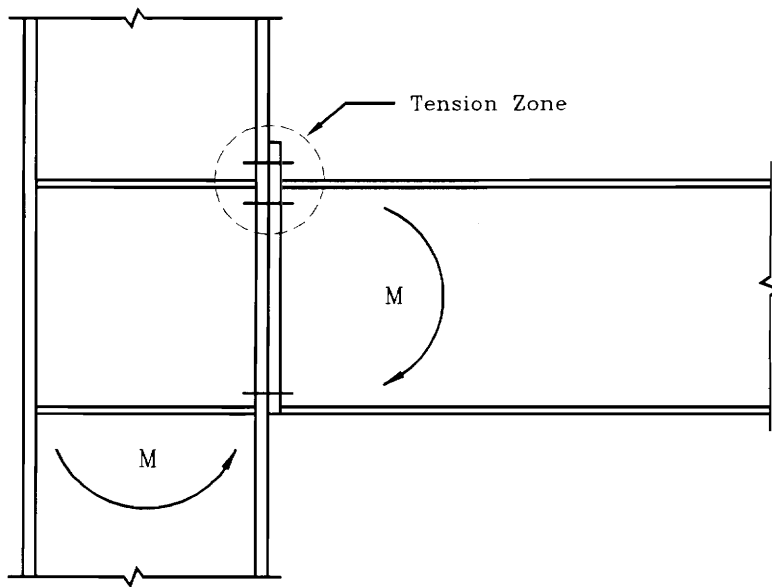
1.1 BACKGROUND

Bolted moment end-plate connections are extensively used as moment-resistant connections in metal buildings and steel portal frame construction. These connections are primarily used to either splice two beams together, commonly called a “splice-plate connection”, Figure 1.1(a), or to connect a beam to a column, Figure 1.1(b). Because of their exceptional moment resistance and ease of erection, moment end-plate connections have become predominant in the metal building industry.

There are two general types of moment end-plate connections: flush end-plates, Figure 1.2, and extended end-plates, Figure 1.3. A flush end-plate is one in which the end-plate does not extend beyond the flanges of the beam section and all rows of bolts are contained within the beam flanges. Flush end-plates may be used with or without stiffeners, which consist of gusset plates welded to both the end-plate and the beam web, as shown in Figure 1.2(b). An extended end-plate connection is one in which the end-plate protrudes beyond the flanges of the beam section to allow for the placement of exterior bolts. Extended end-plates may also be used with or without stiffeners which usually consist of a triangular gusset plate welded to both the end-plate extension and the

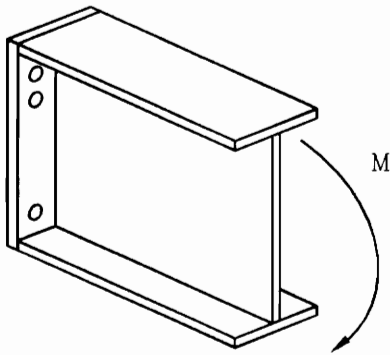


(a) Beam-to-Beam Splice Connection

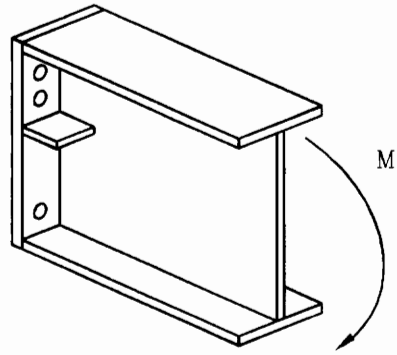


(b) Beam-to-Column Connection

Figure 1.1 Typical Uses of Moment End-Plate Connections

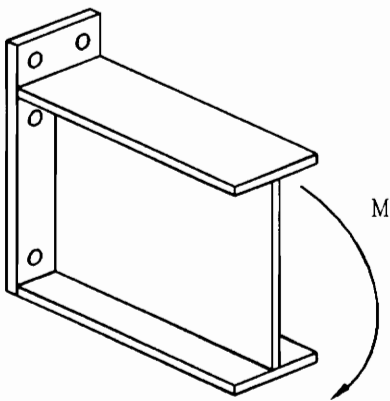


(a) Unstiffened

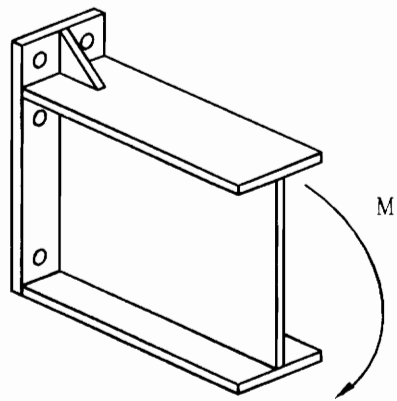


(b) Stiffened

Figure 1.2 Example of a Flush End-Plate Configuration



(a) Unstiffened



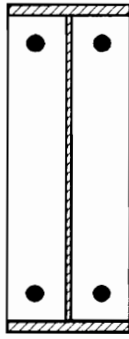
(b) Stiffened

Figure 1.3 Example of an Extended End-Plate Configuration

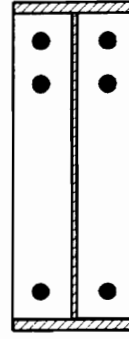
beam tension flange in the plane of the beam web, as shown in Figure 1.3(b). The use of either the flush or extended end-plate connection in a design typically depends on the magnitude of the loads and the desired stiffness of the connection.

The two limit states controlling the design of moment end-plate connections are end-plate yielding and bolt failure. Extensive studies have been conducted in the past on the analysis and design of these connections. From these studies came several different design procedures for determining the end-plate thickness and bolt diameter based on results from the finite-element method, yield-line theory, or experimental test data. Srouji *et al.* (1983b) reported that there is a great deal of variation in the predictions from the different procedures, especially in the case of bolt forces, as some methods assume bolt prying action to be significant, while others assume it to be negligible. Because of this, an extended study was conducted which unified the design procedures for the moment end-plate configurations shown in Figures 1.4 and 1.5 (Srouji *et al.*, 1983a, 1983b; SEI, 1984; Hendrick *et al.*, 1985; Morrison *et al.*, 1985, 1986; Bond and Murray, 1989; Abel and Murray, 1992b). This unified design procedure provides a rational and consistent means of calculating end-plate thickness and bolt forces, yet, requires long and tedious calculations.

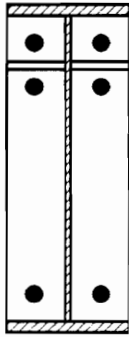
The purpose of the current study is to introduce a simplified and less tedious approach to the design of moment end-plate connections. In the proposed approach, rational assumptions are made allowing the bolt force equations to be minimized, resulting in a simple and straight-forward design procedure. Current literature regarding the design



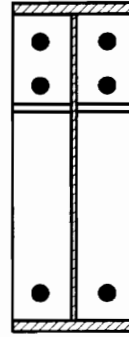
(a) Two-Bolt Unstiffened



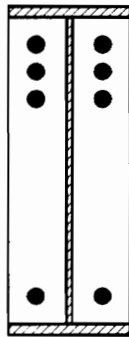
(b) Four-Bolt Unstiffened



**(c) Four-Bolt Stiffened
between tension bolt rows**

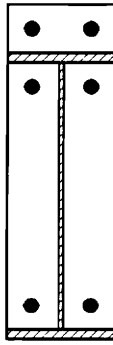


**(d) Four-Bolt Stiffened
outside tension bolt rows**

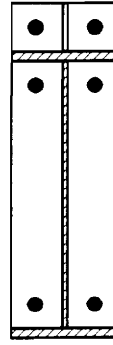


(e) Six-Bolt Unstiffened

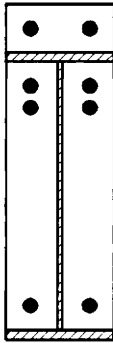
**Figure 1.4 Flush End-Plate Configurations
in Unification Study**



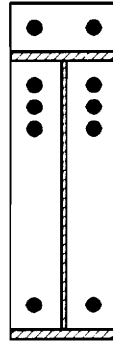
(a) Four-Bolt Unstiffened



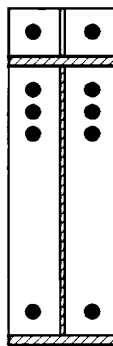
(b) Four-Bolt Stiffened



(c) Multiple Row Unstiffened 1/2



(d) Multiple Row Unstiffened 1/3



(e) Multiple Row Stiffened 1/3

Figure 1.5 Extended End-Plate Configurations
in Unification Study

of moment end-plate connections is first reviewed, followed by the development of yield-line and simplified bolt force design procedures for various flush and extended end-plate configurations. Comparisons between the predictions and extensive experimental results are made, after which conclusions and design recommendations are presented.

1.2 LITERATURE REVIEW

An extensive review of end-plate connection literature prior to 1983 was reported by Srouji *et al.* (1983b). The design procedures and equations for determining end-plate strength and bolt force predictions from several authors were presented, as well as a comparison of the various results. It was found that there was quite a variation in the results of the different prediction methods. The review concluded that yield-line analysis can be used for the design of end-plate strength, and the capacity of the bolts can be predicted from a method proposed by Kennedy *et al.* (1981). Srouji's review spawned an extensive investigation under the guidance of Dr. Thomas M. Murray, who sought to unify the design procedures of moment end-plate connections using yield-line theory and the modified Kennedy method. A review of the reports and findings from this investigation follow an overview of the Kennedy method for bolt predictions.

Kennedy *et al.* (1981) introduced a method for predicting bolt forces with prying action in split-tee connections. The Kennedy split-tee analogy, shown in Figure 1.6, consists of a plate bolted to a rigid support with four bolts and welded to a flange through which a tension load is applied. In Figure 1.6, $2F$ is the applied tension force to the flange, Q is the prying force, and B is the total resulting bolt force.

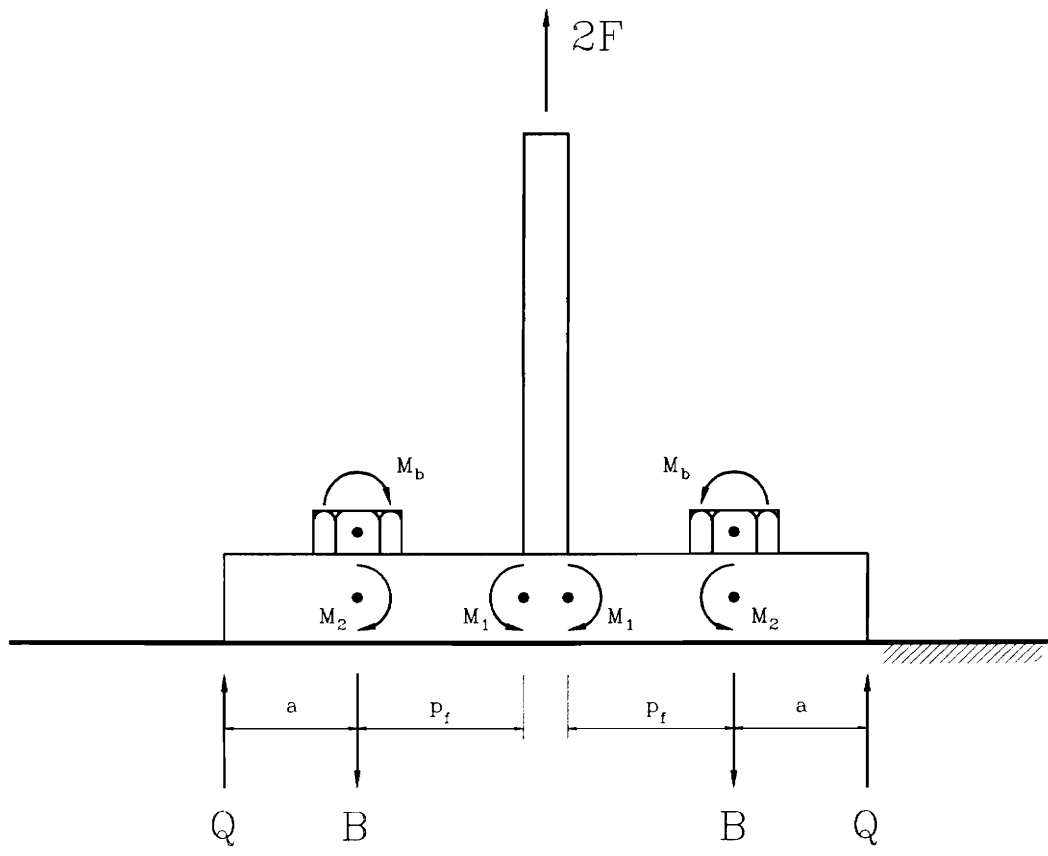
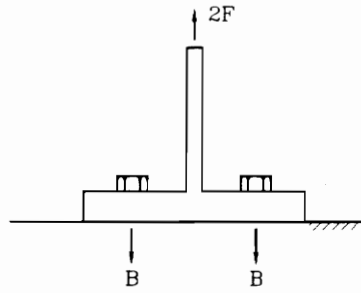


Figure 1.6 Kennedy Split-Tee Analogy
 (after Kennedy *et al.*, 1981)

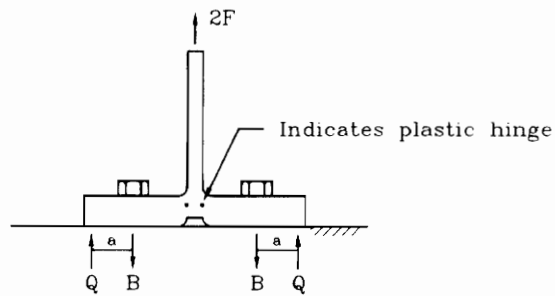
The basic assumption in the Kennedy method is that the plate goes through three stages of behavior as the applied load increases. At the lower levels of applied load, plastic hinges have not developed in the split-tee plate and its behavior is termed **thick plate behavior**, Figure 1.7(a). The prying force, Q , at this stage is assumed to be zero. As the applied load increases, two plastic hinges form at the intersections of the plate centerline and each web face, Figure 1.7(b). This yielding marks the “thick plate limit” and indicates the initiation of the second stage of plate behavior, termed **intermediate plate behavior**. The prying force at this stage is somewhere between zero and the maximum value. As a greater level of load is applied, two additional plastic hinges form at the centerline of the plate and each bolt, Figure 1.7(c). The formation of this second set of plastic hinges marks the “thin plate limit” and indicates the initiation of the third stage of plate behavior, termed **thin plate behavior**. The prying force at this stage is at a maximum, constant value. Once the status of the plate behavior has been determined, the bolt force is calculated by summing the portion of the applied flange force designated to the bolt with the appropriate prying force, $B = F + Q$.

Kennedy *et al.* (1981) establishes the stage of plate behavior by comparing the plate thickness, t_p , with a thick plate limit, t_1 , and a thin plate limit, t_{11} . The thick plate limit is found by iteration using:

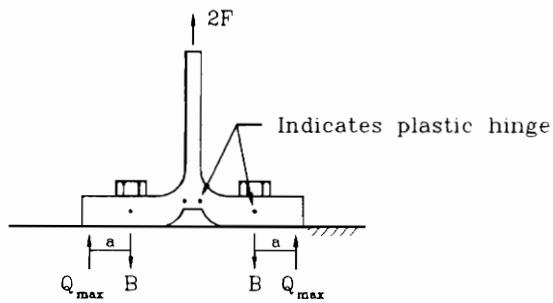
$$t_1 = \sqrt{\frac{2 p_f (2 F)}{b_f \sqrt{F_{py}^2 - 3 \left(\frac{F}{b_f t_1} \right)^2}}} \quad (1.1)$$



(a) First Stage -- Thick Plate Behavior



(b) Second Stage -- Intermediate Plate Behavior



(c) Third Stage -- Thin Plate Behavior

Figure 1.7 Kennedy Split-Tee Behavior
(after Morrison *et al.*, 1985, 1986)

and the thin plate limit is found by iteration using:

$$t_{11} = \sqrt{\frac{p_f(2F) - \pi d_b^3 F_{yb} / 8}{\sqrt{\frac{b_f}{2} \sqrt{F_{py}^2 - 3 \left(\frac{F}{b_f t_{11}} \right)^2} + w' \sqrt{F_{py}^2 - 3 \left(\frac{F}{2 w' t_{11}} \right)^2}}} \quad (1.2)$$

where $2F$ = applied flange force, b_f = beam flange width, F_{py} = plate yield stress, d_b = bolt diameter, F_{yb} = nominal strength of the bolts, designated in Table J3.1 of AISC (1986), w' = width of plate per bolt at a bolt line minus the bolt hole diameter, and p_f = pitch distance from the flange face to the center of the bolt line. If $t_p > t_1$, the plate behaves as a thick plate and the prying force is zero. Hence, the bolt force, B , for thick plate behavior is simply the applied flange force, $2F$, divided by the number of bolts, 4, or:

$$B = F/2 ; \quad \text{if } t_p > t_1 \quad (\text{thick plate behavior}) \quad (1.3)$$

If $t_1 > t_p > t_{11}$, the plate is in the intermediate stage and some prying force is included in the bolt force. The prying force, Q , is calculated by:

$$Q = \frac{p_f(F)}{a} - \frac{\pi d_b^3 F_{yb}}{32 a} - \frac{b_f t_p^2}{8 a} \sqrt{F_{py}^2 - 3 \left(\frac{2F}{b_f t_p} \right)^2} \quad (1.4)$$

where the distance, a , has been suggested to be between $2d_b$ and $3d_b$. The bolt force for intermediate plate behavior is therefore:

$$B = F/2 + Q ; \quad \text{if } t_1 > t_p > t_{11} \quad (\text{intermediate plate behavior}) \quad (1.5)$$

If $t_p < t_{11}$, the plate behaves as a thin plate and the prying force in the bolts is at a maximum and constant value, Q_{max} , calculated by:

$$Q_{\max} = \frac{w' t_p^2}{4 a} \sqrt{F_{py}^2 - 3 \left(\frac{F'}{w' t_p} \right)^2} \quad (1.6)$$

where F' is:

$$F' = \frac{t_p^2 F_{py} (0.85 b_f / 2 + 0.80 w') + \pi d_b^3 F_{yb} / 8}{4 p_f} \quad (1.7)$$

The bolt force for thin plate behavior is therefore:

$$B = F/2 + Q_{\max} ; \quad \text{if } t_p < t_{11} \quad (\text{thin plate behavior}) \quad (1.8)$$

It was noted that the quantities under the radicals in Equations 1.4 and 1.6 can be negative. A negative value for these terms indicates that the plate has yielded locally in shear before the bolt prying action force could be developed, making the connection inadequate for the applied loads.

Srouji *et al.* (1983b) used yield-line analysis and the Kennedy method of bolt force predictions in the first of many studies aimed at moment end-plate design unification. He presented yield-line design methodology for four end-plate configurations: two-bolt flush unstiffened (Figure 1.4(a)), four-bolt flush unstiffened (Figure 1.4(b)), four-bolt extended unstiffened (Figure 1.5(a)), and four-bolt extended stiffened (Figure 1.5(b)). Bolt force predictions including prying action were produced for the two-bolt and four-bolt flush unstiffened configurations. These predictions were based on a modified version of the Kennedy method, which assumes the far interior bolts in the four-bolt flush unstiffened configuration carry 1/6 of the total applied flange force. An experimental investigation was conducted to verify the end-plate and bolt force predictions. Eight two-bolt flush

unstiffened moment end-plate connection tests were conducted and reported in Srouji *et al.* (1983a). In addition, six four-bolt flush unstiffened moment end-plate connection tests were conducted, the results of which are reported in Srouji *et al.* (1984). It was concluded that yield-line analysis and the modified Kennedy method are accurate means of predicting end-plate strength and the bolt forces. In addition, the moment-rotation plots of the experimental tests indicate that the two configurations tested can be classified as Type I connections, AISC (1989).

Hendrick *et al.* (1984) continued Srouji's work by analyzing and testing two four-bolt flush stiffened end-plate configurations: those with the stiffener between the tension bolt rows (Figure 1.4(c)), and those with the stiffener outside the tension bolt rows (Figure 1.4(d)). Analysis included the use of yield-line theory for end-plate strength predictions and Srouji's modified Kennedy approach for bolt force predictions. Eight full scale tests were conducted to verify the prediction methods for the four-bolt stiffened configuration. It was concluded that additional modifications to the Kennedy method of bolt force predictions were necessary in regards to the distance "a" in Figure 1.6. An empirical equation for a was derived from regression analysis:

$$a = 3.682(t_p/d_b)^3 - 0.085 \quad (1.9)$$

In addition, Hendrick *et al.* changed the assumption regarding the fraction of applied flange force carried by the far inner bolts from 1/6 to 1/8. These modifications were carried into the analyses of the tests previously conducted by Srouji *et al.*, and reported in Hendrick *et al.* (1985), which contained a unification of the design procedures for the four

end-plate configurations tested thus far by Srouji and Hendrick: two-bolt flush unstiffened, four bolt flush unstiffened, four-bolt flush stiffened between the tension bolt rows, and four-bolt flush stiffened outside the tension bolt rows. Analytical predictions for end-plate strength using yield-line theory and bolt forces using Hendrick's modified Kennedy approach correlated well with all of the test data. In addition, it was concluded that the four end-plate configurations exhibit adequate moment-rotation stiffness to be classified as Type I connections, AISC (1989).

Three tests were analyzed and conducted by SEI (1984) which included two multiple row extended unstiffened 1/3 configurations (Figure 1.5(d)), and one multiple row extended stiffened 1/3 configuration (Figure 1.5(e)). Note that the designation "1/3" in the multiple row extended configuration reflects the number of bolt rows outside and inside, respectively, of the beam tension flange. The tests were analyzed using yield-line analysis for end-plate predictions and the modified Kennedy method for bolt force predictions. Modifications to the Kennedy method were necessary for determining how much of the applied flange force was carried by the outer and inner bolts in these extended end-plate configurations. Factors, designated as " α " and " β ," were incorporated into the Kennedy procedure for this purpose, and were calculated based on the results of the yield-line analysis. The results correlated well with the experimental results.

Four-bolt extended stiffened (Figure 1.5(b)) and multiple row extended unstiffened 1/3 (Figure 1.5(d)) configurations were analyzed and tested by Morrison *et al.* (1985) and Morrison *et al.* (1986), respectively. Analysis procedures included the use of yield-line

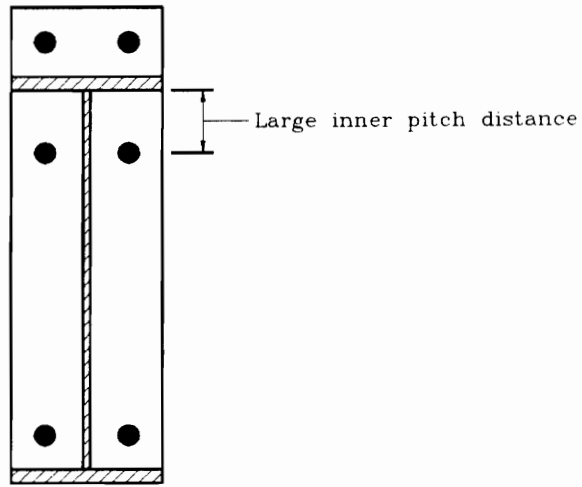
theory and modified Kennedy bolt force predictions. Once again, modifications to the Kennedy method were necessary for determining how much of the applied flange force was carried by the outer and inner bolts in the extended end-plate configurations. Unlike SEI (1984), which used the yield-line results to determine the modification factors, Morrison's modification factors came directly from the experimental results of six four-bolt extended stiffened tests and six multiple row extended unstiffened 1/3 tests. It was concluded from these tests that the outer bolts do not exhibit prying action, and therefore carry the majority of the applied flange force. The factors incorporated into the modified Kennedy analysis, α and β , account for this phenomenon. It was additionally concluded that the four-bolt extended stiffened and multiple row extended unstiffened 1/3 configurations contain adequate stiffness to be classified as Type I connections, AISC (1989).

Five full-scale flush unstiffened end-plate configurations with six bolts at the tension flange (Figure 1.4(e)) were analyzed and tested by Bond and Murray (1989). The analysis procedures set forth previously in the unification studies were adopted for end-plate strength and bolt force calculations. Modifications to the Kennedy bolt prediction method were made with regards to the disbursement of the applied flange force among the bolts. New factors, different from those proposed by Morrison *et al.* (1986), were introduced which proportioned the applied flange force to each of the three lines of bolts. These factors were extrapolated from the test results. Once the modifications were implemented, predictions correlated well with the test data. In addition, it was concluded

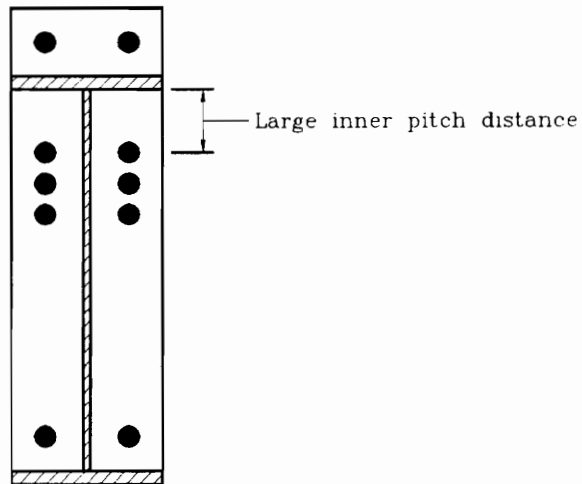
that the six-bolt flush unstiffened end-plate connection can be classified as a Type I connection, AISC (1989).

Abel and Murray (1992b) added a ninth configuration to the unification of moment end-plate design: the four-bolt extended unstiffened configuration (Figure 1.5(a)). Analysis was conducted using the previously set forth yield-line analysis and modified Kennedy method. Four full scale tests were conducted to verify the predictions. It was concluded that the outer and inner rows of bolts each carry half of the applied flange force, however, when the bolt force prediction controls in the analysis, no prying action exists in the outer bolts. As with the other configurations, the four-bolt extended unstiffened moment end-plate connection contains adequate moment-rotation stiffness to be classified as a Type I connection, AISC (1989).

Additional end-plate configurations have also been tested but not fully analyzed by the unified methods. Two tests on a multiple row extended unstiffened 1/2 configuration (Figure 1.5(c)) were conducted by Abel and Murray (1992a). Two four-bolt extended unstiffened configurations with large pitch distances between the face of the beam tension flange and the first interior row of bolts, Figure 1.8(a), were tested and reported by Borgsmiller *et al.* (1995). And lastly, two multiple row extended unstiffened 1/3 configurations with large inner pitch distances, Figure 1.8(b), were conducted, one by Rodkey and Murray (1993) and one by Borgsmiller *et al.* (1995).



(a) Four-Bolt Unstiffened



(b) Multiple Row Unstiffened 1/3

Figure 1.8 Extended End-Plate Configurations with Large Inner Pitch Distances Used in this Study

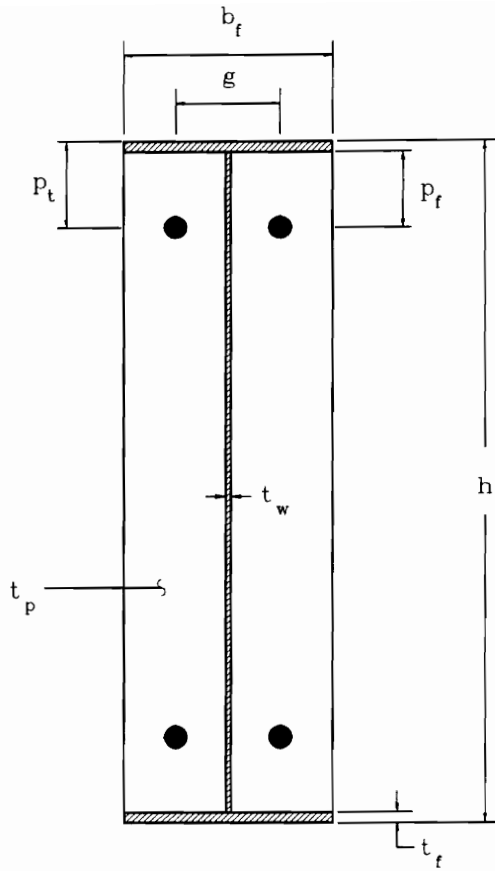
1.3 SCOPE OF RESEARCH

As previously mentioned, the purpose of this research is to develop a simplified design procedure for moment end-plate connections, stemming from the existing unified design procedure. The simplified approach is based on rational assumptions made with regards to the bolt behavior. These assumptions decrease the amount of bolt force calculations in the Kennedy method. The proposed design procedure will provide criteria for:

- Determination of end-plate thickness by yield-line theory given end-plate geometry, beam geometry, and material yield stress, e.g., strength criterion.
- Determination of bolt forces including prying effects by a *simplified* Kennedy method given end-plate geometry, end-plate thickness, bolt diameter, and bolt proof load, e.g., bolt force criterion.

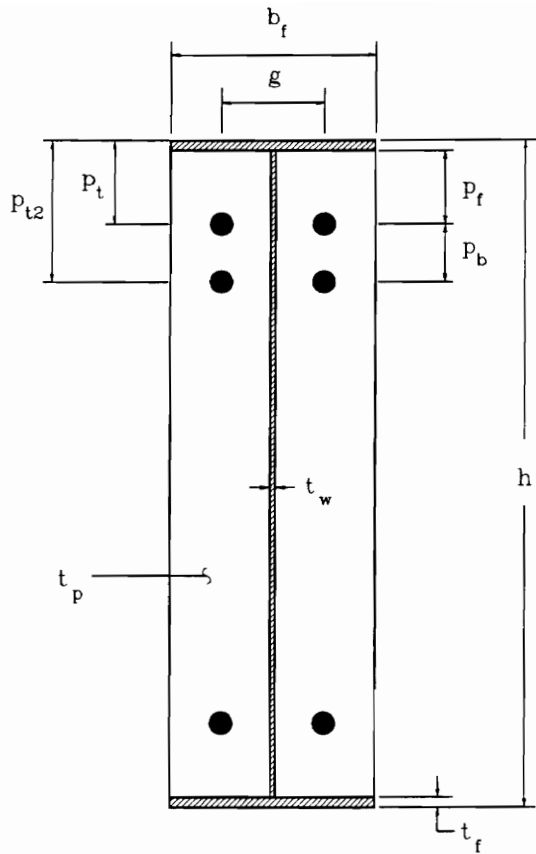
The objectives of this study were accomplished by developing end-plate strength prediction and simplified bolt force prediction equations for the five flush end-plate configurations in Figure 1.4 and the five extended end-plate configurations in Figure 1.5. In addition, the new approach was adapted to include extended end-plate configurations having large pitch distances between the inner face of the beam tension flange and the first row of interior bolts. Two such configurations were included and are shown in Figure 1.8. Note that the designations “1/2” and “1/3” in the descriptions of the multiple row extended configurations reflect on the number of bolt rows outside and inside, respectively, of the beam tension flange. The predictions were then compared to the

experimental results of the previously conducted full-scale tests in the unification study to verify the accuracy of the proposed simplified approach. Figures 1.9 through 1.17 present the various parameters that define the end-plate geometry for each of the nine configurations tested in the unification study. These geometric parameters varied within the limits shown in the table accompanying each figure. All bolts in the tests were type A325. Nomenclature is defined in Appendix A.



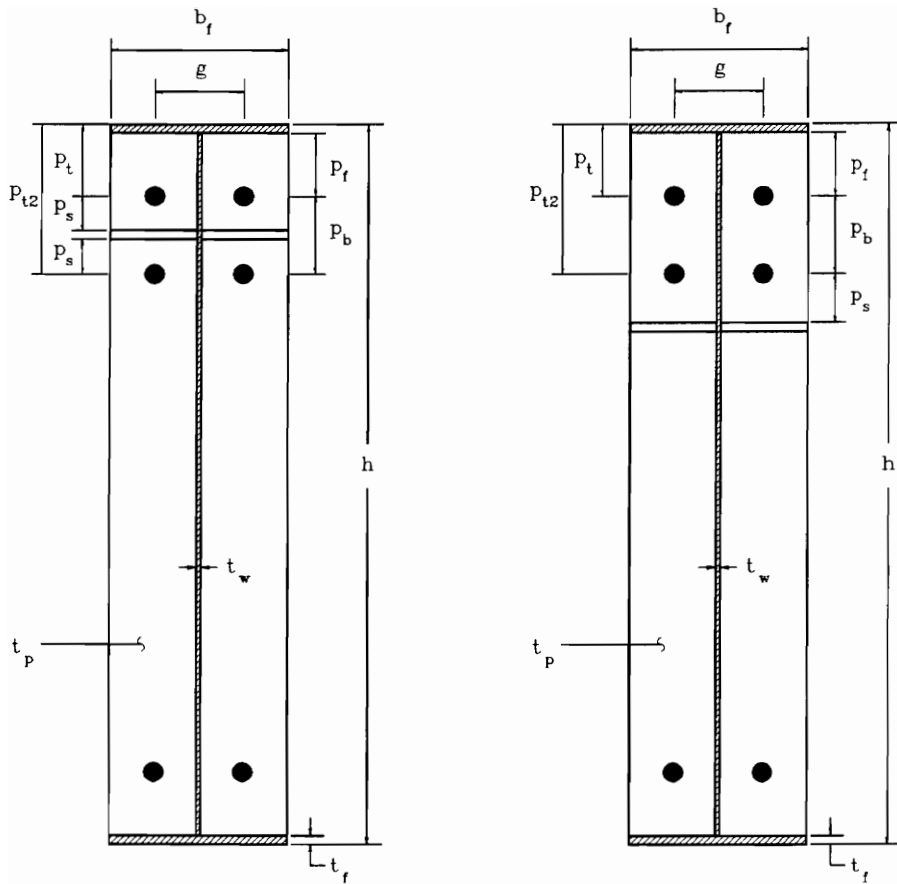
Parameter	Low (in.)	High (in.)
d_b	5/8	3/4
t_p	3/8	1/2
p_f	1 5/16	1 7/8
g	2 1/4	3 3/4
h	10	24
b_f	5	6
t_f	3/16	1/4

Figure 1.9 Limits of Geometric Parameters for the Two-Bolt Flush Unstiffened Moment End-Plate Connection Tests in the Unification Study (after Srouji *et al.*, 1983a)



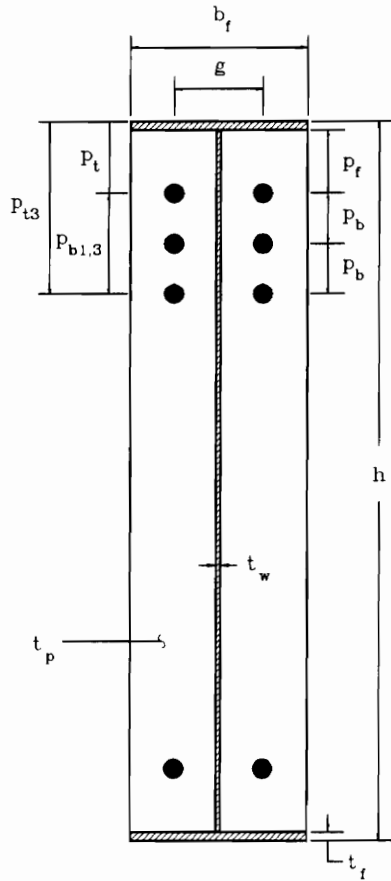
Parameter	Low (in.)	High (in.)
d_b	5/8	3/4
t_p	3/8	1/2
p_f	1 3/8	1 7/8
p_b	3	3
g	2 3/4	3 1/2
h	16	24
b_f	6	6
t_f	1/4	1/4

Figure 1.10 Limits of Geometric Parameters for the Four-Bolt Flush Unstiffened Moment End-Plate Connection Tests in the Unification Study (after Srouji *et al.*, 1983b, 1984)



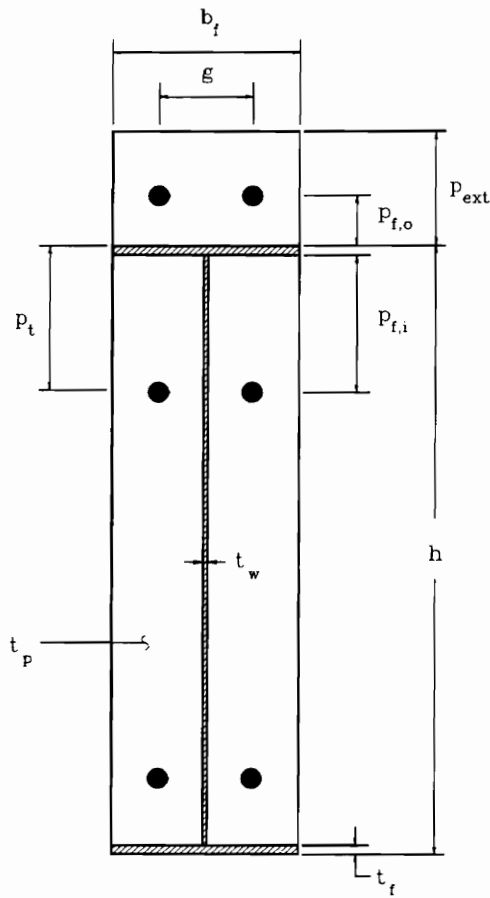
Parameter	Low (in.)	High (in.)
d_b	5/8	3/4
t_p	3/8	1/2
p_f	1 3/8	1 7/8
p_b	1 7/8	3
g	2 3/4	3 1/2
h	16	24
b_f	6	6
t_f	1/4	3/8

Figure 1.11 Limits of Geometric Parameters for the Four-Bolt Flush Stiffened Moment End-Plate Connection
Tests in the Unification Study
(after Hendrick *et al.*, 1984)



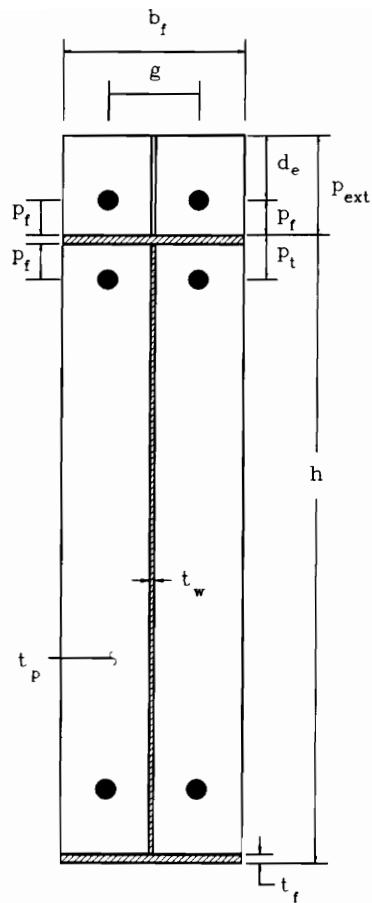
Parameter	Low (in.)	High (in.)
d_b	3/4	1
t_p	3/8	1/2
p_f	1 1/2	2
p_b	2 1/2	2 1/2
g	3	4
h	28	36
b_f	6	10
t_f	3/8	3/8

Figure 1.12 Limits of Geometric Parameters for the Six-Bolt Flush Unstiffened Moment End-Plate Connection Tests in the Unification Study (after Bond and Murray, 1989)



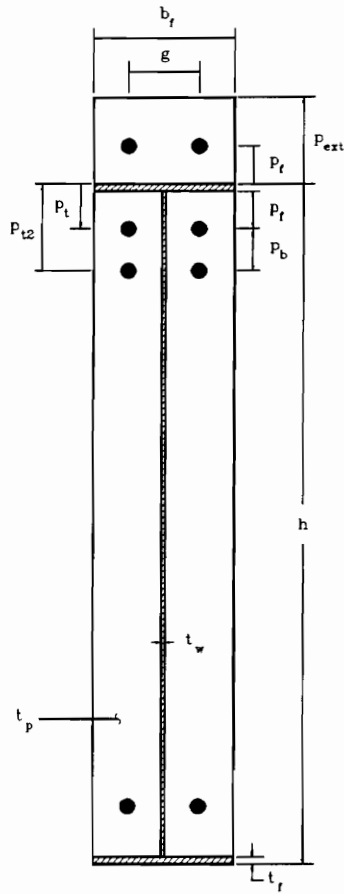
Parameter	Low (in.)	High (in.)
d_b	1/2	1 1/4
t_p	3/8	7/8
$p_{f,i}$	1 1/4	4
$p_{f,o}$	1 1/4	2 1/2
p_{ext}	2 1/2	4
g	2 1/2	7
h	16.2	64
b_f	5	10 1/4
t_f	1/4	1

Figure 1.13 Limits of Geometric Parameters for the Four-Bolt Extended Unstiffened Moment End-Plate Connection Tests in the Unification Study (after Abel and Murray, 1992b; Borgsmiller *et al.*, 1995)



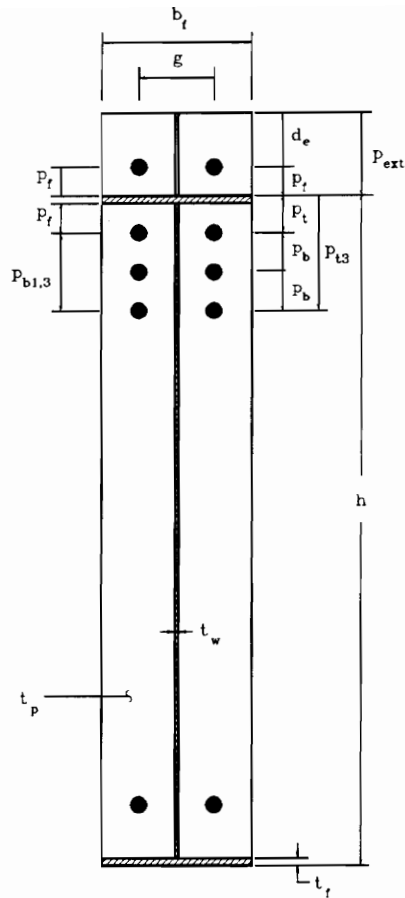
Parameter	Low (in.)	High (in.)
d_b	5/8	1
t_p	3/8	5/8
p_f	1	1 3/4
p_{ext}	2 1/2	3 1/2
g	2 3/4	4 1/2
h	15 3/4	24
b_f	6	8
t_f	3/8	1/2

Figure 1.14 Limits of Geometric Parameters for the Four-Bolt Extended Stiffened Moment End-Plate Connection Tests in the Unification Study (after Morrison *et al.*, 1985)



Parameter	Low (in.)	High (in.)
d_b	3/4	3/4
t_p	3/8	3/4
p_f	1 1/4	1 1/4
p_b	2 1/4	2 1/4
p_{ext}	2 1/2	2 1/2
g	3	3
h	26	26
b_f	6	6
t_f	7/16	7/16

Figure 1.15 Limits of Geometric Parameters for the Multiple Row Extended Unstiffened 1/2 Moment End-Plate Connection Tests in the Unification Study (after Abel and Murray, 1992a)



Parameter	Low (in.)	High (in.)
d_b	1	1
t_p	3/4	3/4
p_f	1 5/8	1 5/8
p_b	3	3
p_{ext}	3 3/8	3 3/8
g	3 1/2	3 1/2
h	62	62
b_f	10	10
t_f	1	1

Figure 1.17 Limits of Geometric Parameters for the Multiple Row Extended Stiffened 1/3 Moment End-Plate Connection Tests in the Unification Study (after SEI, 1984)

CHAPTER II

CONNECTION STRENGTH USING YIELD-LINE THEORY

2.1 GENERAL

A yield line is a continuous formation of plastic hinges along a straight or curved line in a plate or slab structure. A failure mechanism is assumed to exist when the yield lines form a kinematically valid collapse mechanism. Yield-line theory is therefore analogous to plastic design theory in which elastic deformations are negligible compared to the plastic deformations resulting from the yield lines. Because of this, it can be assumed that the yield lines divide the plate or slab into rigid plane regions allowing its deformed shape to be geometrically defined. Much of the yield-line theory development is related to reinforced concrete slabs; however, the principles and findings are applicable to steel plates.

In determining the location of a yield line in a steel plate, the following guidelines have been established by Srouji *et al.* (1983b):

- Axes of rotation generally lie along lines of support.
- Yield lines pass through the intersection of the axes of rotation of adjacent plate segments.
- Along a yield line, the bending moment is assumed to be constant and equal to the plastic moment of the plate.

Yield-line mechanisms can be analyzed using two methods: the equilibrium method and the virtual work method. The latter method is more suitable for application to steel end-plates and is used herein. In this method, the external work done by the applied loads in moving through a small arbitrary virtual deflection is set equal to the internal work done by the plate as it rotates along the yield lines to accommodate this virtual deflection. For a selected yield-line pattern and loading, a specific plastic moment is required of the plate along these hinge lines. It is important to note that this method is an upper bound approach to the strength of the plate, meaning that all of the possible yield-line patterns must be investigated to ensure that the least upper bound to the strength has been found. The failure mechanism for a plate with a given plastic moment capacity consists of the yield-line pattern which produces the *smallest* failure load. Conversely, for a given loading, the appropriate mechanism is that which produces the *largest* required plastic moment capacity of the plate.

To determine the controlling failure load or the required plate moment capacity, an arbitrary succession of all possible yield-line patterns must be selected using the three previously mentioned guidelines. By equating the internal and external work, the relation between the applied loads and the ultimate resisting moment is obtained. The resulting equation is then solved for either the unknown failure load or unknown plate moment capacity. By comparing the different values obtained from the various mechanisms, the controlling minimum load or maximum required plate capacity is identified.

The internal work stored in a yield-line mechanism is the sum of the internal work stored in each yield line forming the mechanism. The internal work per unit length stored in a single yield line is obtained by multiplying the normal moment on the yield line with the normal rotation of the yield line. Thus, the work stored in the n^{th} yield line of length L_n is (Srouji *et al.*, 1983b):

$$w_i = \int_{L_n} m_p \theta_n ds = m_p \theta_n L_n \quad (2.1)$$

where m_p is the plastic moment capacity of the plate, θ_n is the relative normal rotation of line n , and ds is the elemental length of line n . The internal work stored by an entire yield-line mechanism can be written as (Srouji *et al.*, 1983b):

$$W_i = \sum_{n=1}^N m_p \theta_n L_n \quad (2.2)$$

where N is the number of yield lines in the mechanism.

For complicated yield-line patterns, the expressions for the relative plate rotation are somewhat tedious to obtain. It is therefore more convenient to resolve the internal work components in the x - and y - directions. This results in the following form of Equation 2.2 (Srouji *et al.*, 1983b):

$$W_i = \sum_{n=1}^N (m_{px} \theta_{nx} L_{nx} + m_{py} \theta_{ny} L_{ny}) \quad (2.3)$$

where m_{px} and m_{py} are the x - and y - components of the plate moment capacity per unit length, θ_{nx} and θ_{ny} are the x - and y - components of the relative normal rotation of the plate

segments, and L_{nx} and L_{ny} are the x- and y- components of the n^{th} yield line length. For steel plates:

$$m_{px} = m_{py} = m_p = \frac{F_{py}t_p^2}{4} \quad (2.4)$$

where F_{py} is the yield stress of the end-plate material and t_p is the plate thickness. The values of θ_{nx} and θ_{ny} are obtained by drawing convenient straight lines, parallel to the x- and y- axes, on the two plate segments intersecting at the yield line. The relative rotation of the plate segments can then be visualized by “looking down” the axes of these straight lines at the deformed shape of the plate in the x-z and y-z planes. The values of the relative rotations from each viewpoint can then be calculated by selecting straight lines with known displacements at the ends.

Each moment end-plate configuration has a different expression for internal work, W_i , due to unique yield-line mechanisms. However, the external work, W_e , is the same for all end-plate configurations. The external work done due to a unit displacement at the outside of the beam tension flange, resulting in a rotation of the beam cross-section about the outside of the beam compression flange, is given by (Srouji *et al.*, 1983b):

$$W_e = M_u \theta = M_u \left(\frac{1}{h} \right) \quad (2.5)$$

where M_u is the ultimate beam moment at the end-plate, and θ is the virtual rotation at the connection, equal to $1/h$, where h is the total depth of the beam section. Figure 2.1 shows

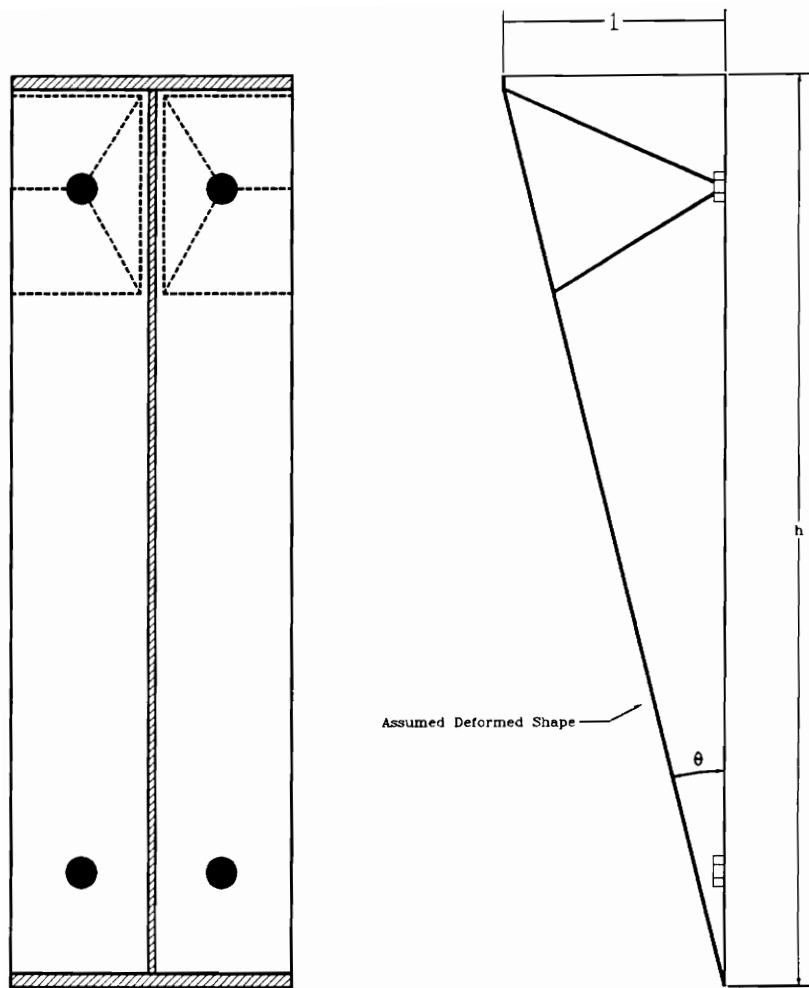


Figure 2.1 Virtual Displacements in a Two-Bolt Flush Unstiffened End-Plate Configuration

θ in the plastic deformed shape of a two-bolt flush unstiffened moment end-plate configuration.

2.2 APPLICATION TO FLUSH MOMENT END-PLATES

Yield-line analysis was performed on the five flush end-plate configurations shown in Figure 1.4. The five configurations are: two-bolt unstiffened, four-bolt unstiffened, four-bolt stiffened between the tension bolt rows, four-bolt stiffened outside the bolt rows, and six bolt unstiffened. Studies have been done on all five of these configurations in the past; hence, the equations and procedures herein are based on these studies.

2.2.1 Two-Bolt Flush Unstiffened Moment End-Plates

A study was done by Srouji, *et al.* (1983b) to determine the behavior of two-bolt flush unstiffened moment end-plate connections. The following discussion is based on that study.

The yield-line mechanism in Figure 2.2 is the controlling yield-line pattern for the two-bolt flush unstiffened moment end-plate connection. The geometric parameters are also defined in the figure. The external work, W_e , is calculated for all end-plate configurations using Equation 2.5. The internal work in this yield-line mechanism is given by:

$$W_i = \frac{4 m_p}{h} (h - p_t) \left[\frac{b_f}{2} \left(\frac{1}{p_f} + \frac{1}{s} \right) + \frac{2}{g} (p_f + s) \right] \quad (2.6)$$

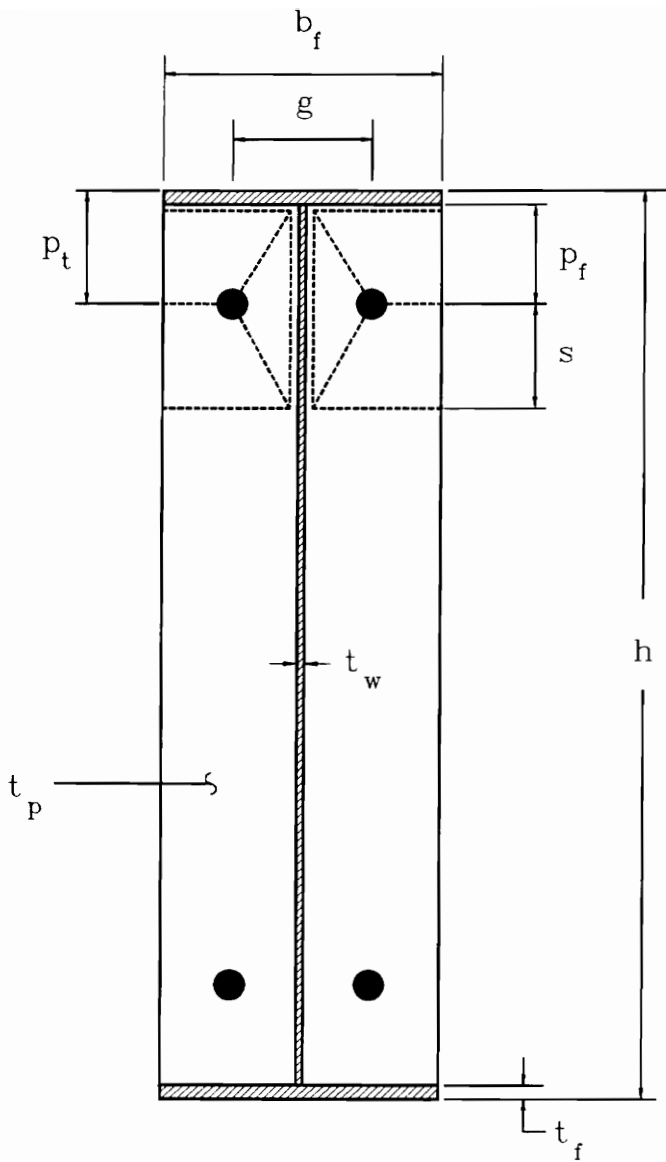


Figure 2.2 Yield-Line Mechanism for Two-Bolt Flush Unstiffened Moment End-Plate (after Srouji *et al.*, 1983b)

where m_p is given by Equation 2.4. The moment capacity of the end-plate, M_{pl} , is found by equating the external and internal work expressions, resulting in:

$$M_{pl} = 4 m_p (h - p_t) \left[\frac{b_f}{2} \left(\frac{1}{p_f} + \frac{1}{s} \right) + \frac{2}{g} (p_f + s) \right] \quad (2.7)$$

Implementing m_p and rearranging M_{pl} results in an expression for the required end-plate thickness, t_p , in terms of the desired ultimate load, M_u :

$$t_p = \left[\frac{M_u / F_{py}}{(h - p_t) \left[\frac{b_f}{2} \left(\frac{1}{p_f} + \frac{1}{s} \right) + \frac{2}{g} (p_f + s) \right]} \right]^{1/2} \quad (2.8)$$

The unknown dimension, s , in Figure 2.2 is found by differentiating the internal work expression, Equation 2.6, with respect to s and equating to zero. The resulting expression for s is:

$$s = \frac{1}{2} \sqrt{b_f g} \quad (2.9)$$

2.2.2 Four-Bolt Flush Unstiffened Moment End-Plates

A study was performed by Srouji *et al.* (1983b) on the behavior of four-bolt flush unstiffened moment end-plate connections. The following discussion is based on that study.

The controlling yield-line mechanism and geometric parameters for the four-bolt flush unstiffened moment end-plate are shown in Figure 2.3. The internal work for the mechanism, W_i , and resulting capacity of the end-plate, M_{pl} , are:

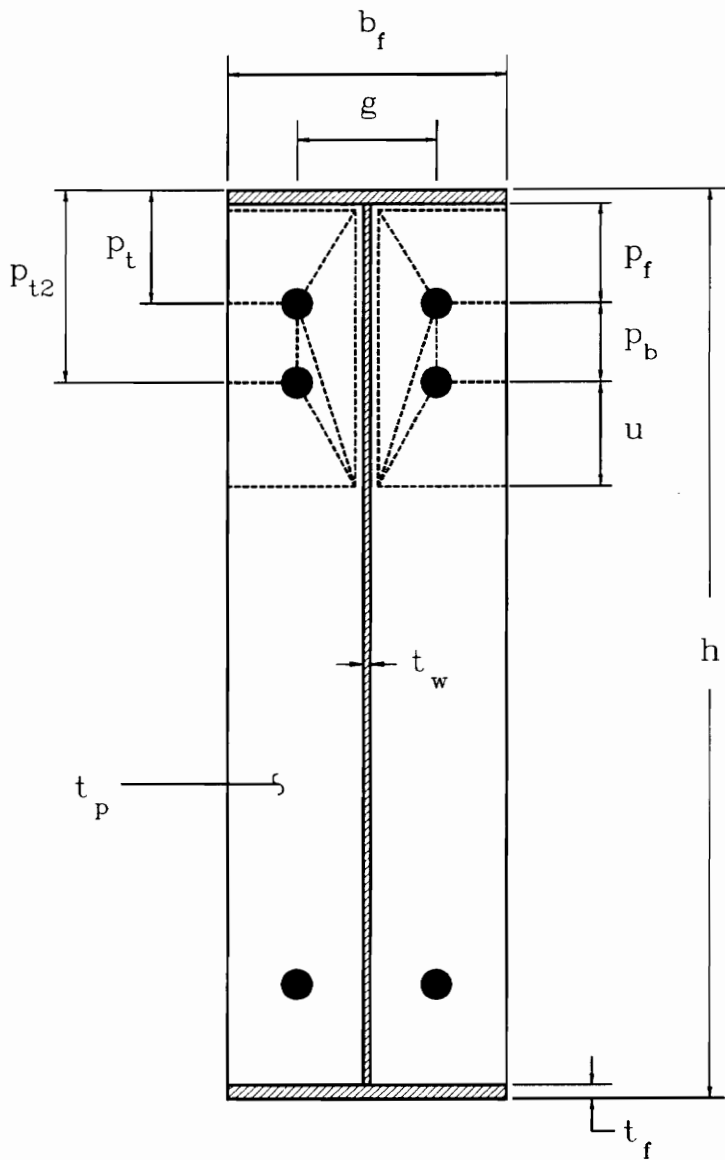


Figure 2.3 Yield-Line Mechanism for Four-Bolt Flush Unstiffened Moment End-Plate
 (after Srouji *et al.*, 1983b)

$$W_i = \frac{4m_p}{h} \left[\frac{b_f}{2} \left(\frac{h-p_t}{p_f} + \frac{h-p_{t2}}{u} \right) + 2(p_f+p_b+u) \left(\frac{h-p_t}{g} \right) \right] \quad (2.10)$$

$$M_{pl} = 4m_p \left[\frac{b_f}{2} \left(\frac{h-p_t}{p_f} + \frac{h-p_{t2}}{u} \right) + 2(p_f+p_b+u) \left(\frac{h-p_t}{g} \right) \right] \quad (2.11)$$

By rearranging the equation for M_{pl} , the required end-plate thickness for a given loading is expressed as:

$$t_p = \left[\frac{M_u / F_{py}}{\frac{b_f}{2} \left(\frac{h-p_t}{p_f} + \frac{h-p_{t2}}{u} \right) + 2(p_f+p_b+u) \left(\frac{h-p_t}{g} \right)} \right]^{1/2} \quad (2.12)$$

The unknown dimension, u , in Figure 2.3 is found by differentiating the internal work expression with respect to u and equating to zero. The resulting expression for u is:

$$u = \frac{1}{2} \sqrt{b_f g \left(\frac{h-p_{t2}}{h-p_t} \right)} \quad (2.13)$$

2.2.3 Four-Bolt Flush Stiffened Moment End-Plates

A study on the behavior of four-bolt flush stiffened moment end-plate connections was done by Hendrick *et al.* (1985). The following discussion is based on that study.

Two configurations of four-bolt flush stiffened end-plates were investigated: those stiffened with a gusset plate between the tension bolt rows, Figure 1.4(c), and those stiffened with a gusset plate on the outside of the tension bolt rows, Figure 1.4 (d). The controlling yield-line mechanism for the configuration with the stiffener between the

tension bolt rows is shown in Figure 2.4(a). Included in the figure are the geometric parameters. The internal work stored in this yield-line mechanism is:

$$W_i = \frac{4m_p}{h} \left\{ (h-p_t) \left[\frac{b_f}{2} \left(\frac{1}{p_f} + \frac{1}{p_s} \right) + \frac{2}{g} (p_f + p_s) \right] + (h-p_{t2}) \left[\frac{b_f}{2} \left(\frac{1}{p_s} + \frac{1}{s} \right) + \frac{2}{g} (p_s + s) \right] \right\} \quad (2.14)$$

On equating the internal and external work expressions, the following expression is obtained for the end-plate strength:

$$M_{pl} = 4m_p \left\{ (h-p_t) \left[\frac{b_f}{2} \left(\frac{1}{p_f} + \frac{1}{p_s} \right) + \frac{2}{g} (p_f + p_s) \right] + (h-p_{t2}) \left[\frac{b_f}{2} \left(\frac{1}{p_s} + \frac{1}{s} \right) + \frac{2}{g} (p_s + s) \right] \right\} \quad (2.15)$$

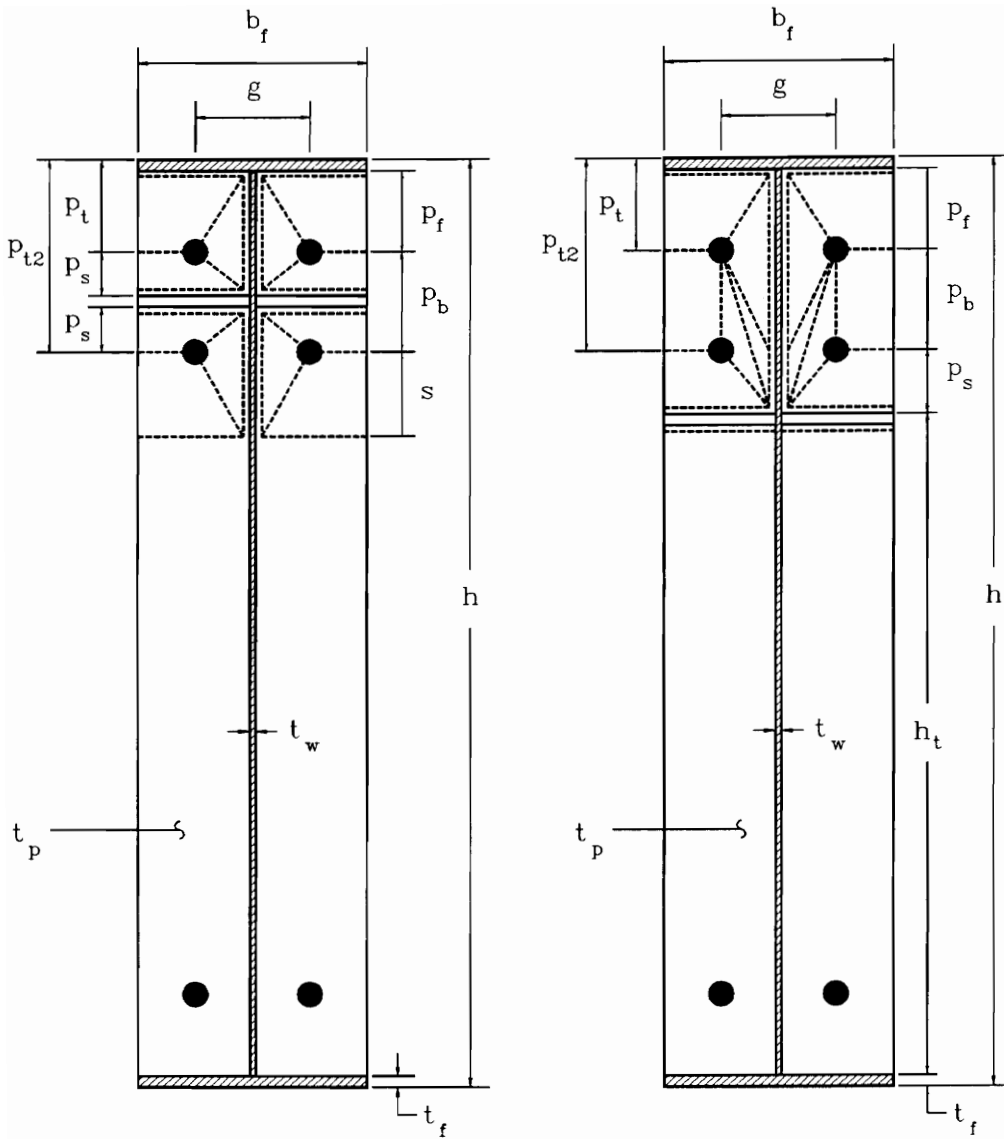
where m_p is calculated from Equation 2.4. This expression for the plate capacity can be solved for the plate thickness, t_p , in terms of a desired ultimate moment of the connection, M_u :

$$t_p = \left\{ \frac{M_u / F_{py}}{(h-p_t) \left[\frac{b_f}{2} \left(\frac{1}{p_f} + \frac{1}{p_s} \right) + \frac{2}{g} (p_f + p_s) \right] + (h-p_{t2}) \left[\frac{b_f}{2} \left(\frac{1}{p_s} + \frac{1}{s} \right) + \frac{2}{g} (p_s + s) \right]} \right\}^{1/2} \quad (2.16)$$

The unknown quantity, s , is found by differentiating the internal work expression, Equation 2.14, with respect to s and equating to zero. The resulting expression for s is:

$$s = \frac{1}{2} \sqrt{b_f g} \quad (2.17)$$

The controlling yield-line mechanism and geometric parameters for the four-bolt flush stiffened end-plate with the stiffener on the outside of the tension bolt rows is shown in Figure 2.4(b). The internal work and resulting end-plate capacity of this mechanism are:



(a) Stiffener Between the Tension Bolt Rows

(b) Stiffener Outside the Tension Bolt Rows

Figure 2.4 Yield-Line Mechanisms for Four-Bolt Flush Stiffened Moment End-Plate (after Hendrick *et al.*, 1985)

$$W_i = \frac{4m_p}{h} \left\{ (h-p_t) \left[\frac{b_f}{2p_f} + \frac{2}{g}(p_f+p_b) \right] + \frac{b_f}{4} + 1.25(h-p_{t2}) \left[\frac{b_f}{2} \left(\frac{1}{p_s} + \frac{1}{2h_t} \right) + \frac{g}{10p_s} + \frac{2}{g} \left(\frac{p_b}{5} + p_s \right) \right] \right\} \quad (2.18)$$

$$M_{pl} = 4m_p \left\{ (h-p_t) \left[\frac{b_f}{2p_f} + \frac{2}{g}(p_f+p_b) \right] + \frac{b_f}{4} + 1.25(h-p_{t2}) \left[\frac{b_f}{2} \left(\frac{1}{p_s} + \frac{1}{2h_t} \right) + \frac{g}{10p_s} + \frac{2}{g} \left(\frac{p_b}{5} + p_s \right) \right] \right\} \quad (2.19)$$

Rearranging M_{pl} and inserting m_p gives the expression for the required plate thickness:

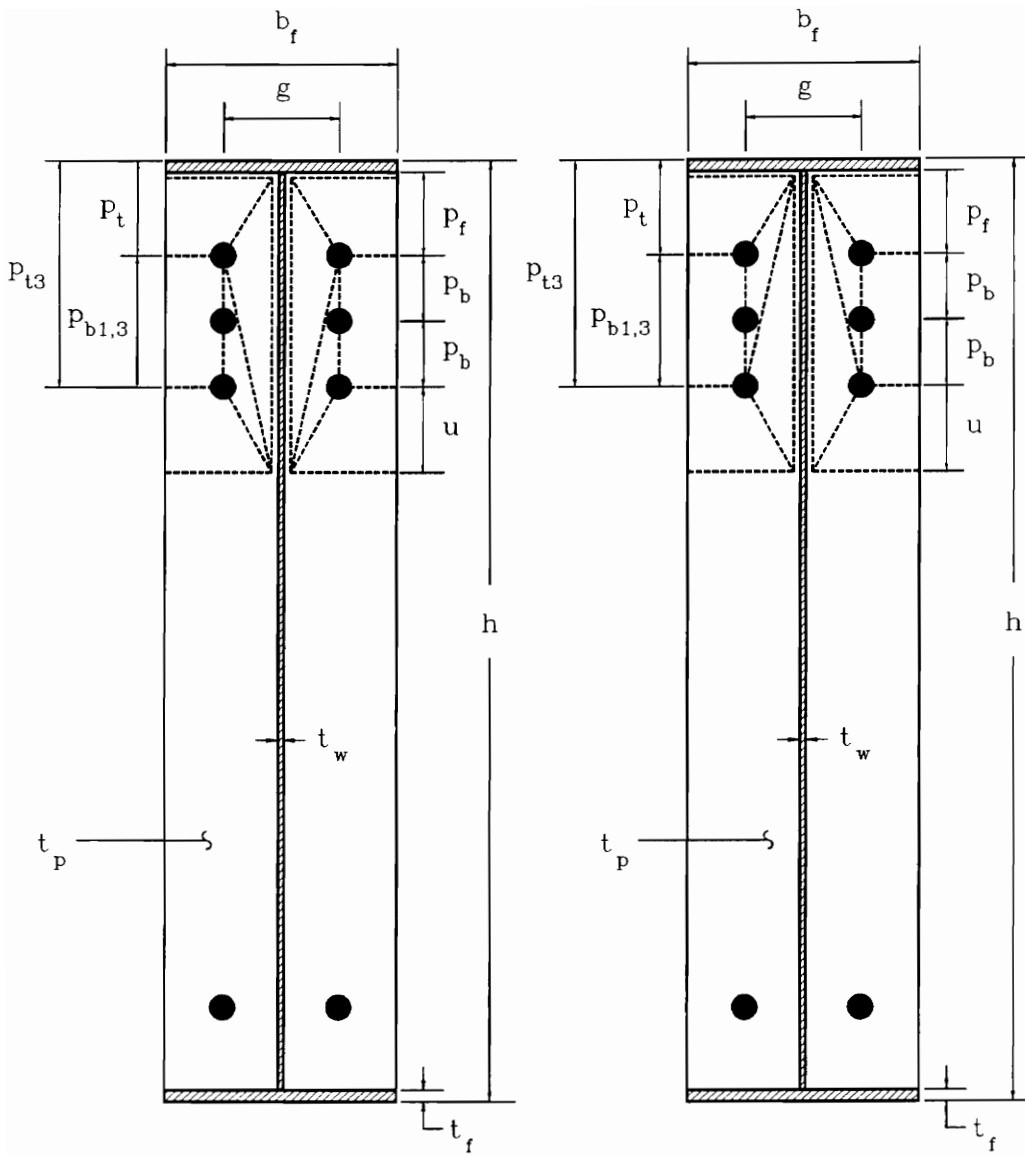
$$t_p = \left\{ \frac{M_u/F_{py}}{\left((h-p_t) \left[\frac{b_f}{2p_f} + \frac{2}{g}(p_f+p_b) \right] + \frac{b_f}{4} + 1.25(h-p_{t2}) \left[\frac{b_f}{2} \left(\frac{1}{p_s} + \frac{1}{2h_t} \right) + \frac{g}{10p_s} + \frac{2}{g} \left(\frac{p_b}{5} + p_s \right) \right] \right)} \right\}^{1/2} \quad (2.20)$$

where p_s is the distance from the furthest interior bolt centerline to the face of the stiffener plate on the outside of the tension bolt rows.

2.2.4 Six-Bolt Flush Unstiffened Moment End-Plates

A study was conducted by Bond and Murray (1989) on the behavior of six-bolt flush unstiffened moment end-plate connections. The following discussion is based on that study.

The two controlling yield-line mechanisms and geometric parameters for the six-bolt flush unstiffened end-plate configuration are shown in Figure 2.5. One of these two yield-line patterns will govern the analysis based on the variable geometric parameters of the specific end-plate. The yield-line patterns of these mechanisms differ in the location of a single pair of yield lines within the depth of the beam near the beam tension flange. In the first mechanism, Mechanism I, this particular yield line begins at the first bolt from the



(a) Mechanism I

(b) Mechanism II

Figure 2.5 Yield-Line Mechanisms for Six-Bolt Flush Unstiffened Moment End-Plate (after Bond and Murray, 1989)

inside of the beam tension flange and ends at the face of the beam web a distance u to the inside of the furthest interior tension bolt, as shown in Figure 2.5(a). In the second mechanism, Mechanism II, the distinguishing yield line begins at the intersection of the inside face of the beam tension flange and the face of the beam web, and ends at the furthest interior bolt, as shown in Figure 2.5(b). Both patterns are symmetric about the beam web. The equations for W_i , M_{pl} , and t_p for each mechanism are as follows:

Mechanism I:

$$W_i = \frac{4m_p}{h} \left[\frac{b_f}{2} \left(\frac{h-p_t}{p_f} + \frac{h-p_{t3}}{u} \right) + 2(p_f + p_{b1,3} + u) \left(\frac{h-p_t}{g} \right) \right] \quad (2.21)$$

$$M_{pl} = 4m_p \left[\frac{b_f}{2} \left(\frac{h-p_t}{p_f} + \frac{h-p_{t3}}{u} \right) + 2(p_f + p_{b1,3} + u) \left(\frac{h-p_t}{g} \right) \right] \quad (2.22)$$

$$t_p = \left[\frac{M_u / F_{py}}{\frac{b_f}{2} \left(\frac{h-p_t}{p_f} + \frac{h-p_{t3}}{u} \right) + 2(p_f + p_{b1,3} + u) \left(\frac{h-p_t}{g} \right)} \right]^{1/2} \quad (2.23)$$

where the unknown parameter, u , is found by taking the derivative of the internal work expression, Equation 2.21, with respect to u and setting equal to zero:

$$u = \frac{1}{2} \sqrt{b_f g \left(\frac{h-p_{t3}}{h-p_t} \right)} \quad (2.24)$$

Mechanism II:

$$W_i = \frac{4m_p}{h} \left[\frac{b_f}{2} \left(\frac{h-p_t}{p_f} + \frac{h-p_{t3}}{u} \right) + \frac{2}{g} (p_f + p_{b1,3}) (h-t_f) + \frac{2u}{g} (h-p_{t3}) + \frac{g}{2} \right] \quad (2.25)$$

$$M_{pl} = 4m_p \left[\frac{b_f}{2} \left(\frac{h-p_t}{p_f} + \frac{h-p_{t3}}{u} \right) + \frac{2}{g} (p_f + p_{b1,3})(h-t_f) + \frac{2u}{g} (h-p_{t3}) + \frac{g}{2} \right] \quad (2.26)$$

$$t_p = \left[\frac{M_u / F_{py}}{\frac{b_f}{2} \left(\frac{h-p_t}{p_f} + \frac{h-p_{t3}}{u} \right) + \frac{2}{g} (p_f + p_{b1,3})(h-t_f) + \frac{2u}{g} (h-p_{t3}) + \frac{g}{2}} \right]^{1/2} \quad (2.27)$$

where the unknown parameter, u , is found as described earlier:

$$u = \frac{1}{2} \sqrt{b_f g} \quad (2.28)$$

2.3 APPLICATION TO EXTENDED MOMENT END-PLATES

Yield-line analysis was performed on the five extended end-plate configurations shown in Figure 1.5. The five configurations are: four-bolt unstiffened, four-bolt stiffened, multiple row unstiffened 1/2, multiple row unstiffened 1/3, and multiple row stiffened 1/3. Analytical studies on all of these configurations except for the multiple row unstiffened 1/2 have been performed in the past. Thus, the equations and procedures that follow are based on these studies.

2.3.1 Four-Bolt Extended Unstiffened Moment End-Plates

A study was conducted by Srouji *et al.* (1983b) on the behavior of four-bolt extended unstiffened moment end-plate connections. The following discussion is based on that study, however, the equations have been generalized to include end-plate configurations with large inner pitch distances, Figure 1.8(a).

The yield-line mechanism in Figure 2.6 is the controlling yield-line pattern for the four-bolt extended unstiffened moment end-plate. The geometric parameters are also shown in the figure. The external work, W_e , for all end-plate configurations is given by Equation 2.4. The internal work stored in this mechanism, W_i , is expressed as:

$$W_i = \frac{4m_p}{h} \left[\left(\frac{b_f}{2} \left(\frac{1}{p_{f,i}} + \frac{1}{s} \right) + (p_{f,i} + s) \left(\frac{2}{g} \right) \right) (h - p_t) + \frac{b_f}{2} \left(\frac{h}{p_{f,o}} + \frac{1}{2} \right) \right] \quad (2.29)$$

where $p_{f,i}$ is the inner pitch distance, $p_{f,o}$ is the outer pitch distance, and s is the distance between parallel yield lines, to be determined. The ultimate capacity of the end-plate, M_{pl} , is found by equating the external and internal work expressions, resulting in:

$$M_{pl} = 4m_p \left[\left(\frac{b_f}{2} \left(\frac{1}{p_{f,i}} + \frac{1}{s} \right) + (p_{f,i} + s) \left(\frac{2}{g} \right) \right) (h - p_t) + \frac{b_f}{2} \left(\frac{h}{p_{f,o}} + \frac{1}{2} \right) \right] \quad (2.30)$$

Rearranging this expression for M_{pl} results in the required end-plate thickness for a desired ultimate moment, M_u :

$$t_p = \left[\frac{M_u / F_{py}}{\left(\frac{b_f}{2} \left(\frac{1}{p_{f,i}} + \frac{1}{s} \right) + (p_{f,i} + s) \left(\frac{2}{g} \right) \right) (h - p_t) + \frac{b_f}{2} \left(\frac{h}{p_{f,o}} + \frac{1}{2} \right)} \right]^{1/2} \quad (2.31)$$

The unknown dimension, s , in Figure 2.6 is found by differentiating the internal work expression, Equation 2.29, with respect to s and equating to zero. The resulting expression for s is:

$$s = \frac{1}{2} \sqrt{b_f g} \quad (2.32)$$

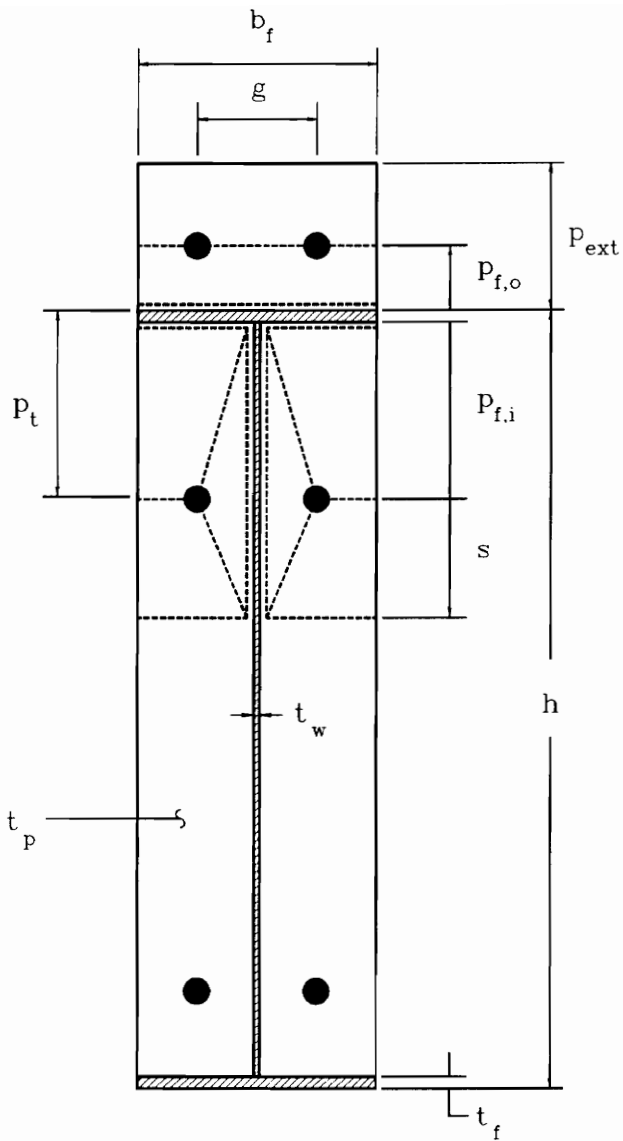


Figure 2.6 Yield-Line Mechanism for Four-Bolt Extended Unstiffened Moment End-Plate (after Srouji *et al.* , 1983b)

2.3.2 Four-Bolt Extended Stiffened Moment End-Plates

A study was conducted by Srouji *et al.* (1983b) on the behavior of four-bolt extended stiffened moment end-plate connections. The following discussion is based on that study.

Figure 2.7 shows the two controlling yield-line mechanisms and geometric parameters for the four-bolt extended stiffened end-plate configuration. The two mechanisms depend on the length of the end-plate extension beyond the exterior bolt line, d_e , and the dimension s . These two parameters determine whether or not a hinge line forms at the extreme edge of the end-plate. The first case, Figure 2.7(a), in which a hinge line does form near the outside edge of the end-plate, is denoted as Case 1. The second case, Figure 2.7(b), in which no hinge line forms above the outside bolt line, is denoted as Case 2. The dimension, s , is found by differentiating the internal work expression with respect to s and equating to zero. The resulting expression for s is:

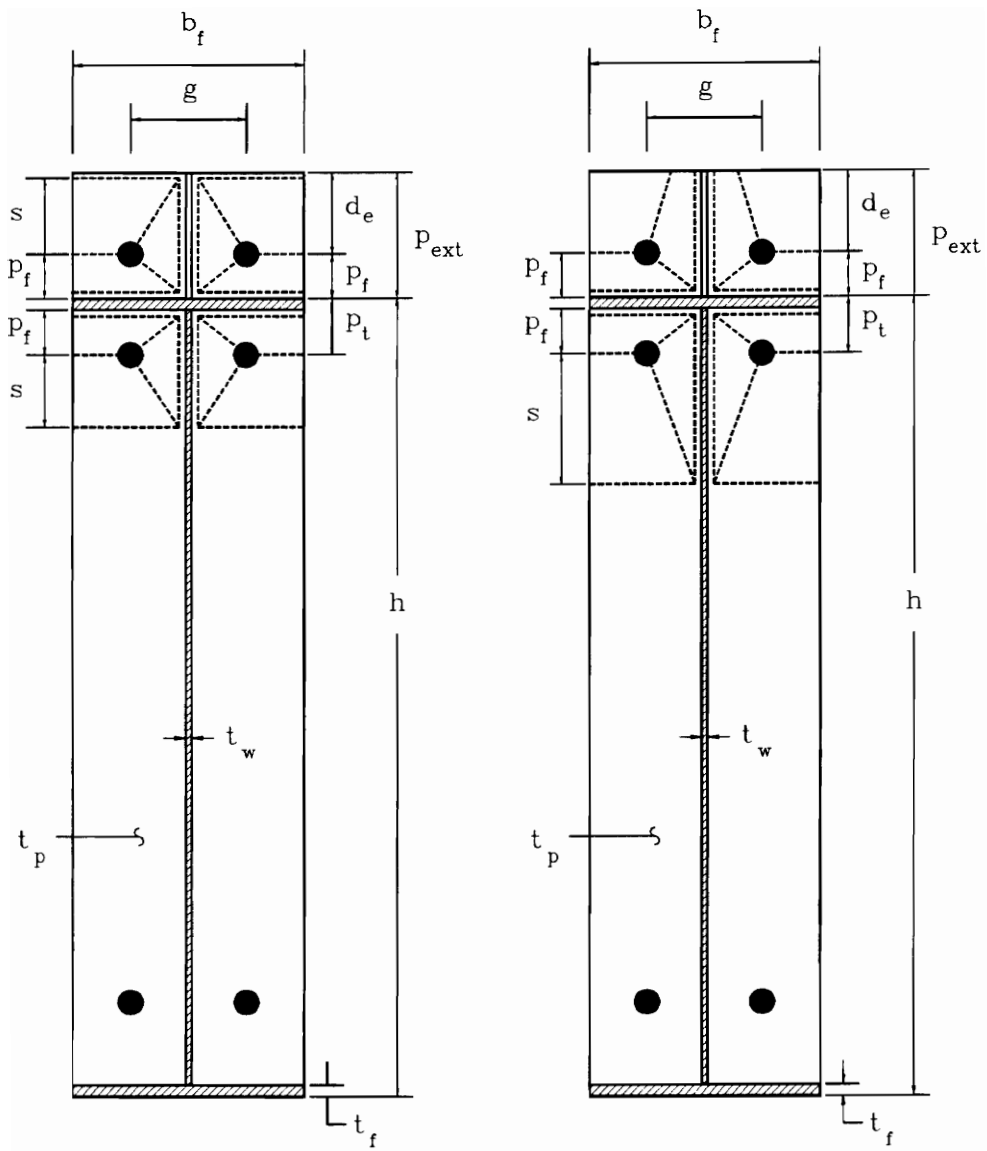
$$s = \frac{1}{2} \sqrt{b_f g} \quad (2.33)$$

The equations for the internal work, W_i , end-plate capacity, M_{pl} , and required plate thickness for a given loading, t_p , for each case are as follows:

Case 1, when $s < d_e$:

$$W_i = \frac{4 m_p}{h} \left[\frac{b_f}{2} \left(\frac{1}{p_f} + \frac{1}{s} \right) + (p_f + s) \left(\frac{2}{g} \right) \right] [(h - p_t) + (h + p_f)] \quad (2.34)$$

$$M_{pl} = 4 m_p \left[\frac{b_f}{2} \left(\frac{1}{p_f} + \frac{1}{s} \right) + (p_f + s) \left(\frac{2}{g} \right) \right] [(h - p_t) + (h + p_f)] \quad (2.35)$$



(a) Case 1, when $s < d_e$

(b) Case 2, when $s > d_e$

Figure 2.7 Yield-Line Mechanisms for Four-Bolt Extended Stiffened Moment End-Plate (after Srouji *et al.*, 1983b)

$$t_p = \left[\frac{M_u / F_{py}}{\left[\frac{b_f}{2} \left(\frac{1}{p_f} + \frac{1}{s} \right) + (p_f + s) \left(\frac{2}{g} \right) \right] [(h - p_t) + (h + p_f)]} \right]^{1/2} \quad (2.36)$$

Case 2, when $s > d_e$:

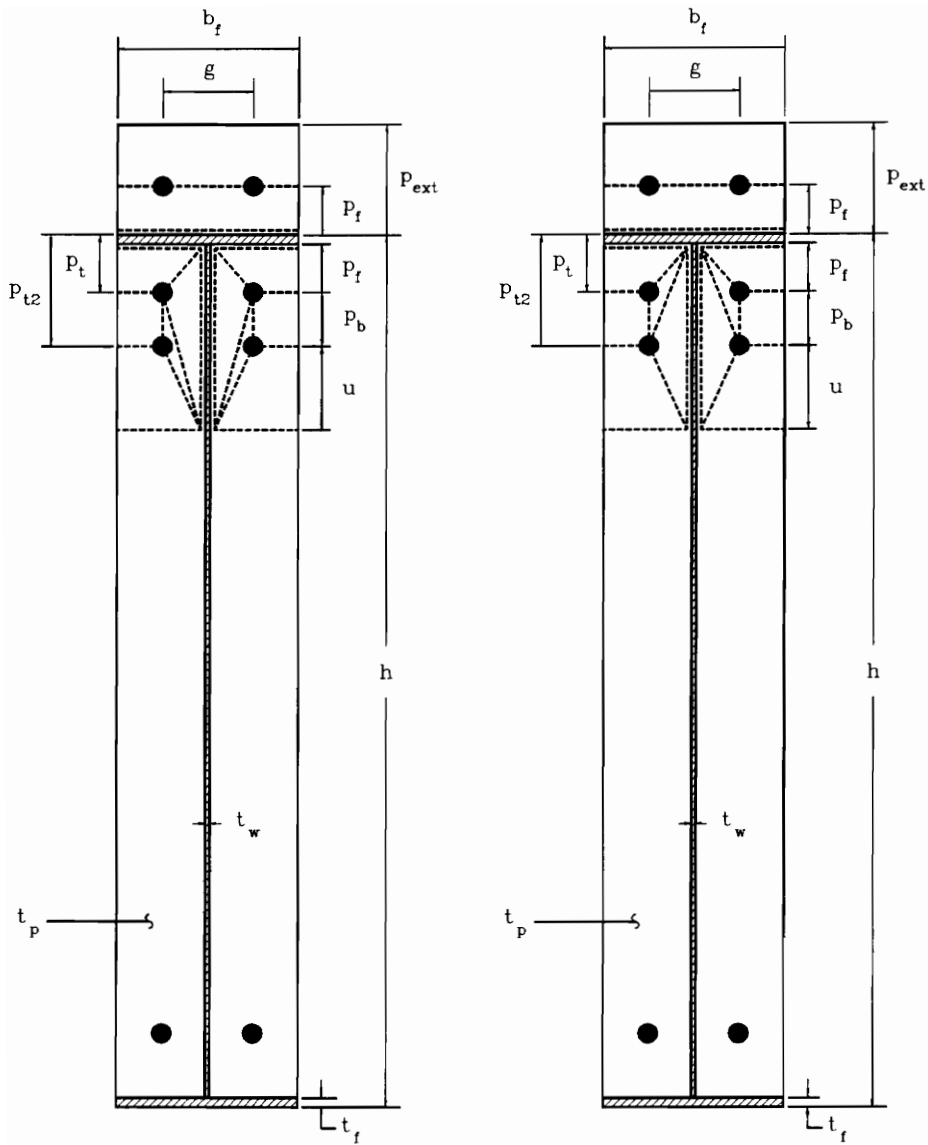
$$W_i = \frac{4 m_p}{h} \left[\frac{b_f}{2} \left(\frac{1}{p_f} + \frac{1}{2s} \right) + (p_f + d_e) \left(\frac{2}{g} \right) \right] [(h - p_t) + (h + p_f)] \quad (2.37)$$

$$M_{pl} = 4 m_p \left[\frac{b_f}{2} \left(\frac{1}{p_f} + \frac{1}{2s} \right) + (p_f + d_e) \left(\frac{2}{g} \right) \right] [(h - p_t) + (h + p_f)] \quad (2.38)$$

$$t_p = \left[\frac{M_u / F_{py}}{\left[\frac{b_f}{2} \left(\frac{1}{p_f} + \frac{1}{2s} \right) + (p_f + d_e) \left(\frac{2}{g} \right) \right] [(h - p_t) + (h + p_f)]} \right]^{1/2} \quad (2.39)$$

2.3.3 Multiple Row Extended Unstiffened 1/2 Moment End-Plates

Two yield-line mechanisms, shown in Figure 2.8, are appropriate for the multiple row extended unstiffened 1/2 moment end-plate connection. These patterns differ in the location of a single pair of yield lines within the depth of the beam near the beam tension flange, much like the patterns for the six-bolt flush unstiffened configuration previously described. In the first mechanism, or Mechanism I, this particular yield line begins at the first bolt from the inside of the beam tension flange and ends at the face of the beam web a distance u to the inside of the innermost bolt line, as shown in Figure 2.8(a). In the second mechanism, Mechanism II, the distinguishing yield line begins at the intersection of the inside face of the beam flange and the face of the beam web, and ends at the furthestmost



(a) Mechanism I

(b) Mechanism II

Figure 2.8 Yield-Line Mechanisms for Multiple Row Extended Unstiffened 1/2 Moment End-Plate

bolt to the inside of the beam tension flange, as shown in Figure 2.8(b). Both yield-line patterns are symmetrical about the beam web. The equations for internal work, W_i , end-plate moment capacity, M_{pl} , and required plate thickness, t_p , for each mechanism are as follows:

Mechanism I:

$$W_i = \frac{4m_p}{h} \left[\frac{b_f}{2} \left(\frac{1}{2} + \frac{h}{p_f} + \frac{h-p_t}{p_f} + \frac{h-p_t}{u} \right) + 2(p_f + p_b + u) \left(\frac{h-p_t}{g} \right) \right] \quad (2.40)$$

$$M_{pl} = 4m_p \left[\frac{b_f}{2} \left(\frac{1}{2} + \frac{h}{p_f} + \frac{h-p_t}{p_f} + \frac{h-p_t}{u} \right) + 2(p_f + p_b + u) \left(\frac{h-p_t}{g} \right) \right] \quad (2.41)$$

$$t_p = \left[\frac{M_u / F_{py}}{\frac{b_f}{2} \left(\frac{1}{2} + \frac{h}{p_f} + \frac{h-p_t}{p_f} + \frac{h-p_t}{u} \right) + 2(p_f + p_b + u) \left(\frac{h-p_t}{g} \right)} \right]^{1/2} \quad (2.42)$$

The dimension, u , is found by taking the derivative of the internal work expression, Equation 2.40, with respect to u , and setting equal to zero. The resulting expression is:

$$u = \frac{1}{2} \sqrt{b_f g \left(\frac{h-p_t}{h-p_t} \right)} \quad (2.43)$$

Mechanism II:

$$W_i = \frac{4m_p}{h} \left[\frac{b_f}{2} \left(\frac{1}{2} + \frac{h}{p_f} + \frac{h-p_t}{p_f} + \frac{h-p_t}{u} \right) + \frac{2}{g} (p_f + p_b) (h-t_f) + \frac{2u}{g} (h-p_t) + \frac{g}{2} \right] \quad (2.44)$$

$$M_{pl} = 4m_p \left[\frac{b_f}{2} \left(\frac{1}{2} + \frac{h}{p_f} + \frac{h-p_t}{p_f} + \frac{h-p_t}{u} \right) + \frac{2}{g} (p_f + p_b) (h-t_f) + \frac{2u}{g} (h-p_t) + \frac{g}{2} \right] \quad (2.45)$$

$$t_p = \left[\frac{M_u / F_{py}}{\frac{b_f}{2} \left(\frac{1}{2} + \frac{h}{p_f} + \frac{h-p_t}{p_f} + \frac{h-p_{t2}}{u} \right) + \frac{2}{g} (p_f + p_b)(h-t_f) + \frac{2u}{g} (h-p_{t2}) + \frac{g}{2}} \right]^{1/2} \quad (2.46)$$

The unknown dimension, u , is found as described earlier, resulting in:

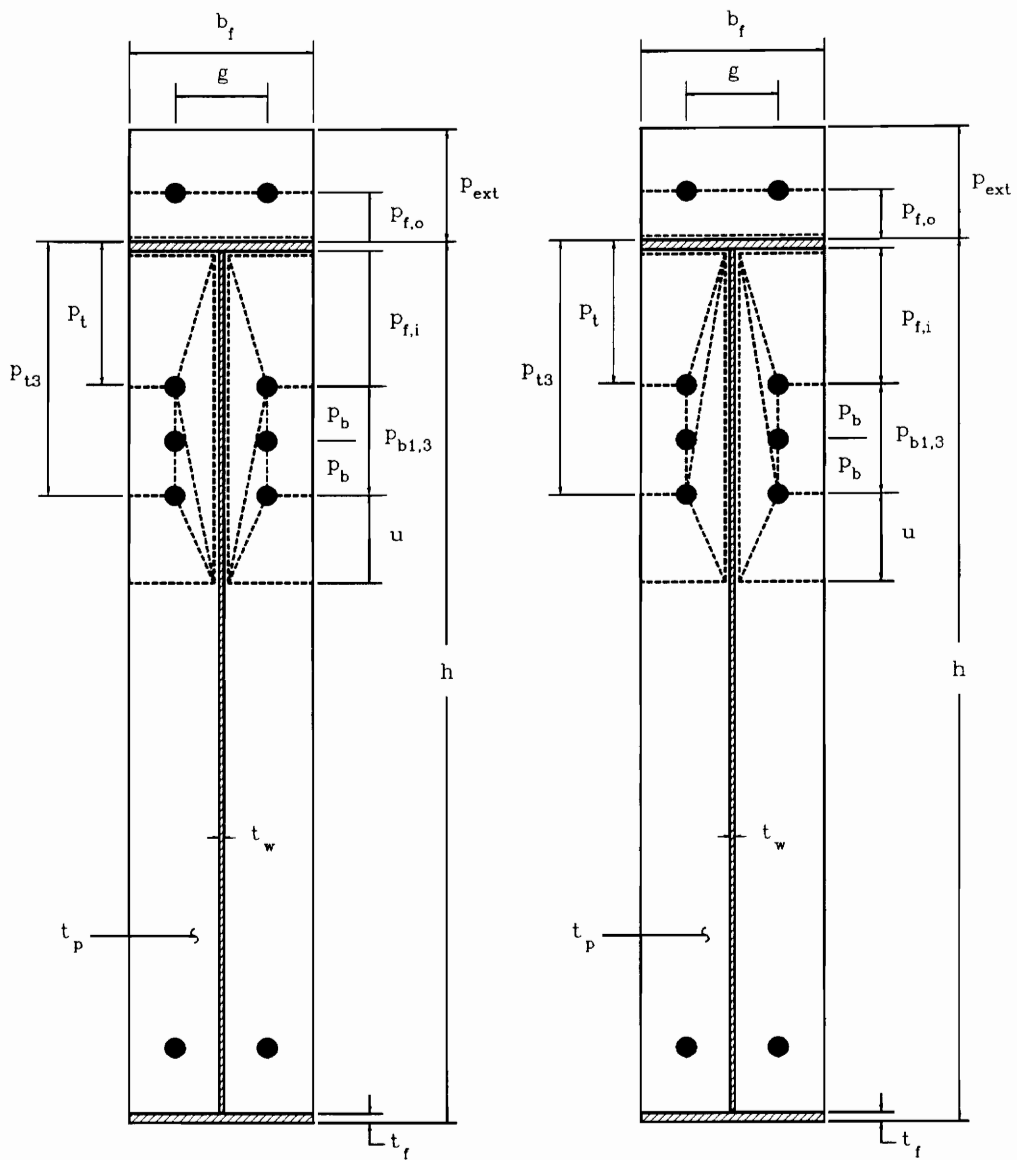
$$u = \frac{1}{2} \sqrt{b_f g} \quad (2.47)$$

2.3.4 Multiple Row Extended Unstiffened 1/3 Moment End-Plates

A study of the behavior of multiple row extended unstiffened 1/3 moment end-plate connections was performed by SEI (1984) and Morrison *et al.* (1986). The following discussion is based on those studies, however, the equations have been generalized to include end-plate configurations with large inner pitch distances, Figure 1.8(b).

Two yield-line mechanisms, shown in Figure 2.9, are appropriate for the multiple row extended unstiffened 1/3 moment end-plate configuration. The yield-line patterns of these mechanisms differ in the location of a single pair of yield lines within the depth of the beam near the beam tension flange, similar to those for the multiple row extended unstiffened 1/2 configuration just described. Mechanism I is shown in Figure 2.9(a) and Mechanism II is shown in Figure 2.9(b). The geometric parameters are also shown in the figure. The equations for W_i , M_{pl} , t_p , and u for each mechanism are as follows:

Mechanism I:



(a) Mechanism I

(b) Mechanism II

Figure 2.9 Yield-Line Mechanisms for Multiple Row Extended Unstiffened 1/3 Moment End-Plate (after SEI, 1984)

$$W_i = \frac{4m_p}{h} \left[\frac{b_f}{2} \left(\frac{1}{2} + \frac{h}{p_{f,o}} + \frac{h-p_t}{p_{f,i}} + \frac{h-p_{t3}}{u} \right) + 2(p_{f,i} + p_{b1,3} + u) \left(\frac{h-p_t}{g} \right) \right] \quad (2.48)$$

$$M_{pl} = 4m_p \left[\frac{b_f}{2} \left(\frac{1}{2} + \frac{h}{p_{f,o}} + \frac{h-p_t}{p_{f,i}} + \frac{h-p_{t3}}{u} \right) + 2(p_{f,i} + p_{b1,3} + u) \left(\frac{h-p_t}{g} \right) \right] \quad (2.49)$$

$$t_p = \left[\frac{M_u / F_{py}}{\frac{b_f}{2} \left(\frac{1}{2} + \frac{h}{p_{f,o}} + \frac{h-p_t}{p_{f,i}} + \frac{h-p_{t3}}{u} \right) + 2(p_{f,i} + p_{b1,3} + u) \left(\frac{h-p_t}{g} \right)} \right]^{1/2} \quad (2.50)$$

$$u = \frac{1}{2} \sqrt{b_f g \left(\frac{h-p_{t3}}{h-p_t} \right)} \quad (2.51)$$

Mechanism II:

$$W_i = \frac{4m_p}{h} \left[\frac{b_f}{2} \left(\frac{1}{2} + \frac{h}{p_{f,o}} + \frac{h-p_t}{p_{f,i}} + \frac{h-p_{t3}}{u} \right) + \frac{2}{g} (p_{f,i} + p_{b1,3}) (h-t_f) + \frac{2u}{g} (h-p_{t3}) + \frac{g}{2} \right] \quad (2.52)$$

$$M_{pl} = 4m_p \left[\frac{b_f}{2} \left(\frac{1}{2} + \frac{h}{p_{f,o}} + \frac{h-p_t}{p_{f,i}} + \frac{h-p_{t3}}{u} \right) + \frac{2}{g} (p_{f,i} + p_{b1,3}) (h-t_f) + \frac{2u}{g} (h-p_{t3}) + \frac{g}{2} \right] \quad (2.53)$$

$$t_p = \left[\frac{M_u / F_{py}}{\frac{b_f}{2} \left(\frac{1}{2} + \frac{h}{p_{f,o}} + \frac{h-p_t}{p_{f,i}} + \frac{h-p_{t3}}{u} \right) + \frac{2}{g} (p_{f,i} + p_{b1,3}) (h-t_f) + \frac{2u}{g} (h-p_{t3}) + \frac{g}{2}} \right]^{1/2} \quad (2.54)$$

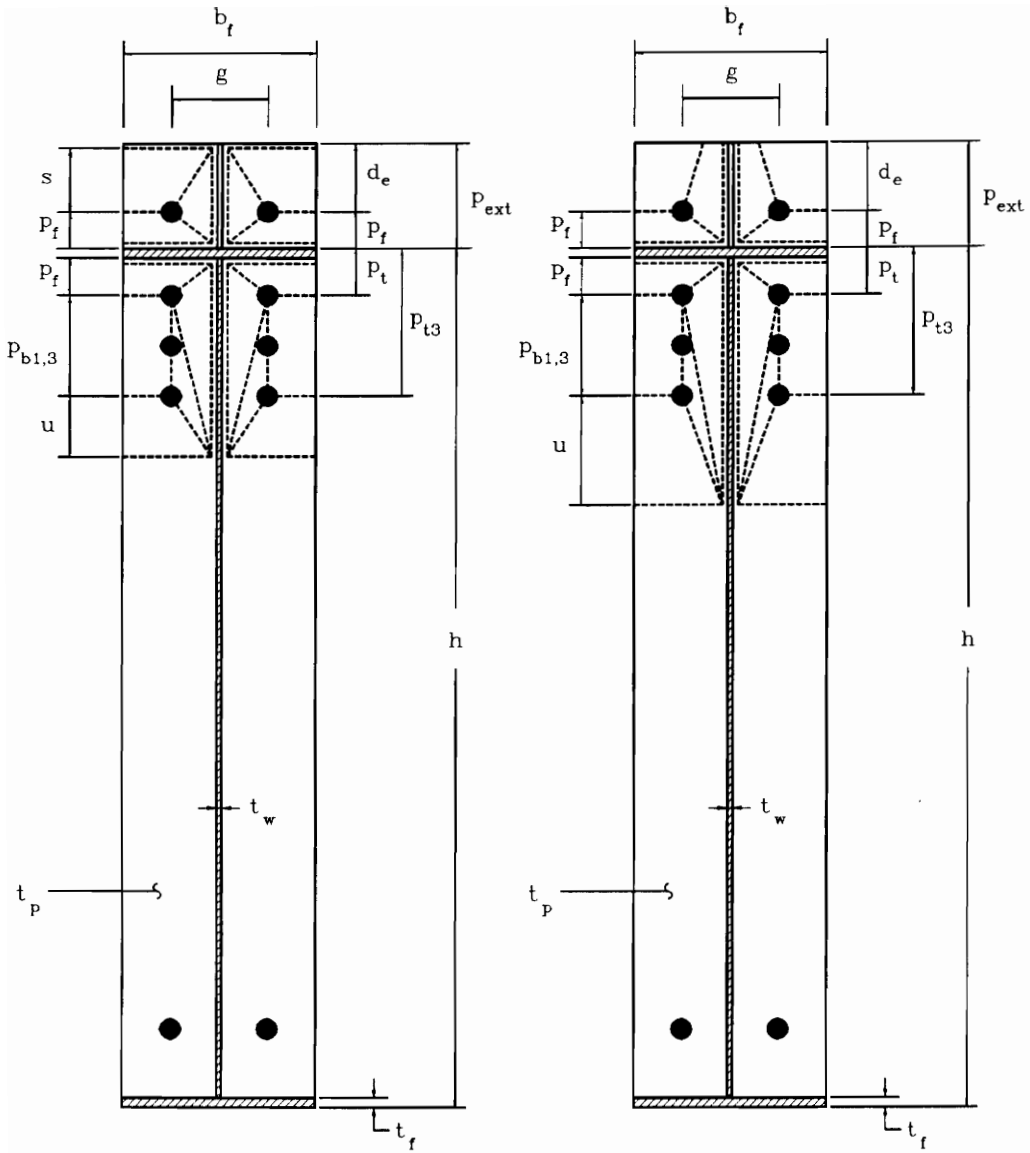
$$u = \frac{1}{2} \sqrt{b_f g} \quad (2.55)$$

2.3.5 Multiple Row Extended Stiffened 1/3 Moment End-Plates

A study was conducted by SEI (1984) on the behavior of multiple row extended stiffened 1/3 moment end-plate connections. The equations and discussion herein are based on that study.

The two yield-line mechanisms shown in Figure 2.10 and Figure 2.11 control the analysis of multiple row extended stiffened 1/3 end-plate configurations. The two mechanisms differ by the location of a single pair of yield lines--the same distinguishing pair of yield lines just described for the multiple row extended unstiffened 1/3 configuration. Mechanism I is shown in Figure 2.10, and Mechanism II is shown in Figure 2.11. For each mechanism, there are two cases, which depend on the length of the end-plate extension beyond the exterior bolt line, d_e , and the dimension s . These parameters determine whether or not a yield line forms at the extreme edge of the end-plate. The first case for each mechanism, in which a hinge line does form near the outside edge of the end-plate, is denoted as Case 1, Figures 2.10(a) and 2.11(a). The second case for each mechanism, in which no yield line forms above the outside bolt line is denoted as Case 2, Figures 2.10(b) and 2.11(b). The dimension, s , is found by differentiating the internal work expressions with respect to s and equating to zero. The resulting expression for both mechanisms is:

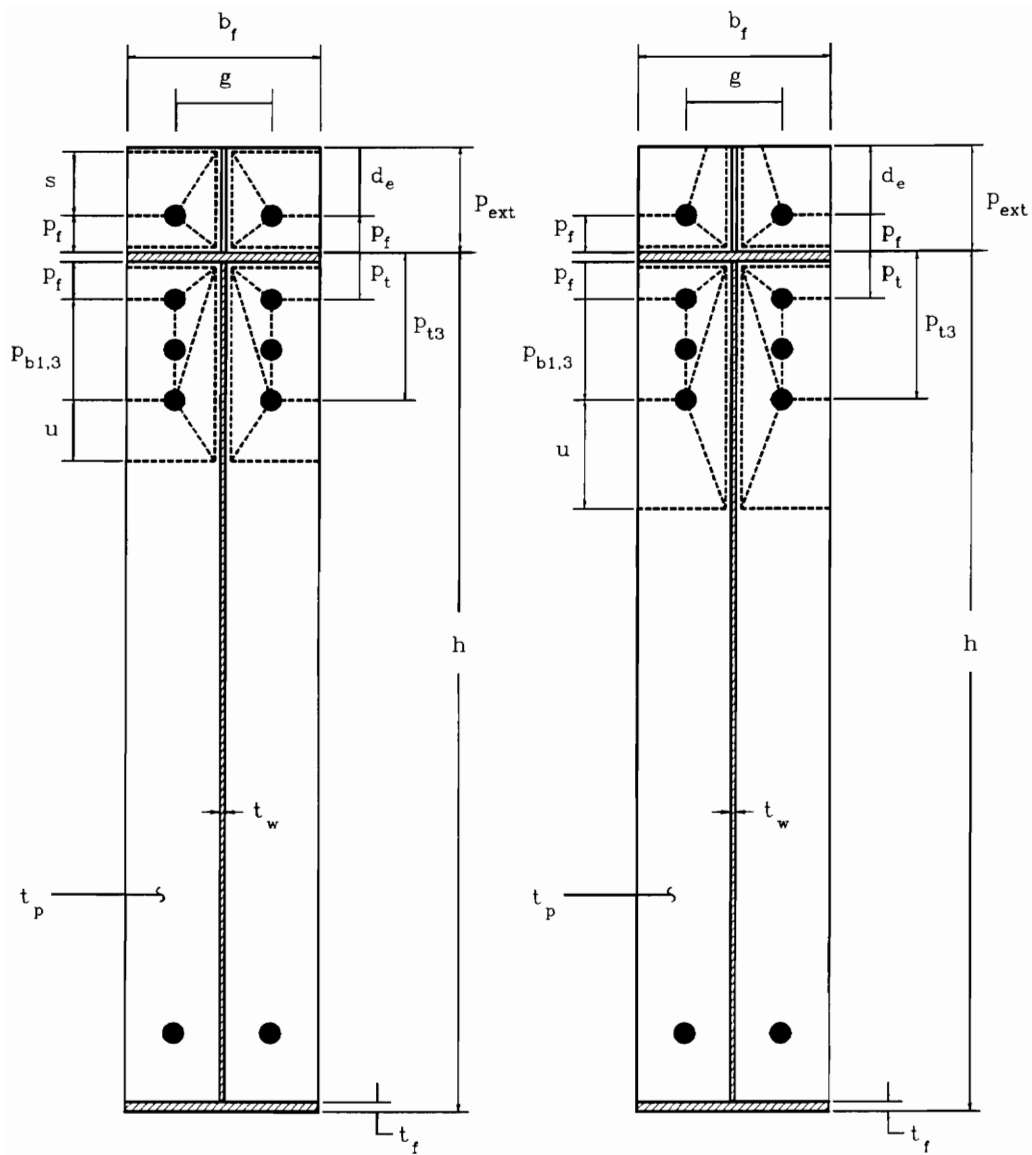
$$s = \frac{1}{2} \sqrt{b_f g} \quad (2.56)$$



(a) Case 1, when $s < d_e$

(b) Case 2, when $s > d_e$

Figure 2.10 Yield-Line Mechanism I for Multiple Row Extended Stiffened 1/3 Moment End-Plate (after SEI, 1984)



(a) Case 1, when $s < d_e$

(b) Case 2, when $s > d_e$

Figure 2.11 Yield-Line Mechanism II for Multiple Row Extended Stiffened 1/3 Moment End-Plate (after SEI, 1984)

The equations for the internal work, W_i , end-plate capacity, M_{pl} , and required end-plate thickness, t_p , for a desired ultimate load are as follows for each mechanism and case:

Mechanism I:

Case 1, when $s < d_e$:

$$W_i = \frac{4m_p}{h} \left[\frac{b_f}{2} \left(1 + \frac{h}{p_f} + \frac{h-p_t}{p_f} + \frac{h-p_{t3}}{u} + \frac{h+p_f}{s} \right) + 2(p_f + p_{b1,3} + u) \left(\frac{h-p_t}{g} \right) + \frac{2}{g} (s+p_f)(h+p_f) \right] \quad (2.57)$$

$$M_{pl} = 4m_p \left[\frac{b_f}{2} \left(1 + \frac{h}{p_f} + \frac{h-p_t}{p_f} + \frac{h-p_{t3}}{u} + \frac{h+p_f}{s} \right) + 2(p_f + p_{b1,3} + u) \left(\frac{h-p_t}{g} \right) + \frac{2}{g} (s+p_f)(h+p_f) \right] \quad (2.58)$$

$$t_p = \left[\frac{M_u / F_{py}}{\frac{b_f}{2} \left(1 + \frac{h}{p_f} + \frac{h-p_t}{p_f} + \frac{h-p_{t3}}{u} + \frac{h+p_f}{s} \right) + 2(p_f + p_{b1,3} + u) \left(\frac{h-p_t}{g} \right) + \frac{2}{g} (s+p_f)(h+p_f)} \right]^{1/2} \quad (2.59)$$

The unknown parameter, u , in Figure 2.10 is found from differentiating the internal work expression, Equation 2.57, with respect to u , and setting equal to zero, resulting in:

$$u = \frac{1}{2} \sqrt{b_f g \left(\frac{h-p_{t3}}{h-p_t} \right)} \quad (2.60)$$

Case 2, when $s > d_e$:

$$W_i = \frac{4m_p}{h} \left[\frac{b_f}{2} \left(1 + \frac{h}{p_f} + \frac{h-p_t}{p_f} + \frac{h-p_{t3}}{u} + \frac{h+p_f}{2s} \right) + 2(p_f + p_{b1,3} + u) \left(\frac{h-p_t}{g} \right) + \frac{2}{g} (d_e + p_f)(h+p_f) \right] \quad (2.61)$$

$$M_{pl} = 4m_p \left[\frac{b_f}{2} \left(1 + \frac{h}{p_f} + \frac{h-p_t}{p_f} + \frac{h-p_{t3}}{u} + \frac{h+p_f}{2s} \right) + 2(p_f + p_{b1,3} + u) \left(\frac{h-p_t}{g} \right) + \frac{2}{g} (d_e + p_f)(h+p_f) \right] \quad (2.62)$$

$$t_p = \left[\frac{M_u / F_{py}}{\frac{b_f}{2} \left(1 + \frac{h}{p_f} + \frac{h-p_t}{p_f} + \frac{h-p_{t3}}{u} + \frac{h+p_f}{2s} \right) + 2(p_f + p_{b1,3} + u) \left(\frac{h-p_t}{g} \right) + \frac{2}{g} (d_e + p_f)(h+p_f)} \right]^{1/2} \quad (2.63)$$

where u is the same as for Case 1, Equation 2.60.

Mechanism II:

Case 1, when $s < d_e$:

$$W_i = \frac{4m_p}{h} \left[\frac{b_f}{2} \left(1 + \frac{h}{p_f} + \frac{h-p_t}{p_f} + \frac{h-p_{t3}}{u} + \frac{h+p_f}{s} \right) + \frac{2}{g} (p_f + p_{b1,3})(h-t_f) + \frac{2u}{g} (h-p_{t3}) + \frac{2}{g} (s+p_f)(h+p_f) + \frac{g}{2} \right] \quad (2.64)$$

$$M_{pl} = 4m_p \left[\frac{b_f}{2} \left(1 + \frac{h}{p_f} + \frac{h-p_t}{p_f} + \frac{h-p_{t3}}{u} + \frac{h+p_f}{s} \right) + \frac{2}{g} (p_f + p_{b1,3})(h-t_f) + \frac{2u}{g} (h-p_{t3}) + \frac{2}{g} (s+p_f)(h+p_f) + \frac{g}{2} \right] \quad (2.65)$$

$$t_p = \left[\frac{M_u / F_{py}}{\frac{b_f}{2} \left(1 + \frac{h}{p_f} + \frac{h-p_t}{p_f} + \frac{h-p_{t3}}{u} + \frac{h+p_f}{s} \right) + \frac{2}{g} (p_f + p_{b1,3})(h-t_f) + \frac{2u}{g} (h-p_{t3}) + \frac{2}{g} (s+p_f)(h+p_f) + \frac{g}{2}} \right]^{1/2} \quad (2.66)$$

The unknown dimension, u , in Figure 2.11 is found as described earlier resulting in:

$$u = \frac{1}{2} \sqrt{b_f g} \quad (2.67)$$

Case 2, when $s > d_e$:

$$W_i = \frac{4m_p}{h} \left[\frac{b_f}{2} \left(1 + \frac{h}{p_f} + \frac{h-p_t}{p_f} + \frac{h-p_{t3}}{u} + \frac{h+p_f}{2s} \right) + \frac{2}{g} (p_f + p_{b1,3})(h-t_f) + \frac{2u}{g} (h-p_{t3}) + \frac{2}{g} (d_e + p_f)(h+p_f) + \frac{g}{2} \right] \quad (2.68)$$

$$M_{pl} = 4m_p \left[\frac{b_f}{2} \left(1 + \frac{h}{p_f} + \frac{h-p_t}{p_f} + \frac{h-p_{t3}}{u} + \frac{h+p_f}{2s} \right) + \frac{2}{g} (p_f + p_{b1,3})(h-t_f) + \frac{2u}{g} (h-p_{t3}) + \frac{2}{g} (d_e + p_f)(h+p_f) + \frac{g}{2} \right] \quad (2.69)$$

$$t_p = \left[\frac{M_u / F_{py}}{\frac{b_f}{2} \left(1 + \frac{h}{p_f} + \frac{h-p_t}{p_f} + \frac{h-p_{t3}}{u} + \frac{h+p_f}{2s} \right) + \frac{2}{g} (p_f + p_{b1,3})(h-t_f) + \frac{2u}{g} (h-p_{t3}) + \frac{2}{g} (d_e + p_f)(h+p_f) + \frac{g}{2}} \right]^{1/2} \quad (2.70)$$

where the unknown parameter, u , is the same as for Case 1, Equation 2.67.

CHAPTER III

CONNECTION STRENGTH USING SIMPLIFIED BOLT ANALYSIS

3.1 GENERAL

Yield-line theory predicts a moment capacity for end-plate connections which is controlled by yielding of the plate. It does not predict the connection capacity based on bolt failure. Because both the plate and the bolts are essential to the connection performance, it is necessary to analyze the capacity of the connection based on bolt forces including prying action. Experimental tests have shown that prying action in the bolts arises when the end-plate deforms out of its original flat state, as shown in Figure 3.1 (Srouji *et al.*, 1983a, 1983b, 1984; Hendrick *et al.*, 1984; SEI, 1984, Morrison *et al.*, 1985, 1986; Bond and Murray, 1989; Abel and Murray, 1992b). As the plate deforms, contact points are made between the plates, giving rise to the points of application of prying forces. A simplified form of a method introduced by Kennedy *et al.* (1981) has been adopted for predicting the connection moment capacity for the limit state of bolt rupture which includes prying action.

As described in Chapter I, the primary assumption in the Kennedy method is that, as the end-plate deforms out of its original state, it displays one of three stages of behavior depending on the thickness of the plate and the magnitude of the applied load. The three

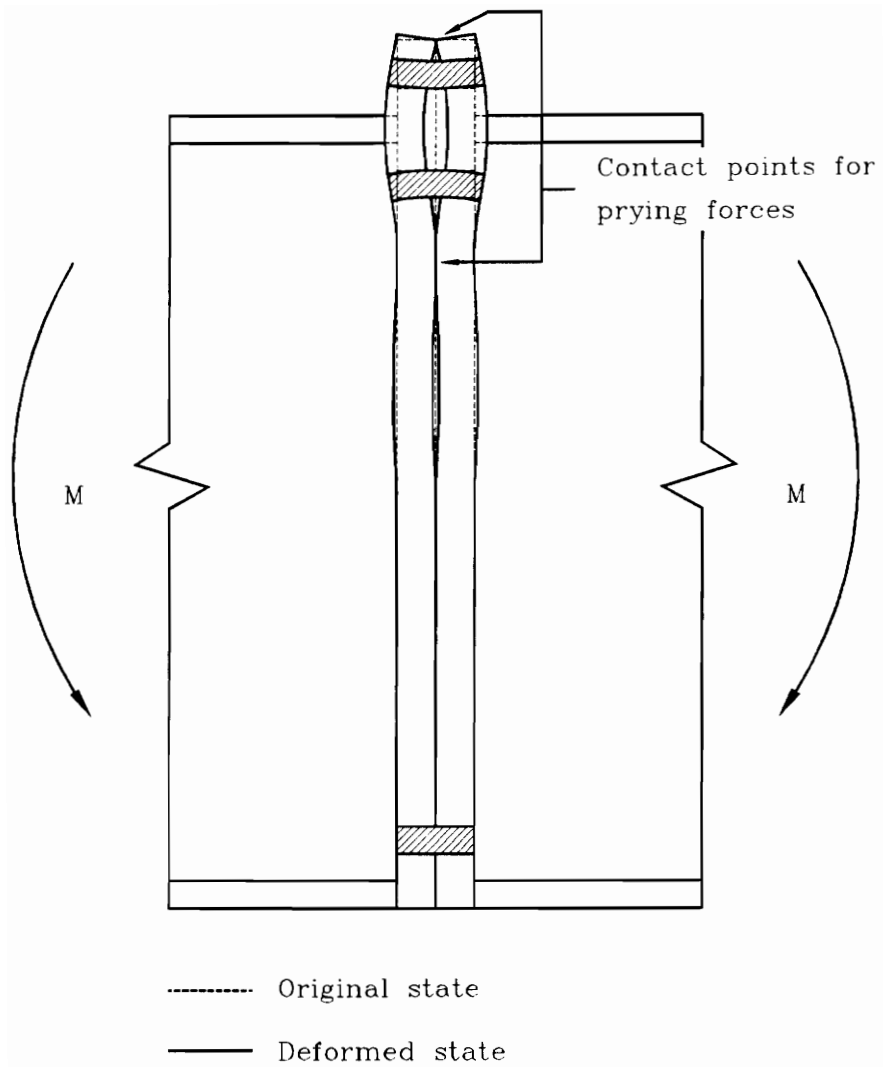


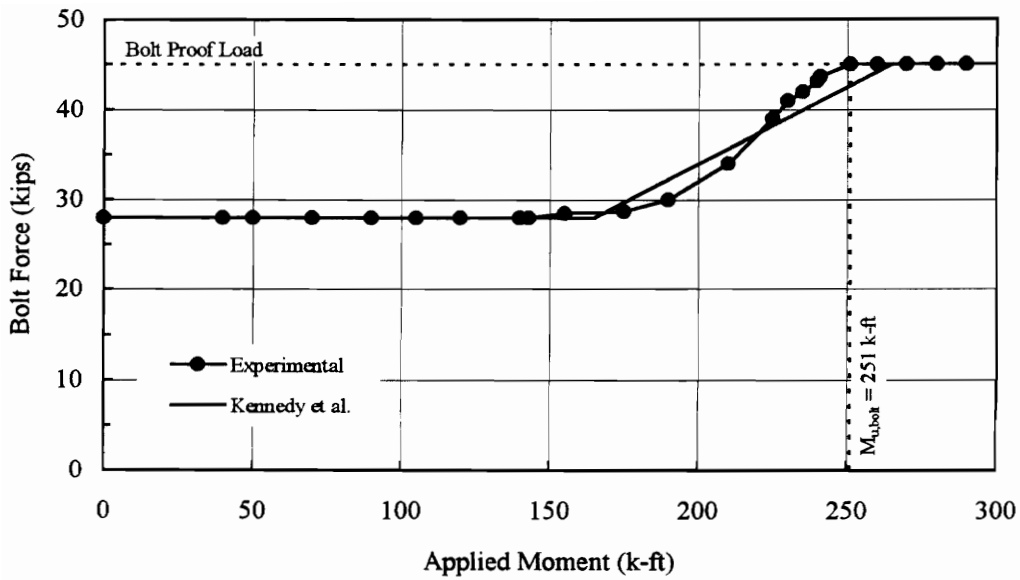
Figure 3.1 Prying Forces as a Result of Plate Bending

stages of plate behavior are thick, intermediate, and thin (Figure 1.7). Each stage of plate behavior has a corresponding equation for calculating a prying force which is incorporated into the bolt force calculation. Once the stage of plate behavior is determined, the prying force, and hence, the bolt force can be calculated. The moment at which bolt failure occurs, $M_{u,bolt}$, is designated as the moment at which one of the bolts first reaches its proof load, as shown in the sample applied moment versus bolt force plot in Figure 3.2(a). The bolt proof load, P_t , is calculated by multiplying the bolt cross-sectional area, A_b , with the nominal strength of the bolt, F_{yb} , defined in Table J3.2, AISC (1986):

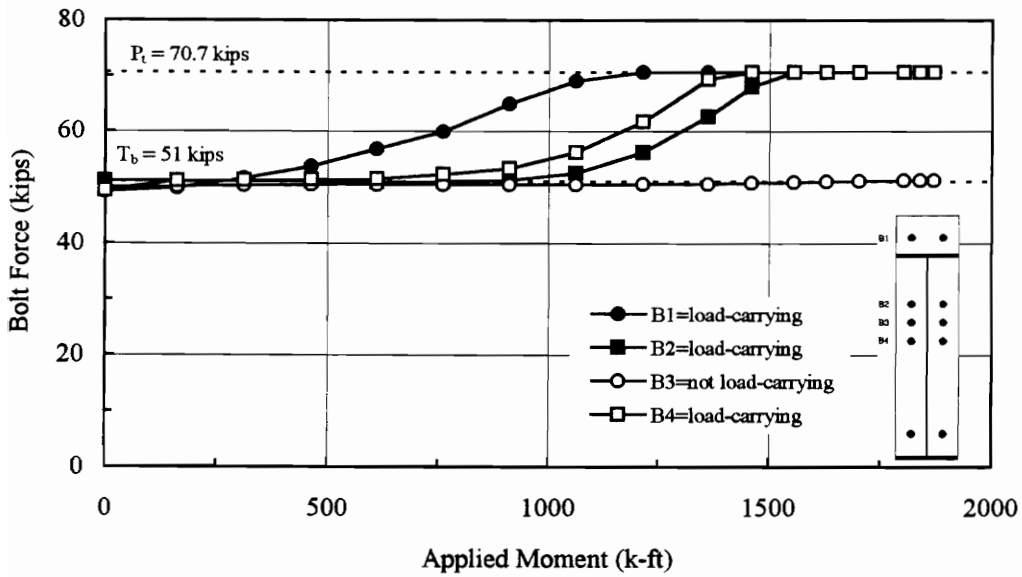
$$P_t = A_b F_{yb} \quad (3.1)$$

The modified Kennedy method has been proven to be quite accurate for predicting bolt forces with prying action in end-plate connections at any stage of loading (Srouji *et al.*, 1983a, 1983b, 1984; Hendrick *et al.*, 1984; SEI, 1984, Morrison *et al.*, 1985, 1986; Bond and Murray, 1989; Abel and Murray, 1992b). The correlation between the modified Kennedy method and experimental bolt force is shown in the sample plot in Figure 3.2(a). As discussed in Chapter I, extensive calculations and iterations are involved in the modified Kennedy method. However, when considering the ultimate moment capacity of the connection, these calculations can be reduced considerably.

After reviewing the results of previously conducted connection tests, two rational assumptions were devised in order to minimize the bolt force calculations in the Kennedy method. The first assumption considers bolt yielding. It was evident that, in most of the tests, the connection continued carrying load beyond the point at which the first bolt



(a) Kennedy *et al.* Prediction
(after Abel and Murray, 1992a)



(b) Determination of Load-Carrying Bolts
(after Borgsmiller *et al.*, 1995)

Figure 3.2 Sample Applied Moment vs. Bolt Force Plots

reached its proof load, $M_{u,bolt}$ (Figure 3.2(a) and (b)). Because the proof load of a bolt designates the point at which yielding commences, and because of the ductile nature of steel, it can be assumed that bolts that have reached their proof load can continue yielding without rupture until the other bolts reach their proof load as well. This assumption is justified by the notable yield plateau on bolt stress-strain graphs obtained by Abel and Murray (1992b). The second assumption is a conservative one, and states that when a bolt reaches its proof load, the plate behaves as a “thin” plate and the maximum possible prying force, Q_{max} , can be incorporated into the bolt analysis. It is important to note that, because of the second assumption, this simplified method is only applicable when predicting the ultimate capacity of the connection. In other words, this simplified approach is geared towards calculating the maximum possible applied moment when the bolts have reached their proof load, P_t .

When calculating the connection strength using the simplified approach, all load-carrying bolt forces are set equal to their proof load, P_t , the maximum possible prying force for a given end-plate configuration, Q_{max} , is calculated, and the two are incorporated into the analysis of the connection moment capacity for the limit state of bolt rupture. If a bolt does not carry any load, its force is always equal to the minimum pretension force, T_b , specified in Table J3.1, AISC (1986). A “load-carrying bolt” is one that has been experimentally proven to carry load in an end-plate connection. For instance bolts B_1 , B_2 , and B_4 in Figure 3.2(b) show an increase in bolt load as the applied moment increases,

whereas B_3 stays at approximately the pretension force, 51 kips, throughout the entire test. The load-carrying bolts in this hypothetical test are therefore B_1 , B_2 , and B_4 .

To illustrate the simplified approach, consider the schematic of a two-bolt flush unstiffened end-plate configuration shown in Figure 3.3. In the figure, M_q = ultimate moment capacity of the connection as controlled by bolt rupture with prying action, F_f = the total applied flange force resulting from the applied moment, B = the bolt force in one bolt, equal to the bolt proof load, P_t , and Q_{max} = the maximum possible prying force in one bolt resulting from the plate deformation. Summing the moments results in:

$$\begin{aligned} M_q &= 2 P_t d_1 - 2 Q_{max} (d_1 - a) \\ &= 2[(P_t - Q_{max}) d_1 + Q_{max}(a)] \end{aligned} \quad (3.2)$$

The term, $Q_{max}(a)$, in this equation only constitutes approximately 2% of M_q . Hence, in the spirit of simplification and in keeping things conservative, it can be assumed that the $Q_{max}(a)$ term is negligible, resulting in the following expression for M_q :

$$M_q = 2(P_t - Q_{max}) d_1 \quad (3.3)$$

Based on this simplified equation of equilibrium, a simpler model of the connection indicates that the bolt force can be taken as $(P_t - Q_{max})$ rather than having two sets of forces, P_t and Q_{max} . This further simplified model is shown in Figure 3.4.

If the bolt force is considered to be $(P_t - Q_{max})$, care must be taken to ensure that it is not less than the minimum pretension of the bolt, T_b . If this is the case, the value for T_b is used instead of $(P_t - Q_{max})$ in Equation 3.3. The calculation of M_q is therefore expressed as:

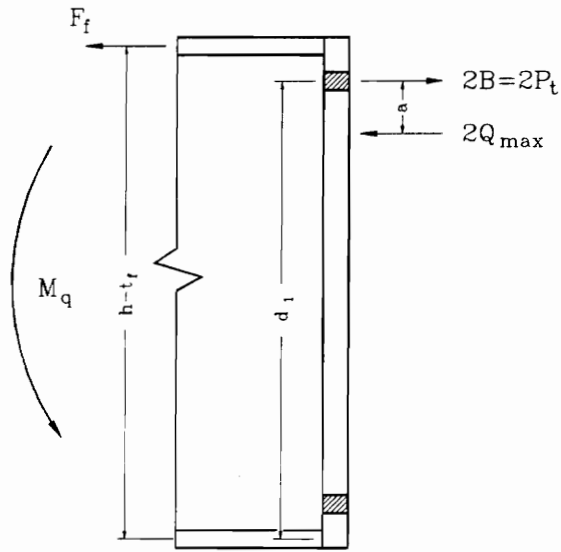


Figure 3.3 Bolt Analysis for Two-Bolt Flush Unstiffened Moment End-Plates

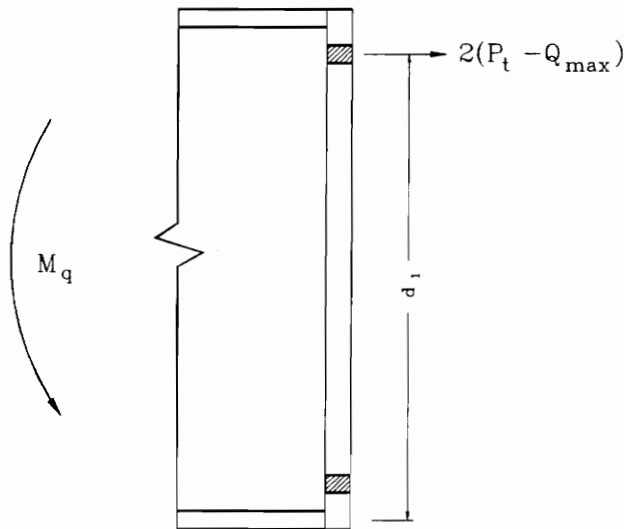


Figure 3.4 Simplified Bolt Force Model for Two-Bolt Flush Unstiffened Moment End-Plates

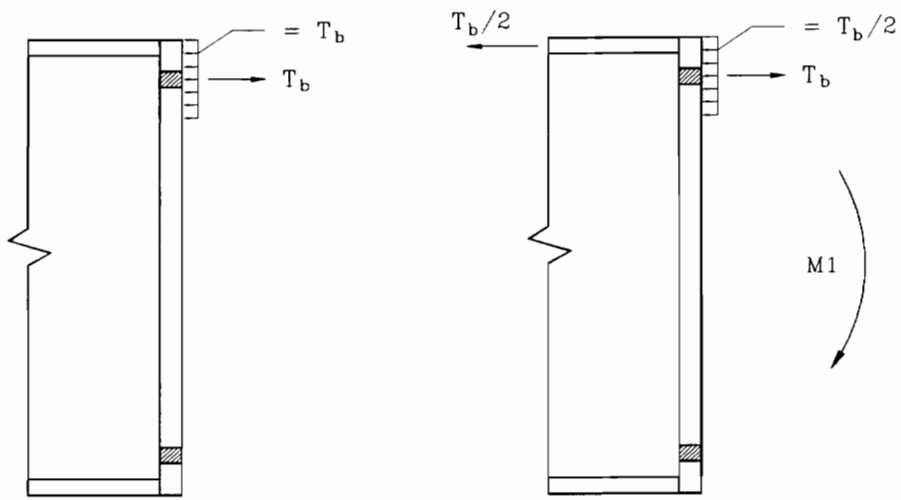
$$M_{q} = \max \left\{ \begin{array}{l} 2(P_t - Q_{\max}) d_1 \\ 2(T_b) d_1 \end{array} \right. \quad (3.4)$$

The pretension phenomenon is depicted in Figure 3.5. By pretensioning the bolts, the plates are compressed an equivalent amount as the bolt pretension. As load is applied to the connection, no load is applied into the bolt until the precompression of the plates is diminished. Once this happens, the bolt load increases beyond the pretension force until it reaches its proof load.

The procedure used in calculating M_q for the two-bolt flush unstiffened configuration can be generalized to include any configuration. The predicted ultimate moment capacity of the connection for the limit state of bolt rupture including prying action in any end-plate configuration is calculated by:

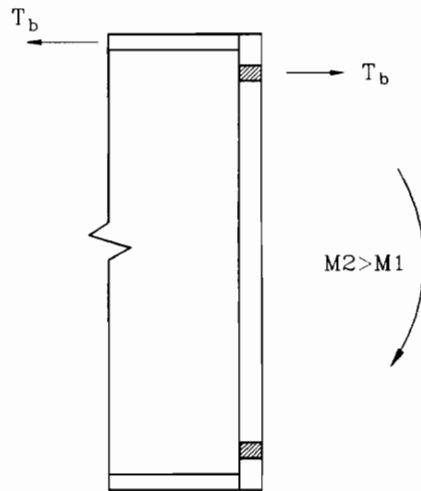
$$M_q = \max \left\{ \begin{array}{l} \sum_{i=1}^{N_i} 2(P_t - Q_{\max})_i d + \sum_{j=1}^{N_j} 2(T_b)_j d \\ \sum_{n=1}^N 2(T_b)_n d \end{array} \right. \quad (3.5)$$

where N_i = the number of load-carrying bolt rows, N_j = the number of non-load-carrying bolt rows, N = the total number of bolt rows, d = the distance from the respective bolt row to the compression flange centerline, and “q” signifies that prying action is included. It is noted, and will be demonstrated later, that the general expression for M_q is not always algebraically correct for all end-plate configurations when summing the moments. Much depends on the assumed placement of the prying force, Q_{\max} , and the distance “a”. Because of the fact that it is impossible to pinpoint the exact location of the prying force,



(a) Zero Applied Load

(b) Applied Load Equivalent to $T_b/2$



(c) Applied Load Equivalent to T_b

Figure 3.5 Effects of Bolt Pretension

and in keeping the design of all end-plate configurations unified, Equation 3.5 has been adopted to predict the ultimate moment of the connection when controlled by bolt force. The maximum possible prying force for an end-plate configuration, Q_{\max} , is calculated using Equation 1.6:

$$Q_{\max} = \frac{w' t_p^2}{4 a} \sqrt{F_{py}^2 - 3 \left(\frac{F'}{w' t_p} \right)^2} \quad (1.6)$$

and F' is:

$$F' = \frac{t_p^2 F_{py} (0.85 b_f / 2 + 0.80 w') + \pi d_b^3 F_{yb} / 8}{4 p_f} \quad (1.7)$$

Kennedy *et al.* (1981) cautioned that, if the quantity under the radical in Equation 1.6 is negative, the end-plate will fail locally in shear before prying forces can be developed, and the connection is inadequate for the applied load. Also, the distance “a” is dependent on whether Q_{\max} is being calculated for an interior bolt or an exterior bolt. For interior bolt calculation and all of those in flush end-plate configurations, a is calculated by Equation 1.9:

$$a_i = 3.682(t_p/d_b)^3 - 0.085 \quad (1.9)$$

When calculating Q_{\max} for an outer bolt, a is the minimum of:

$$a_o = \min \left\{ \begin{array}{l} 3.682(t_p/d_b)^3 - 0.085 \\ p_{\text{ext}} - p_{f,o} \end{array} \right. \quad (3.6)$$

where p_{ext} = the distance from the outer face of the beam tension flange to the edge of the end-plate extension, and $p_{\text{f.o}}$ = the outer pitch distance between the outer face of the beam tension flange and the centerline of the exterior bolt line (Figure 2.5).

The calculations involved in the simplified bolt force analysis are a substantial decrease from those involved in the modified Kennedy analysis used in the previous studies (Srouji *et al.*, 1983a, 1983b; SEI, 1984; Hendrick *et al.*, 1984, 1985; Morrison *et al.*, 1985, 1986; Bond and Murray, 1989; Abel and Murray, 1992b). The need to determine the stage of plate behavior, and hence the need for the complex Equations 1.1, 1.2, and 1.4, is eliminated. Also, the simplified approach eliminates the use of the inconsistent α and β factors which were used to determine the amount of flange force carried by different lines of bolts. The studies of the past, especially those dealing with extended end-plate connections, incorporated α and β factors into the bolt analysis to determine the amount of flange force carried by the outer and inner bolts, respectively (SEI, 1984; Morrison *et al.*, 1985, 1986; Abel and Murray, 1992b). These factors were usually extrapolated from the test results and were inconsistent from one configuration to the next. Because of the assumption that all of the load-carrying bolts can yield, the need for α and β factors in the simplified analysis is eliminated, making it consistent and determinant among all end-plate configurations.

3.2 APPLICATION TO FLUSH MOMENT END-PLATES

Simplified bolt force analysis was performed on the five flush end-plate configurations shown in Figure 1.4. The five configurations are: two-bolt unstiffened,

four-bolt unstiffened, four-bolt stiffened between the tension bolt rows, four-bolt stiffened outside the bolt rows, and six bolt unstiffened. Experimental investigations have been conducted on all five of these configurations. The equations and procedures that follow are supported by the results from these past studies.

3.2.1 Two-Bolt Flush Unstiffened Moment End-Plates

Srouji *et al.* (1983a) performed eight full-scale tests on two-bolt flush unstiffened moment end-plate connections. The model used for the simplified bolt analysis of this configuration was described earlier and is depicted in Figure 3.4. The bolt force versus applied moment plots from Srouji's study indicate that the two tension bolts can both be considered load-carrying bolts. The ultimate moment capacity as controlled by bolt failure was given in Equation 3.4:

$$M_{q_{\max}} = \begin{cases} 2(P_t - Q_{\max})d_1 \\ 2(T_b)d_1 \end{cases} \quad (3.4)$$

where Q_{\max} is calculated from Equation 1.6., and the distance "a" is calculated from Equation 1.9.

3.2.2 Four-Bolt Flush Unstiffened Moment End-Plates

Srouji *et al.* (1983b, 1984) performed six full-scale tests on four-bolt flush unstiffened moment end-plate connections. The model used for the simplified bolt analysis is shown in Figure 3.6. The bolt force versus applied moment plots resulting from Srouji's study indicate that all four of the tension bolts act as load-carrying bolts. The ultimate

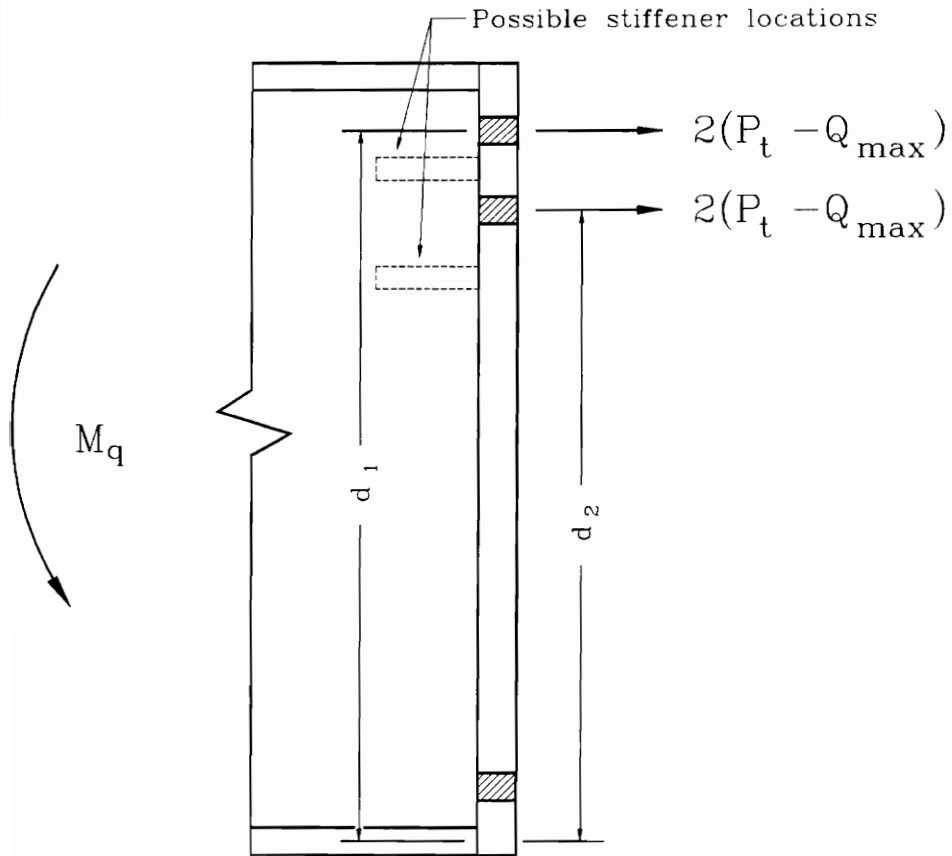


Figure 3.6 Simplified Bolt Force Model for Four-Bolt Flush Unstiffened and Stiffened Moment End-Plates

capacity of the connection for the limit state of bolt rupture is calculated from expanding Equation 3.5:

$$M_q = \max \begin{cases} 2(P_t - Q_{\max})(d_1 + d_2) \\ 2(T_b)(d_1 + d_2) \end{cases} \quad (3.7)$$

where Q_{\max} is calculated from Equation 1.6., and the distance “a” from Equation 1.9. It was noted earlier that the equation for M_q may not demonstrate equilibrium based on the forces in the model of the connection. This is the case when summing the moments of the forces in Figure 3.6. However, as previously discussed, Equation 3.7 accurately predicts the connection capacity and keeps it consistent with other end-plate configurations.

3.2.3 Four-Bolt Flush Stiffened Moment End-Plates

Eight full-scale tests were performed on four-bolt flush stiffened moment end-plate connections by Hendrick et al. (1984). Four of the tests conducted had the stiffener between the tension bolt rows, and four of the tests had the stiffener outside of the tension bolt rows. The simplified bolt analysis model for the four-bolt flush stiffened configuration is the same as that for the four-bolt flush unstiffened configuration depicted in Figure 3.6. In seven of the eight tests in Hendrick’s study, the bolt force versus applied moment plot indicates that all four bolts carry load. The one test in which this is not indicated, instrumentation problems arose in the outer bolts during the test procedure. It is therefore assumed that all four of the tension bolts are load-carrying bolts. Calculation of the ultimate moment is the same as for the four-bolt flush unstiffened configuration:

$$M_{q_{\max}} = \begin{cases} 2(P_t - Q_{\max})(d_1 + d_2) \\ 2(T_b)(d_1 + d_2) \end{cases} \quad (3.7)$$

where Q_{\max} and a are calculated as described above.

3.2.4 Six-Bolt Flush Unstiffened Moment End-Plates

Five full-scale tests were conducted by Bond and Murray (1989) on six-bolt flush unstiffened moment end-plate connections. The analytical bolt model for the six-bolt flush unstiffened configuration is shown in Figure 3.7. There are inconsistencies in the 1989 report regarding whether the middle line of bolts carries any of the applied flange force. Originally, it was stated that, due to the deformed shape of the plate, no prying action in the middle bolt line occurs, as shown in Figure 3.8. Further on, however, prying force in the middle bolts was explained and included in the bolt force calculations. The bolt force versus applied moment plots in the appendices indicate that prying action does exist in the middle line of bolts, and that they carry a slight portion of the applied load. However, to be consistent with the bolt analysis procedures for the multiple row extended 1/3 configurations, yet to be described, it is assumed that the middle line of bolts does not carry any of the applied flange force. This assumption is also justified by earlier statements regarding uncertainty in the placement of prying forces. It is therefore assumed that the two bolts adjacent the beam tension flange and the furthest interior two bolts are load-carrying bolts, and the force in the middle line of bolts is always equal to the minimum pretension. The ultimate moment of the connection controlled by bolt proof load, M_q , is calculated by expanding Equation 3.5 as follows:

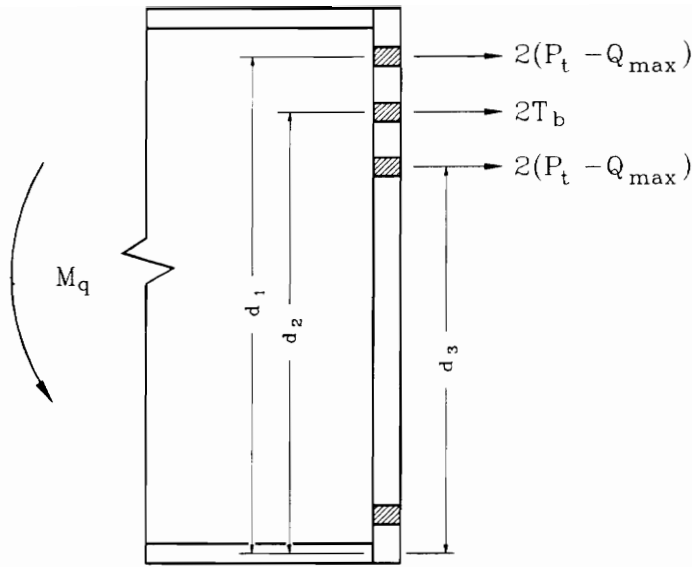


Figure 3.7 Simplified Bolt Force Model for Six-Bolt Flush Unstiffened Moment End-Plates

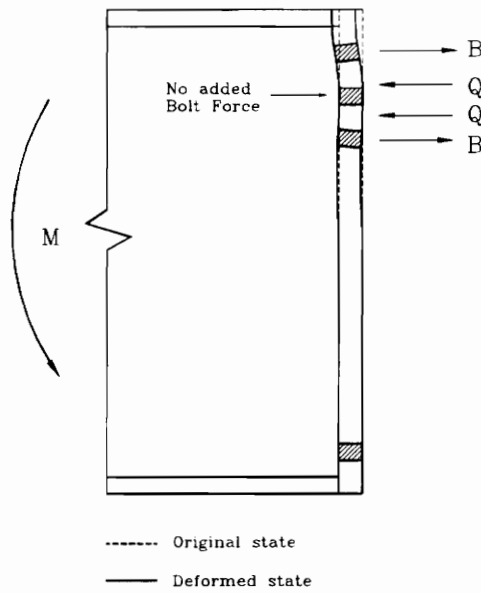


Figure 3.8 Deformed Shape of Multiple Row End-Plates

$$M_{q_{\max}} = \begin{cases} 2(P_t - Q_{\max})(d_1 + d_3) + 2(T_b)d_2 \\ 2(T_b)(d_1 + d_2 + d_3) \end{cases} \quad (3.8)$$

where Q_{\max} is calculated from equation 1.6, and the distance “a” from Equation 1.9.

3.3 APPLICATION TO EXTENDED MOMENT END-PLATES

Ultimate moment predictions based on the simplified bolt analysis of the five extended end-plate connections shown in Figure 1.5 were performed. The five configurations are: four-bolt unstiffened, four-bolt stiffened, multiple row unstiffened 1/2, multiple row unstiffened 1/3, and multiple row stiffened 1/3. Experimental investigations on all five configurations have been conducted in the past. The procedures that follow are supported by the results from these investigations.

3.3.1 Four-Bolt Extended Unstiffened Moment End-Plates

Six tests were conducted on four-bolt extended unstiffened moment end-plate connections. Four of the tests were conducted by Abel and Murray (1992b) and two were conducted by Borgsmiller *et al.* (1995). The two tests conducted by Borgsmiller *et al.* (1995) had large pitch distances between the inner face of the beam tension flange and the first row of interior tension bolts (Figure 1.8(a)). The procedure described herein has been generalized to include such configurations. The simplified bolt force model including prying action is shown in Figure 3.9. It was concluded that all four bolts on the tension side of the connection contribute in carrying the applied load, as observed in the bolt force

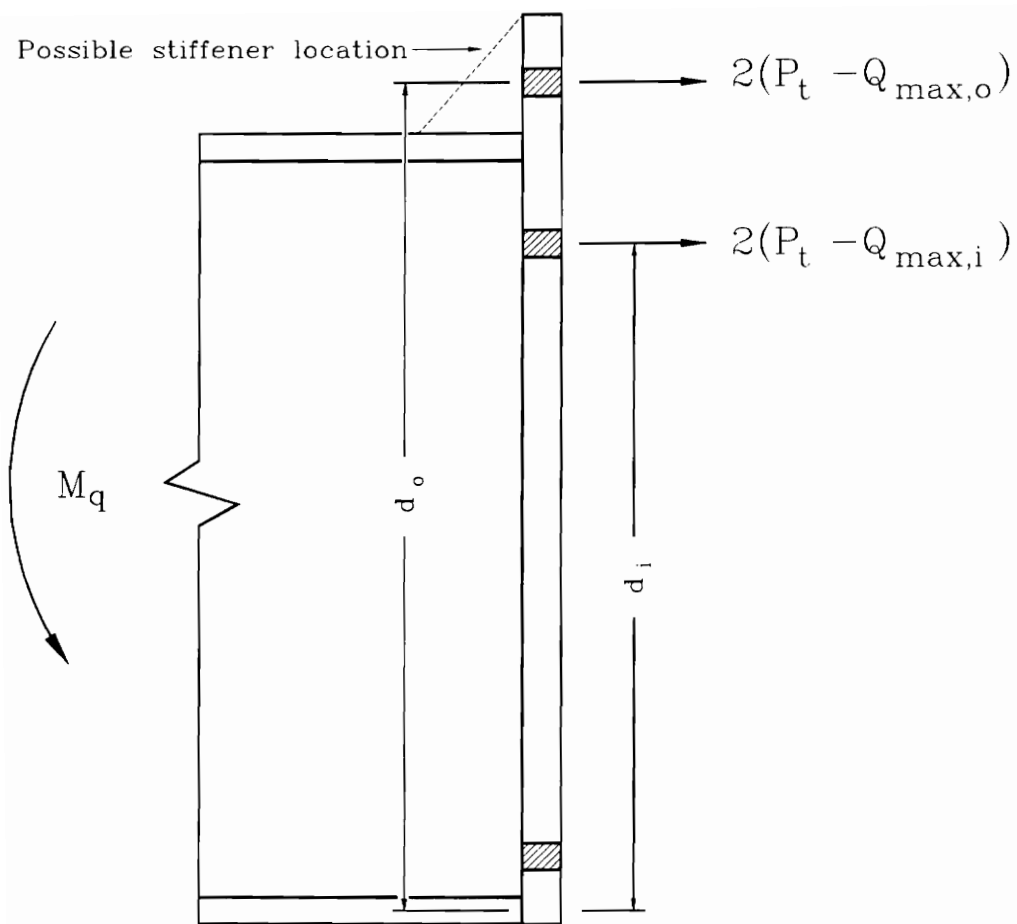


Figure 3.9 Simplified Bolt Force Model for Four-Bolt Extended Unstiffened and Stiffened Moment End-Plates

versus applied moment plots of all six tests. Expanding Equation 3.5 results in the expression for the ultimate connection moment capacity controlled by bolt proof load:

$$M_q = \max \begin{cases} 2(P_t - Q_{\max,o})d_o + 2(P_t - Q_{\max,i})d_i \\ 2(P_t - Q_{\max,o})d_o + 2(T_b)(d_i) \\ 2(P_t - Q_{\max,i})d_i + 2(T_b)(d_o) \\ 2(T_b)(d_o + d_i) \end{cases} \quad (3.9)$$

where $Q_{\max,o}$ and $Q_{\max,i}$ indicate the maximum prying force in the outside and inside bolts, respectively, calculated from Equation 1.6. There are two different F' terms, F'_i and F'_o , in the calculation of the maximum prying force because of the different pitch distances on the inner and outer portions of the end-plate. The expression for computing F' is given in Equation 1.7. The inner pitch distance, $p_{f,i}$, is used in calculating F'_i , and the outer pitch distance, $p_{f,o}$, is used in calculating F'_o . When computing $Q_{\max,o}$, the distance “a” is calculated from Equation 3.6. When computing $Q_{\max,i}$, the distance “a” is calculated from Equation 1.9.

3.3.2 Four-Bolt Extended Stiffened Moment End-Plates

Six full-scale experimental tests were performed by Morrison *et al.* (1985) on the four-bolt extended stiffened moment end-plate configuration. The analytical model for this configuration is the same as that for the four-bolt extended unstiffened configuration just described, and is shown in Figure 3.9. As with the four-bolt extended unstiffened configuration, all four bolts on the tension side of the connection contribute in carrying the

applied load, and the ultimate moment capacity controlled by bolt failure including prying action is:

$$M_q = \max \begin{cases} 2(P_t - Q_{\max,o})d_o + 2(P_t - Q_{\max,i})d_i \\ 2(P_t - Q_{\max,o})d_o + 2(T_b)(d_i) \\ 2(P_t - Q_{\max,i})d_i + 2(T_b)(d_o) \\ 2(T_b)(d_o + d_i) \end{cases} \quad (3.9)$$

The values for $Q_{\max,o}$ and $Q_{\max,i}$, computed from Equation 1.6, are dependent on the values a_o and a_i , calculated from Equations 3.6 and 1.9, respectively.

3.3.3 Multiple Row Extended Unstiffened 1/2 Moment End-Plates

Abel and Murray (1992a) conducted two full-scale tests on the multiple row extended unstiffened 1/2 moment end-plate connection. The analytical model for the simplified bolt analysis is shown in Figure 3.10. The bolt force versus applied moment plot of one of these tests indicates that the far interior line of bolts maintained a bolt force equal to the pretension force throughout the test. The bolt force of this line of bolts was not plotted against the applied moment for the other test. Therefore, it can be concluded that the far interior line of bolts does not carry any of the applied load, and the exterior bolts and the first interior row of bolts are considered load-carrying bolts. The expression for the ultimate capacity of the connection controlled by the limit state of bolt rupture is:

$$M_q = \max \begin{cases} 2(P_t - Q_{\max,o})d_1 + 2(P_t - Q_{\max,i})d_2 + 2(T_b)d_3 \\ 2(P_t - Q_{\max,o})d_1 + 2(T_b)(d_2 + d_3) \\ 2(P_t - Q_{\max,i})d_2 + 2(T_b)(d_1 + d_3) \\ 2(T_b)(d_1 + d_2 + d_3) \end{cases} \quad (3.10)$$

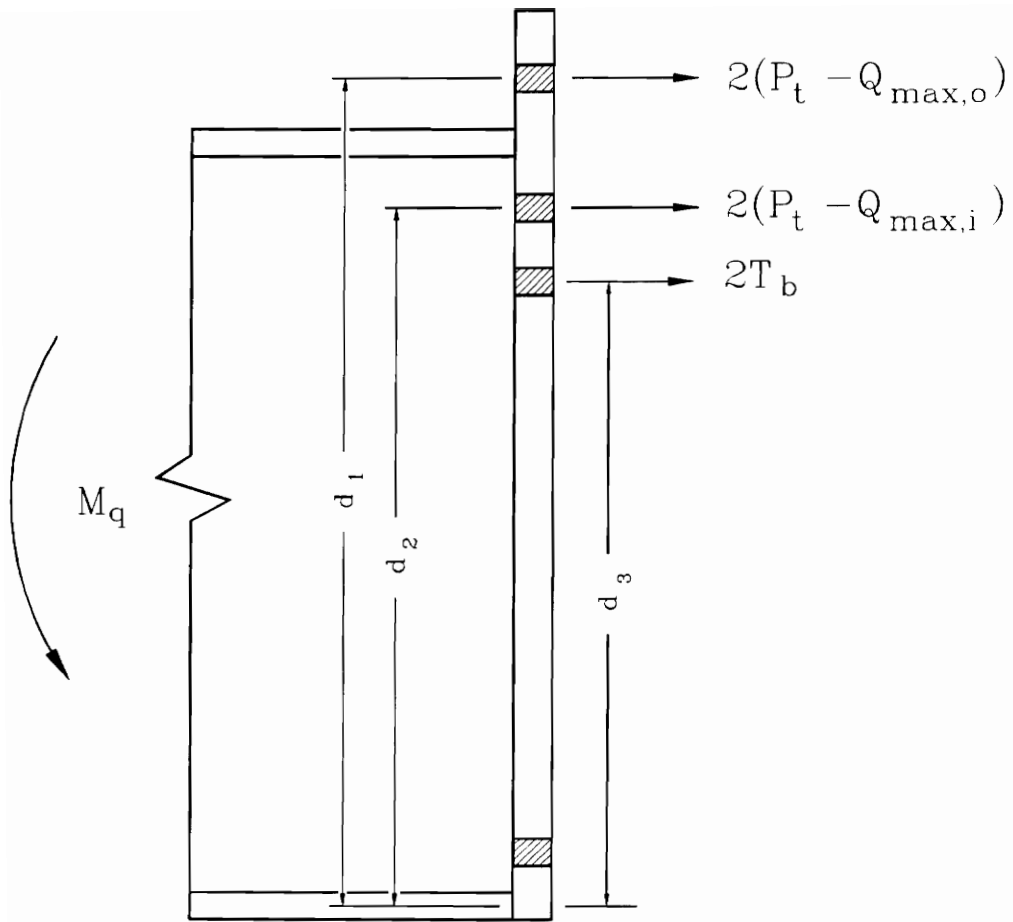


Figure 3.10 Simplified Bolt Force Model for Multiple Row Extended Unstiffened 1/2 Moment End-Plates

where $Q_{\max,o}$ and $Q_{\max,i}$ are calculated from Equation 1.6. The values a_o and a_i in Figure 3.10 are calculated from Equations 3.6 and 1.9, respectively.

3.3.4 Multiple Row Extended Unstiffened 1/3 Moment End-Plates

A total of ten full-scale tests were performed on multiple row extended unstiffened 1/3 moment end-plate connections. One test was conducted by Borgsmiller *et al.* (1995), one test conducted by Rodkey and Murray (1993), six tests conducted by Morrison *et al.* (1986), and two tests conducted by SEI (1984). The tests which were conducted by Borgsmiller *et al.* (1995) and Rodkey and Murray (1993) had large distances between the inner face of the beam tension flange and the first row of interior tension bolts (Figure 1.8(b)). The procedure herein has been generalized to include such configurations. The simplified analytical bolt model is shown in Figure 3.11. The bolt force versus applied moment plots of six of the ten tests indicate that all of the bolts carry a portion of the applied load except for the middle row of interior bolts. In one test, the bolt force of the middle row of interior bolts was not plotted against the applied moment, as the appropriate data was “not available” (Morrison *et al.*, 1986). The deformed shape of the inner portion of the end-plate is similar to that of the six-bolt flush unstiffened configuration shown in Figure 3.8. It was therefore concluded that the load-carrying bolt rows are the exterior, first interior, and far interior lines of bolts. The moment capacity of the connection controlled by bolt rupture is obtained from expanding Equation 3.5:

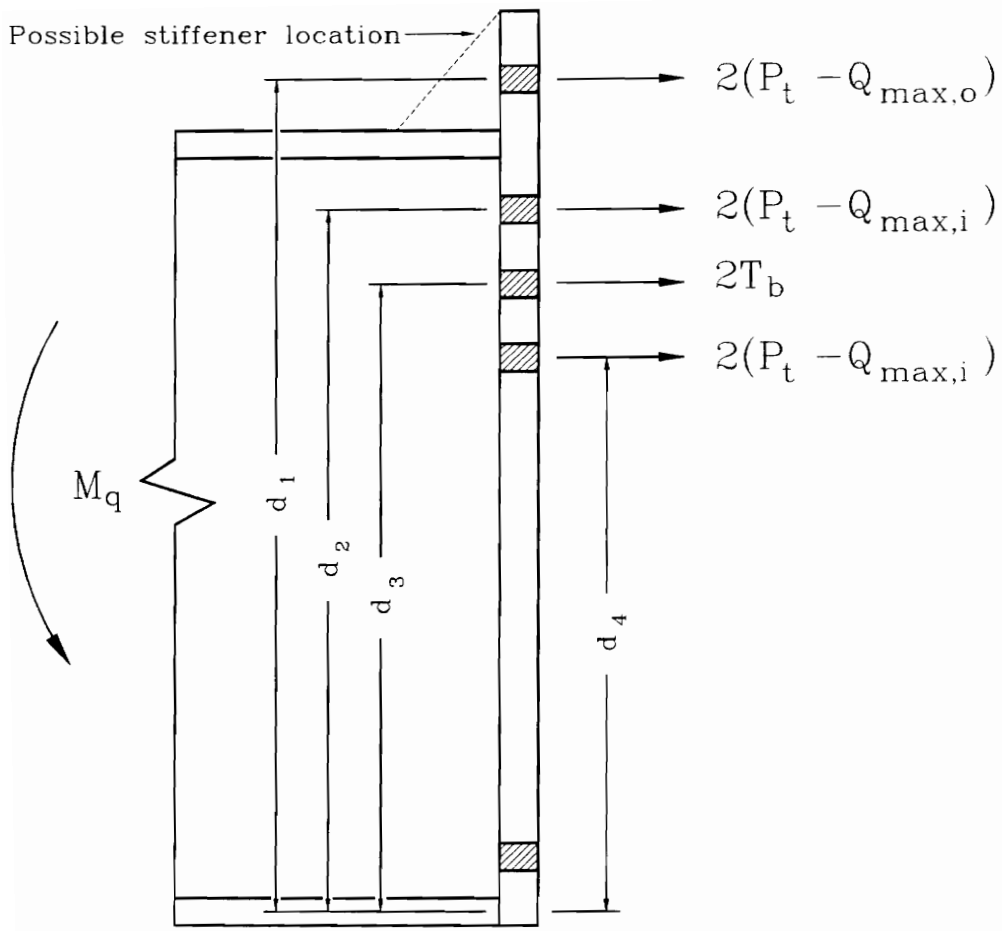


Figure 3.11 Simplified Bolt Force Model for Multiple Row Extended Unstiffened and Stiffened 1/3 Moment End-Plates

$$M_q = \max \begin{cases} 2(P_t - Q_{\max,o})(d_1) + 2(P_t - Q_{\max,i})(d_2 + d_4) + 2(T_b) d_3 \\ 2(P_t - Q_{\max,o})(d_1) + 2(T_b)(d_2 + d_3 + d_4) \\ 2(P_t - Q_{\max,i})(d_2 + d_4) + 2(T_b)(d_1 + d_3) \\ 2(T_b)(d_1 + d_2 + d_3 + d_4) \end{cases} \quad (3.11)$$

where $Q_{\max,o}$ and $Q_{\max,i}$ are calculated from Equation 1.6. Two different values of F' are used in the prying force calculations. F'_i is used in calculating $Q_{\max,i}$ with the large inner pitch distance, $p_{f,i}$, and F'_o is used in calculating $Q_{\max,o}$ with the outer pitch distance, $p_{f,o}$. Both F'_i and F'_o are calculated from Equation 1.7. The values a_o and a_i in Figure 3.11 are calculated from Equations 3.6 and 1.9, respectively.

3.3.5 Multiple Row Extended Stiffened 1/3 Moment End-Plates

One test was performed by SEI (1984) on a multiple row extended stiffened 1/3 moment end-plate connection. The simplified analytical bolt model is the same as for the multiple row extended unstiffened 1/3 configuration just described, and is shown in Figure 3.11. The bolt force versus applied moment plots for this test were limited, so it was assumed that the load-carrying bolts for this configuration are the same as those for the multiple row extended unstiffened 1/3 configuration: exterior line, first interior line, and far interior line. The maximum possible applied moment before the load-carrying bolt forces reach their proof load is calculated the same as for the previous configuration:

$$M_q = \max \begin{cases} 2(P_t - Q_{\max,o})(d_1) + 2(P_t - Q_{\max,i})(d_2 + d_4) + 2(T_b) d_3 \\ 2(P_t - Q_{\max,o})(d_1) + 2(T_b)(d_2 + d_3 + d_4) \\ 2(P_t - Q_{\max,i})(d_2 + d_4) + 2(T_b)(d_1 + d_3) \\ 2(T_b)(d_1 + d_2 + d_3 + d_4) \end{cases} \quad (3.11)$$

$Q_{\max,o}$ and $Q_{\max,i}$ are calculated from Equation 1.6, and the values a_o and a_i in Figure 3.11 are obtained as described above.

CHAPTER IV

COMPARISON OF EXPERIMENTAL RESULTS AND PREDICTIONS

4.1 PREVIOUS EXPERIMENTAL RESULTS

Appendices B through J contain the geometric parameters and calculations for the 52 end-plate connections tested in the past (Srouji *et al.*, 1983a, 1983b, 1984; SEI, 1984; Hendrick *et al.*, 1984, 1985; Morrison *et al.*, 1985, 1986; Bond and Murray, 1989; Abel and Murray, 1992a, 1992b; Rodkey and Murray, 1993; Borgsmiller *et al.*, 1995). The test designations in the appendices follow the following format:

$$XX - d_b - t_p - h$$

where d_b = nominal bolt diameter, t_p = end-plate thickness, h = beam depth, and the "XX" is the configuration identification, defined for each as:

F1 =	two-bolt flush unstiffened (one row of tension bolts)
F2 =	four-bolt flush unstiffened (two rows of tension bolts)
FB2 =	four-bolt flush stiffened between the two tension bolt rows
FO2 =	four-bolt flush stiffened outside the two tension bolt rows
MRF =	six-bolt, multiple row flush unstiffened (three rows of tension bolts)
EF _y =	four-bolt extended unstiffened, F _y refers to nominal plate yield stress

- ES = four-bolt extended stiffened
- MRE1/2 = multiple row extended unstiffened, 1 exterior tension bolt row, 2 interior tension bolt rows
- MRE1/3 = multiple row extended unstiffened, 1 exterior tension bolt row, 3 interior tension bolt rows
- MRES1/3 = multiple row extended stiffened, 1 exterior tension bolt row, 3 interior tension bolt rows

The yield strength of the connection end-plate material, F_{py} , shown in the appendices was determined by standard ASTM coupon tests. All bolts were A325 with a nominal tensile strength, F_{yb} , equal to 90 ksi, as specified in Table J3.2, AISC (1986). In the tests conducted by Abel and Murray (1992b), the strength of the A325 bolts was measured by tensile tests conducted in a universal testing machine. Also shown in Appendices B through J are the appropriate yield-line mechanisms and simplified bolt force models for each end-plate configuration.

All tests were splice moment connections under pure moment, as shown in Figure 4.1. The test beam was simply supported and loaded with two equal concentrated loads symmetrically placed. Load was applied by a hydraulic ram via a load cell and spreader beam, as shown in Figure 4.2. Lateral support for both the test specimen and the spreader beam was provided by lateral brace mechanisms bolted to steel wide flange frames anchored to the laboratory reaction floor.

To compare the experimental results to the predicted strength of the connections, it was necessary to determine the experimental failure load of each test. Depending on the shape of the applied moment versus end-plate separation plot from the experimental tests,

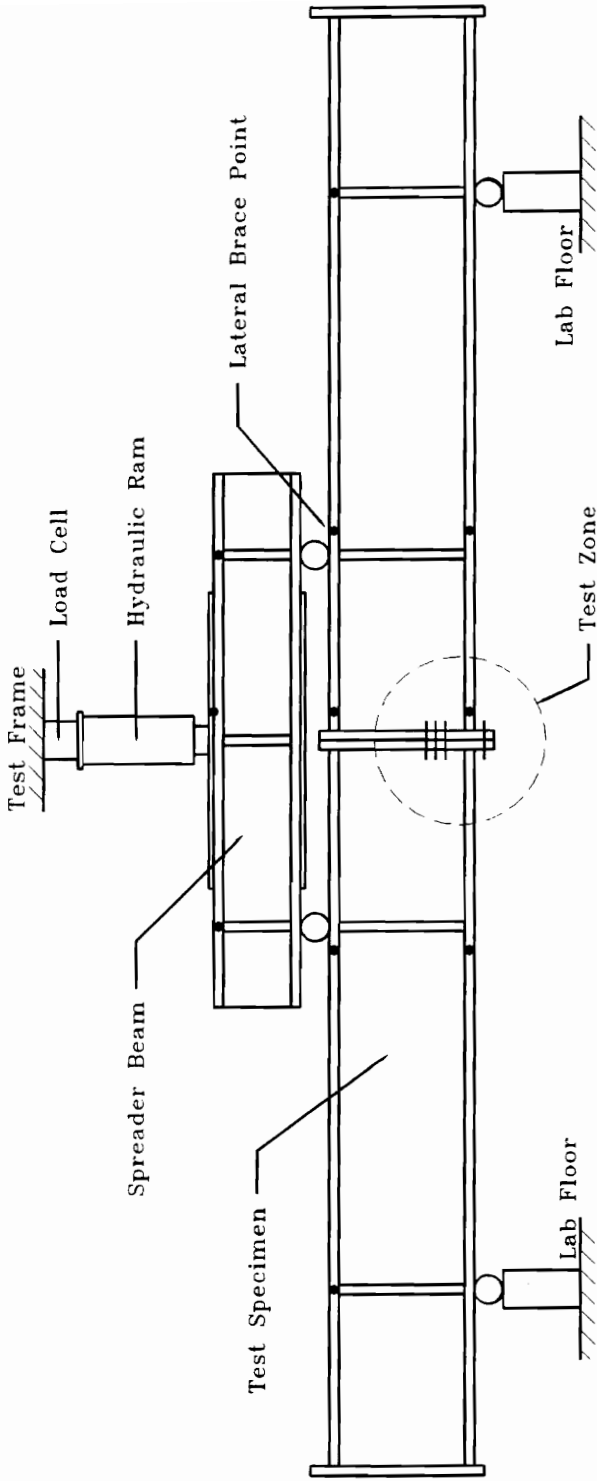


Figure 4.1 Longitudinal Elevation of Laboratory Test Setup

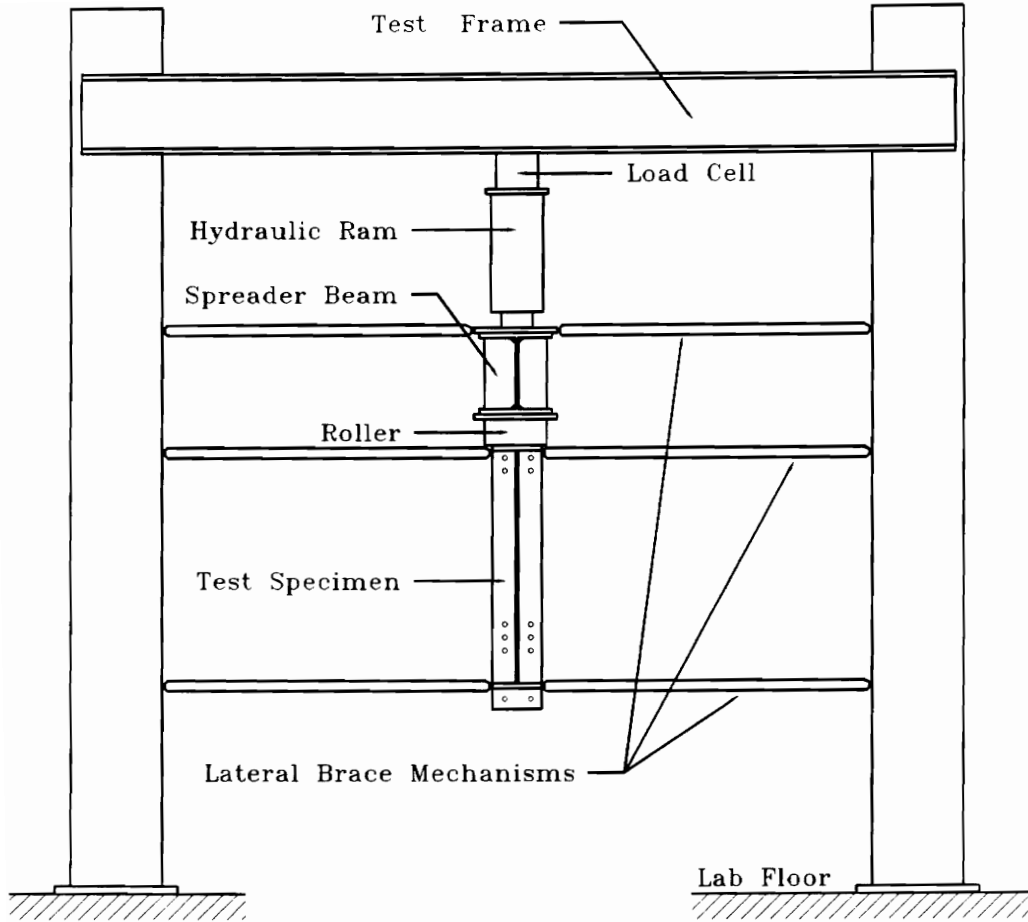


Figure 4.2 Cross-section of Laboratory Test Setup

one of two different failure loads was identified, M_u or M_y . Applied moment versus end-plate separation plots came as a result of placing measuring devices on the end-plates at or near the beam tension flange during the test procedure. These plots are an indication as to whether or not the end-plate yields. If the plot has a nearly horizontal yield plateau, such as Plot A in Figure 4.3, the failure load of the specimen is taken as the maximum applied load in the test, M_u . From a design standpoint, this is acceptable since the maximum applied load in the test closely correlates to the point at which the connection yields. A connection displaying this behavior is in relatively little danger of experiencing excessive deformations under service loads. Plot B in Figure 4.3 shows a curve with no distinct yield point and a sloped yield plateau. Connections displaying this type of applied moment versus end-plate separation behavior would experience large deformations under working loads if the design failure load were assumed to be the maximum applied moment in the test. Therefore, the failure load is determined to be near the point at which the connection yields, M_y . This experimental yield moment is established by dividing the applied moment versus end-plate separation plot into two linear segments which intersect at the yield moment, as shown in Figure 4.4.

The maximum applied moment, M_u , and experimental yield moment, M_y , for each of the 52 tests were determined and can be found in Appendices B through J. It was necessary to establish a numerical threshold for distinguishing which value, M_u or M_y , to use for the experimental failure load, M_{fail} . In some cases, it was difficult to determine whether some of the applied moment versus plate separation plots displayed the behavior

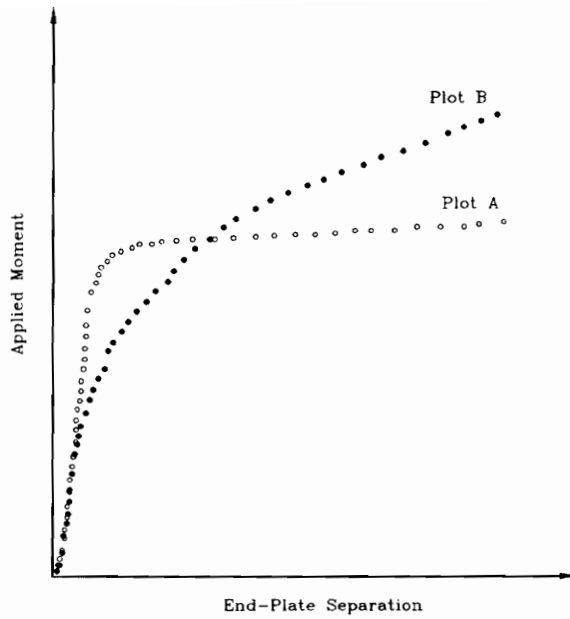


Figure 4.3 Sample of Applied Moment vs. End-Plate Separation Plots

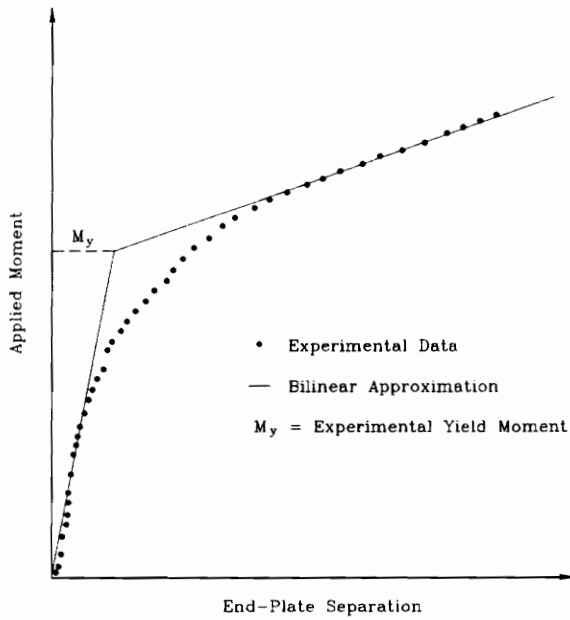


Figure 4.4 Determination of Experimental Yield Moment

of Plot A or Plot B in Figure 4.3. This threshold was empirically established through the ratio of M_y to M_u , and is expressed as follows:

$$M_{fail} = M_y \quad \text{if } M_y/M_u < 0.75 \quad (4.1)$$

$$M_{fail} = M_u \quad \text{if } M_y/M_u > 0.75 \quad (4.2)$$

It should be noted that this threshold is an approximate one, and that if the M_y/M_u ratio is approximately equal to 0.75, +/- 0.02, either value, M_y or M_u , can be taken as the experimental failure load. The values corresponding to the appropriate experimental failure load of each test are shown shaded in the appendices.

4.2 DETERMINATION OF THE PREDICTED CONNECTION STRENGTH

Prediction of the ultimate strength of moment end-plate connections was presented for two limit states. Chapter II described the prediction of the ultimate strength for the limit state of plate yielding, M_{pl} , using yield-line theory. Chapter III described the prediction of the connection strength for the limit state of bolt fracture including prying action, M_q , using a simplified version of the Kennedy method. Appendices B through J show the calculations of M_{pl} and M_q for each of the connections tested. Notice that the asterisk (*) next to Q_{max} in the appendices indicates that $(P_t - Q_{max}) < T_b$, which plays a crucial role in the calculation of M_q .

Once the connection strength predictions for the end-plate yield and bolt rupture limit states have been calculated, a final, controlling connection strength prediction, M_{pred} , must be chosen. To do so, an important assumption is necessary: the end-plate must sufficiently yield in order for prying action to occur in the bolts. If the end-plate does not

substantially deform out of its original state, there can be no points of application for prying forces (Figure 3.1). This concept was originally introduced by Kennedy *et al.* (1981), as they presented the three stages of plate behavior caused by increasing load. The circumstance initiating the different stages of plate behavior is the formation of plastic hinges, or end-plate yielding.

The outcome of this assumption is the concept of a “prying action threshold.” Until this threshold is reached, the plate behaves as a thick plate, and no prying action takes place in the bolts. Beyond the threshold, maximum prying action occurs in the bolts due to the sufficient deformation of the plate. The prying action threshold is taken as 90% of the full strength of the plate as determined by yield-line analysis, or $0.90M_{pl}$. Thorough review of the past experimental data lead to the conclusion that the plate begins deforming out of its original state at approximately 80% of the full strength of the plate, or $0.80M_{pl}$. However, to assume maximum prying action in the bolts at the point at which yielding in the plates commences would be unreasonably conservative. Therefore, it was assumed that the plate has deformed sufficiently at 90% of the plate strength to warrant the use of maximum prying action in the bolts. The predicted strength of the connection is controlled by the following guidelines:

$$\text{If applied moment} < 0.90M_{pl} \quad \text{thick plate behavior} \quad (4.3)$$

$$\text{If applied moment} > 0.90M_{pl} \quad \text{thin plate behavior} \quad (4.4)$$

If the plate behaves as a thick plate, no prying action is considered in the bolts. Calculation of the connection strength for the limit state of bolt rupture with no prying

action, M_{np} , follows the same philosophy outlined in Chapter III, except Q_{max} is set equal to zero and all of the bolts in the connection are assumed to carry load. The connection strength for the limit state of bolt rupture with no prying action is therefore calculated from a revised version of Equation 3.5:

$$M_{np} = \sum_{i=1}^N 2(P_t)_i d_i \quad (4.5)$$

where N = the number of bolt rows, d_i = the distance from the respective bolt row to the compression flange centerline, and “np” signifies that no prying action is included.

Once M_{np} , M_q , and M_{pl} are known, the controlling prediction of the connection strength, M_{pred} , can be determined. As mentioned earlier, the prying action threshold has been identified as 90% of the plate strength, or $0.90M_{pl}$. If the strength for the limit state of bolt rupture with no prying action, M_{np} , is less than the prying action threshold, the connection will fail by bolt rupture before the plate can yield and before prying action can take place in the bolts, a “thick” plate failure. If the strength for the limit state of bolt rupture with no prying action, M_{np} , is greater than the prying action threshold, prying action takes place in the bolts, because the plate yields before the bolts rupture. If the strength for the limit state of bolt rupture with prying action, M_q , is less than the strength of the plate, M_{pl} , the connection will fail by means of bolt rupture with prying action before the plate can fully yield. However, if M_q is greater than M_{pl} , the connection will fail by plate yielding. In summary:

$$M_{pred} = M_{np} \quad \text{if } M_{np} < 0.90M_{pl} \quad (4.6)$$

$$M_{pred} = M_q \quad \text{if } 0.90M_{pl} \leq M_{np} \text{ and } M_q \leq M_{pl} \quad (4.7)$$

$$M_{\text{pred}} = M_{\text{pl}} \quad \text{if } M_{\text{pl}} < M_{\text{q}} \quad (4.8)$$

The final predicted strength of each of the 52 tests is shown in Appendices B through J. Comparison of the experimental results to the predictions is necessary to verify the simplified approach.

4.3 FLUSH MOMENT END-PLATE COMPARISONS

The predicted and experimental results for the flush moment end-plate connection tests are listed in Table 4.1. Twenty-seven tests, comprising four different configurations, were examined. Included in the table are M_{q} , M_{pl} , $0.90M_{\text{pl}}$, M_{np} , M_{pred} , M_{y} , and M_{u} . Note that in the cases where $M_{\text{pl}} < M_{\text{q}}$, it was not necessary to calculate either $0.90M_{\text{pl}}$ or M_{np} as the connection strength was controlled by M_{pl} , thus the dashes in the columns containing $0.90M_{\text{pl}}$ and M_{np} . Also in the table are design ratios, comparing M_{pred} to M_{y} and M_{u} . A design ratio smaller than 1.0 is conservative, and one larger than 1.0 is unconservative. The shaded values are the ratios corresponding to the applicable failure load, determined by the M_{y} to M_{u} ratio as described above. If $M_{\text{y}}/M_{\text{u}} < 0.75$, the applicable design ratio is $M_{\text{pred}}/M_{\text{y}}$; if $M_{\text{y}}/M_{\text{u}} > 0.75$, the applicable design ratio is $M_{\text{pred}}/M_{\text{u}}$. The appropriate design ratios are shown shaded in the appendices as well. In all but five of the flush end-plate tests, the experimental failure load was designated as the maximum applied load in the test, and the applicable design ratio is $M_{\text{pred}}/M_{\text{u}}$. This indicates that the applied moment versus end-plate separation curve for most flush configurations resembles Plot A in Figure 4.3.

Table 4.1 Flush Moment End-Plate Predicted and Experimental Results

	TEST ⁽¹⁾	Moments (k-ft)						Design ratios ⁽⁶⁾			
		M_q	M_{pl}	$0.90M_{pl}$	M_{ap}	M_{pred} ⁽²⁾	M_y ⁽³⁾	M_u ⁽⁴⁾	M_y/M_u ⁽⁵⁾	M_{pred}/M_y	M_{pred}/M_u
2-Bolt Flush Unstiff.	Strouji <i>et al.</i> (1983a)	77.2	92.0	82.8	93.6	77.2	75	97.5	0.77	1.03	0.79
	Strouji <i>et al.</i> (1983a)	67.2	56.7	—	—	56.7	47	57	0.82	1.21	0.99
	Strouji <i>et al.</i> (1983a)	53.8	82.6	74.4	63.3	63.3	60	75	0.80	1.05	0.84
	Strouji <i>et al.</i> (1983a)	51.3	62.0	55.8	65.6	51.3	55	63	0.87	0.93	0.81
	Strouji <i>et al.</i> (1983a)	33.0	51.6	46.4	37.4	37.4	32	39.47	0.81	1.17	0.95
	Strouji <i>et al.</i> (1983a)	32.7	32.8	29.5	38.7	32.7	25	33.92	0.74	1.31	0.96
	Strouji <i>et al.</i> (1983a)	118.1	147.6	132.8	145.0	118.1	110	120.25	0.91	1.07	0.98
	Strouji <i>et al.</i> (1983a)	120.8	165.9	149.3	147.4	147.4	125	154.2	0.81	1.18	0.96
	Strouji <i>et al.</i> (1983b, 1984)	94.1	131.5	118.3	112.7	112.7	85	108	0.79	1.33	1.04
	Strouji <i>et al.</i> (1983b, 1984)	89.1	81.4	—	—	81.4	85	85.5	0.99	0.96	0.95
4-Bolt Flush Unstiff.	Strouji <i>et al.</i> (1983b, 1984)	222.6	177.3	—	—	177.3	140	171.8	0.81	1.27	1.03
	Strouji <i>et al.</i> (1983b, 1984)	193.7	136.4	—	—	136.4	110	144.7	0.76	1.24	0.94
	Strouji <i>et al.</i> (1983b, 1984)	138.0	112.2	—	—	112.2	85	115.5	0.74	1.32	0.97
	Strouji <i>et al.</i> (1983b, 1984)	118.2	68.8	—	—	68.8	62	73.2	0.85	1.11	0.94
	Hendrick <i>et al.</i> (1984, 1985)	122.6	96.9	—	—	96.9	85	92.8	0.92	1.14	1.04
	Hendrick <i>et al.</i> (1984, 1985)	122.6	74.9	—	—	74.9	74	74.4	0.99	1.01	1.01
	Hendrick <i>et al.</i> (1984, 1985)	196.1	139.9	—	—	139.9	146	146.2	1.00	0.96	0.96
	Hendrick <i>et al.</i> (1984, 1985)	196.1	107.6	—	—	107.6	110	120.2	0.92	0.98	0.89
	Hendrick <i>et al.</i> (1984, 1985)	92.7	112.3	101.1	118.5	92.7	108	108.4	1.00	0.86	0.86
	Hendrick <i>et al.</i> (1984, 1985)	95.9	82.2	—	—	82.2	85	85	1.00	0.97	0.97
4-Bolt Flush Stiff.	Hendrick <i>et al.</i> (1984, 1985)	212.0	240.8	216.7	252.6	212.0	250	254	0.98	0.85	0.83
	Hendrick <i>et al.</i> (1984, 1985)	212.0	183.2	—	—	183.2	200	207	0.97	0.92	0.89
	Bond and Murray (1989)	456.4	174.1	—	—	174.1	185	365	0.51	0.94	0.48
	Bond and Murray (1989)	588.3	310.3	—	—	310.3	280	399	0.70	1.11	0.78
	Bond and Murray (1989)	431.9	211.2	—	—	211.2	220	365	0.60	0.96	0.58
	Bond and Murray (1989)	649.3	362.6	—	—	362.6	355	459	0.77	1.02	0.79
	Bond and Murray (1989)	641.0	358.0	—	—	358.0	355	379	0.94	1.01	0.94

1 - Test designation: XX- ϕ_p -4-p-h

2 - If $M_{ap} < 0.90M_{pl}$, $M_{pred} = M_{ap}$; If $0.90M_{pl} < M_{ap}$ and $M_q < M_{pl}$, $M_{pred} = M_q$; If $M_{pl} < M_{ap}$, $M_{pred} = M_{pl}$

3 - M_y was determined from the plot of applied moment vs. end-plate separation via two intersecting lines. (see Chapter IV for details)

4 - M_u = the maximum applied moment in the test.

5 - If $M_y/M_u < 0.75$ (+/- 0.02) use M_{pred}/M_y ratio; if $M_y/M_u > 0.75$ (+/- 0.02) use M_{pred}/M_u ratio. Values to be used are shown shaded. (see Chapter IV for details)

6 - If Design ratio > 1.0 , prediction is unconservative; if Design ratio < 1.0 , prediction is conservative

Eight tests were conducted by Srouji *et al.* (1983a) on the two-bolt unstiffened configuration. Design ratios varied from 0.81 to 1.03 and were, with one exception, calculated by M_{pred}/M_y . It can be concluded that the predictions are conservative, but correspond well with the experimental results for two-bolt flush unstiffened end-plate configurations.

Six tests were conducted by Srouji *et al.* (1983b, 1984) on four-bolt unstiffened end-plate configurations. Design ratios varied from 0.94 to 1.04, indicating that the simplified approach adequately predicts the behavior of this configuration.

Four-bolt flush stiffened tests were performed by Hendrick *et al.* (1984, 1985). Four tests were stiffened between the tension bolt rows and four tests were stiffened outside the tension bolt rows. Design ratios varied from 0.83 to 1.04, indicating that, even though slightly conservative, the predictions correlate well with the experimental results of this configuration.

Finally, five tests were conducted by Bond and Murray (1989) on six-bolt flush unstiffened end-plate configurations. In four of the tests, the failure load was designated as the yield moment, M_y , due to a small M_y/M_u ratio. The other test had a designated failure load equal to the maximum applied moment. Design ratios varied from 0.94 to 1.11 indicating that the predictions are slightly unconservative, but still correlate well with the experimental results.

4.4 EXTENDED MOMENT END-PLATE COMPARISONS

The predicted and experimental results for the extended moment end-plate connection tests are listed in Table 4.2. Twenty-five tests, comprising five extended end-plate configurations, were studied. As with the flush end-plate tests, design ratios were computed. The appropriate design ratios, based on the value of M_y/M_u , are shown shaded in the table. In fourteen of the tests, the design ratio was controlled by M_u , and in eleven tests, the design ratio was controlled by M_y . This indicates that, unlike flush end-plate configurations, extended end-plates have a tendency to display either type of behavior shown in Figure 4.3.

Six Four-bolt unstiffened tests were performed by Abel and Murray (1992b) and Borgsmiller *et al.* (1995). The design ratios for five of the six tests varied from 0.80 to 1.07; one test had a design ratio of 1.37. The predicted failure moment for the latter test was controlled by the plate, M_{pl} . Such was the case when Abel and Murray (1992b) analyzed the connection using the unification procedures of past studies. In other words, for this particular test, the simplified approach results in an identical prediction to that of the unified approach. It is also noted that the design ratio comparing M_{pred} to M_u for this test is equal to 0.93. Aside from the one test, the results are somewhat conservative, but compare well with the experimental results.

Six tests were conducted by Morrison *et al.* (1985) on the four-bolt stiffened configuration. Design ratios varied from 0.85 to 1.35, indicating some scatter in the results. However, as was just noted with Abel and Murray (1992b), the prediction of the

Table 4.2 Extended Moment End-Plate Predicted and Experimental Results

	TEST ⁽¹⁾	Moments (k-ft)						M_p/M_u ⁽⁵⁾	Design ratios ⁽⁶⁾		
		M_q	M_{pl}	$0.90M_{pl}$	M_{pr}	M_{pred} ⁽²⁾	M_u ⁽³⁾		M_u ⁽⁴⁾	M_{pred}/M_y	M_{pred}/M_u
4-Bolt Extended Unstiff.	Abel and Murray (1992b)	193.0	398.3	358.5	267.6	267.6	250	259.7	0.96	1.07	1.03
	Abel and Murray (1992b)	195.8	529.4	476.5	267.6	267.6	275	275.1	1.00	0.97	0.97
	Abel and Murray (1992b)	403.5	314.7	—	—	314.7	230	337.8	0.68	1.37	0.93
	Abel and Murray (1992b)	516.9	375.0	—	—	375.0	350	503	0.70	1.07	0.75
	Borgsmiller <i>et al.</i> (1995)	75.2	80.3	72.2	88.5	75.2	70	84.9	0.82	1.07	0.89
	Borgsmiller <i>et al.</i> (1995)	1142.3	1405.2	1264.7	1450.4	1142.3	1350	1423	0.95	0.85	0.80
4-Bolt Extended Stiff.	Morrison <i>et al.</i> (1985)	112.2	108.4	—	—	108.4	80	114.9	0.70	1.35	0.94
	Morrison <i>et al.</i> (1985)	169.3	167.9	—	—	167.9	130	163.4	0.80	1.29	1.03
	Morrison <i>et al.</i> (1985)	199.6	208.7	187.8	257.9	199.6	180	235.1	0.77	1.11	0.85
	Morrison <i>et al.</i> (1985)	212.3	163.3	—	—	163.3	150	203	0.74	1.09	0.80
	Morrison <i>et al.</i> (1985)	400.6	249.8	—	—	249.8	260	349.5	0.74	0.96	0.71
	Morrison <i>et al.</i> (1985)	417.7	364.5	—	—	364.5	280	379.4	0.74	1.30	0.96
Multiple Row Extended	Abel and Murray (1992a)	368.8	802.9	722.7	481.6	481.6	370	372.1	0.99	1.30	1.29
	Abel and Murray (1992a)	348.2	179.0	—	—	179.0	210	309.2	0.68	0.85	0.58
	Borgsmiller <i>et al.</i> (1995)	2081.7	1810.4	—	—	1810.4	1870	1870	1.00	0.97	0.97
	Morrison <i>et al.</i> (1986)	505.5	258.9	—	—	258.9	270	404.9	0.67	0.96	0.64
	Morrison <i>et al.</i> (1986)	900.5	325.6	—	—	325.6	300	425.1	0.71	1.09	0.77
	Morrison <i>et al.</i> (1986)	1114.5	570.0	—	—	570.0	520	866.1	0.60	1.10	0.66
	Morrison <i>et al.</i> (1986)	1727.4	966.7	—	—	966.7	975	975.1	1.00	0.99	0.99
	Morrison <i>et al.</i> (1986)	2697.8	1166.5	—	—	1166.5	1200	1635	0.73	0.97	0.71
	Morrison <i>et al.</i> (1986)	3846.0	1601.6	—	—	1601.6	1600	2329.6	0.69	1.00	0.69
	Rodkey and Murray (1993)	600.0	760.1	684.1	783.7	600.0	690	692.5	1.00	0.87	0.87
	SEI (1984)	1089.7	923.2	—	—	923.2	750	929	0.81	1.23	0.99
	SEI (1984)	2050.7	1896.3	—	—	1896.3	1250	1364	0.92	1.52	1.39
	SEI (1984)	2050.7	2311.0	2079.9	2718.5	2050.7	1600	1834	0.87	1.28	1.12

¹ -- Test designation: XX-d_b-p-h

² -- If $M_{pr} < 0.90M_{pl}$, $M_{pred} = M_{pr}$; if $0.90M_{pl} < M_{pr}$ and $M_u < M_{pl}$, $M_{pred} = M_{pr}$; if $M_{pl} < M_{pr}$, $M_{pred} = M_{pl}$

³ -- M_u was determined from the plot of applied moment vs. end-plate separation via two intersecting lines. (see Chapter IV for details)

⁴ -- M_u = the maximum applied moment in the test.

⁵ -- If $M_p/M_u < 0.75$ (+/- 0.02) use M_{pred}/M_y ratio; if $M_p/M_u > 0.75$ (+/- 0.02) use M_{pred}/M_u ratio. Values to be used are shown shaded. (see Chapter IV for details)

⁶ -- If Design ratio > 1.0 , prediction is unconservative; if Design ratio < 1.0 , prediction is conservative

test having a design ratio equal to 1.35 was controlled by M_{pl} , meaning the result of this study was identical to that in Morrison *et al.* (1985). It is also noted that the design ratio of M_{pred}/M_u for this test was 0.94. Aside from the one test, the predictions from the simplified approach compare well with the experimental results.

Two tests were performed by Abel and Murray (1992a) on the multiple row extended unstiffened 1/2 end-plate configuration. The design ratios from these tests were 0.85 and 1.29, indicating that there is some scatter in the results. Due to the limited testing done on this configuration, it is difficult to determine a conclusion as to the accuracy of the simplified prediction method.

Ten multiple row unstiffened 1/3 connections were tested: one by Borgsmiller *et al.* (1995), six by Morrison *et al.* (1986), one by Rodkey and Murray (1993), and two by SEI (1984). Design ratios from these ten tests ranged from 0.87 to 1.39, indicating scatter in these results. However, aside from the value equal to 1.39, the other nine test design ratios vary from 0.87 to 1.10. The test that produced a design ratio of 1.39 was conducted by SEI (1984), who said, “the yield-line prediction of the failure load [is] not close since the failure was due to large bolt forces and the full strength of the plate was not reached.” This confusing statement would lead to the conclusion that bolt prying action can occur prior to plate bending. However, due to the overwhelming evidence against this statement, it can be concluded that, with the exception of the one test, the simplified procedure accurately predicts the failure load of multiple row extended 1/3 end-plate configurations.

One test was conducted by SEI (1984) on a multiple row extended stiffened 1/3 end-plate connection. The design ratio is 1.12, indicating slightly unconservative results for the limited experimental data.

CHAPTER V

SUMMARY, CONCLUSIONS AND RECOMMENDATIONS

5.1 SUMMARY

This study has introduced a simplified method for the design of moment end-plate connections. The new method calculates the ultimate strength of the connection based on two limit states: end-plate yielding and bolt rupture. Yield-line theory was used for determining the connection strength based on end-plate yielding, and a simplified version of the Kennedy method was used for determining the connection strength as controlled by the bolts with or without prying action. The bolt calculations were reduced substantially from those in the modified Kennedy method, for only the computation of a maximum prying force, Q_{\max} , is involved. A primary assumption in this approach is that the end-plate must substantially yield in order to produce prying forces in the bolts; if the plate is strong enough, no prying action occurs and the bolts are loaded in direct tension.

The simplified approach was used to predict the failure moments of 52 connections, comprising nine different configurations. The predictions were compared to the experimental results from past tests for verification. The nine configurations are:

Flush Configurations

- two-bolt unstiffened
- four-bolt unstiffened
- four-bolt stiffened
- six-bolt unstiffened

Extended Configurations

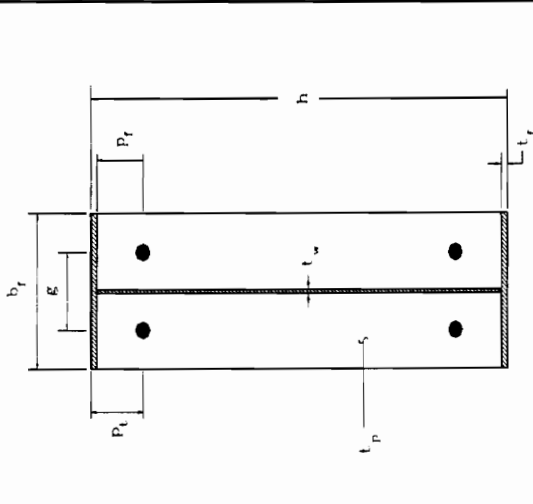
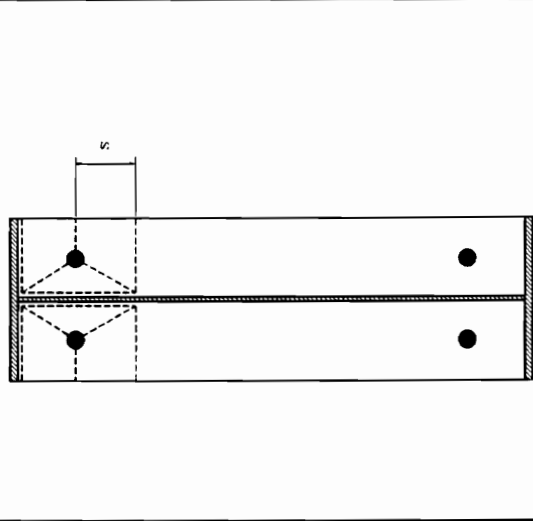
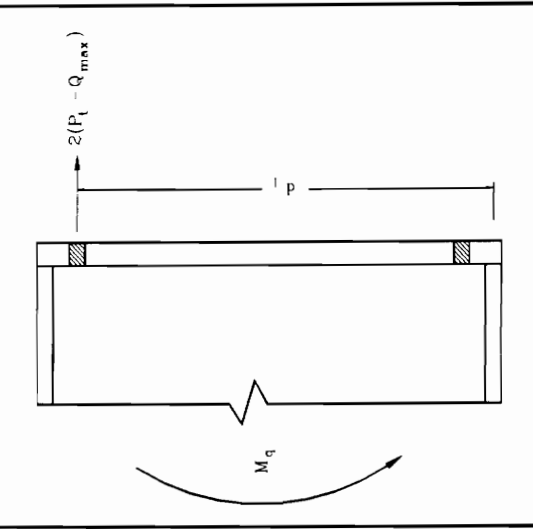
- four-bolt unstiffened
- four-bolt stiffened
- multiple row unstiffened 1/2
- multiple row unstiffened 1/3
- multiple row stiffened 1/3

Tables 5.1 through 5.11 summarize the proposed analysis procedures for these moment end-plate configurations. Table 5.1 lists the equations for bolt prying action, Q_{max} , bolt proof load, P_t , and bolt pretension, T_b , which are common for every end-plate configuration. Tables 5.2 through 5.11 show diagrams of the end-plate geometry, yield-line mechanisms, and simplified bolt force models, as well as equations for calculating the design strength of the connection, ϕM_n . The connection design strength is calculated for the limit states of end-plate yield, M_{pl} , and bolt rupture with or without prying action, M_q , M_{np} . The resistance factors ϕ_r and ϕ_y have been incorporated into the equations to make them applicable to Load and Resistance Factor Design. It is recognized that an in-depth probabilistic study on the proposed analytical models is necessary in order to determine accurate and dependable resistance factors. Such a study is beyond the scope of this research, hence the common resistance factors for yielding and bolt rupture are used. The resistance factor for bolt rupture, ϕ_r , is 0.75, and the resistance factor for end-plate yield, ϕ_y , is 0.90, AISC (1986). It should be noted that the expression for the plastic moment capacity per unit length, $m_p = (F_{py}t_p^2)/4$, has been substituted into the equations for $\phi_y M_{pl}$ in Tables 5.2 through 5.11.

Table 5.1 Summary of Bolt Equations

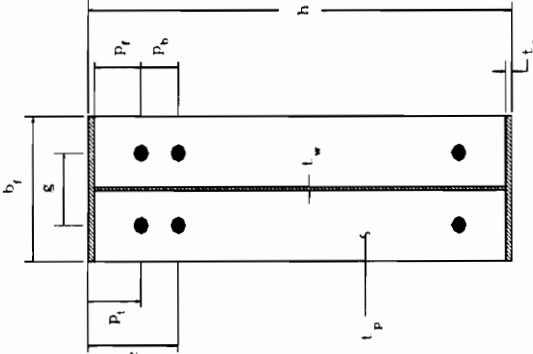
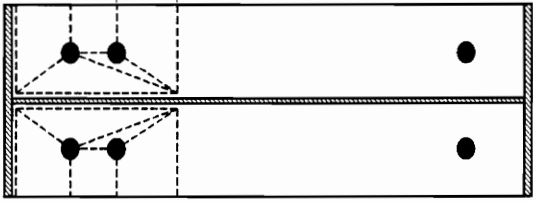
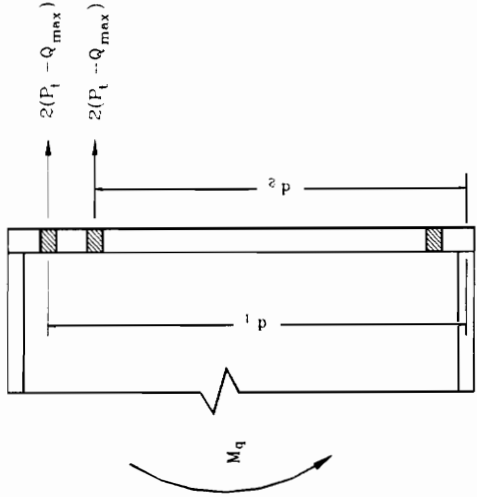
Bolt Proof Load	$P_t = A_b F_{yb} = \frac{\pi d_b^2}{4} (F_{yb})$ $F_{yb} = 90 \text{ ksi, nominal tensile strength of A325 bolts, specified in Table J3.2, AISC (1986)}$	
Bolt Pretension	$T_b = \text{specified force in Table J3.1, AISC (1986)}$	
Maximum Prying Force	Flush Configs.	$Q_{max} = \frac{w't_p^2}{4a} \sqrt{F_{py}^2 - 3 \left(\frac{F'}{w't_p} \right)^2}$ $a = 3.682 \left(\frac{t_p}{d_b} \right)^3 - 0.085$ $F' = \frac{t_p^2 F_{py} (0.85 b_f / 2 + 0.80 w') + \pi d_b^3 F_{yb} / 8}{4 p_f}$
	Extended Configs.	$Q_{max,i} = \frac{w't_p^2}{4a_i} \sqrt{F_{py}^2 - 3 \left(\frac{F'_i}{w't_p} \right)^2}$ $a_i = 3.682 \left(\frac{t_p}{d_b} \right)^3 - 0.085$ $F'_i = \frac{t_p^2 F_{py} (0.85 b_f / 2 + 0.80 w') + \pi d_b^3 F_{yb} / 8}{4 p_{f,i}}$ $Q_{max,o} = \frac{w't_p^2}{4a_o} \sqrt{F_{py}^2 - 3 \left(\frac{F'_o}{w't_p} \right)^2}$ $a_o = \min \left[3.682 \left(\frac{t_p}{d_b} \right)^3 - 0.085, P_{ext} - P_{f,o} \right]$ $F'_o = \frac{t_p^2 F_{py} (0.85 b_f / 2 + 0.80 w') + \pi d_b^3 F_{yb} / 8}{4 p_{f,o}}$
		Inside Bolt Rows
		Outside Bolt Rows

Table 5.2 Summary of Two-Bolt Flush Unstiffened Moment End-Plate Analysis

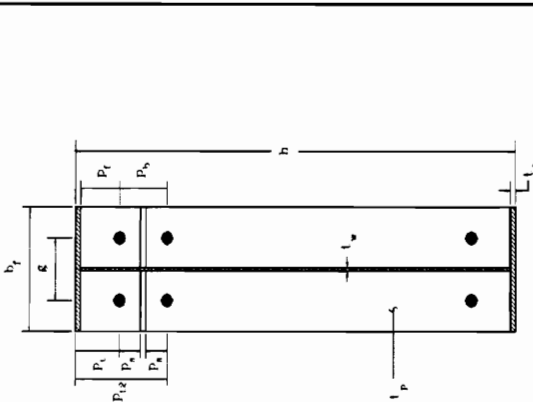
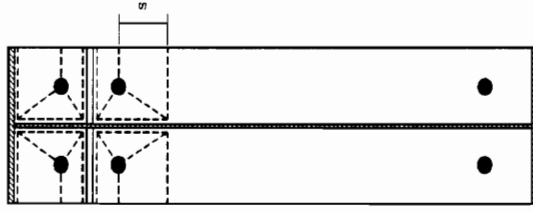
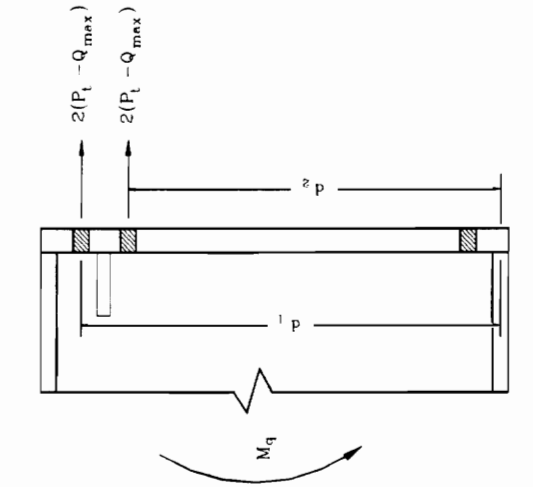
		
Geometry	Yield-Line Mechanism	Bolt Force Model
<p>End-Plate Yield</p> $\phi M_n = \phi_y M_{pl} = \phi_y F_y t_p^2 (h - p_t) \left[\frac{b_f}{2} \left(\frac{1}{p_f} + \frac{1}{s} \right) + \frac{2}{g} (p_f + s) \right]$ $s = \frac{1}{2} \sqrt{b_f g} \quad \phi_y = 0.90$		
<p>Bolt Rupture w/ Prying Action</p> $\phi M_n = \phi_r M_{q \max}$	$\phi_r M_{q \max} = \frac{\phi_r 2(P_t - Q_{\max}) d_1}{\max \left[\phi_r 2(T_b) d_1 \right]}$ $\phi_r = 0.75$	
<p>Bolt Rupture No Prying Action</p> $\phi M_n = \phi_r M_{np} = \phi_r 2(P_t) d_1$	$\phi_r = 0.75$	

Plastic Moment Capacity per unit length, $M_p = (F_y t_p^2) / 4$ subbed in for $\phi_y M_p$ in Tables 5.2 - 5.11

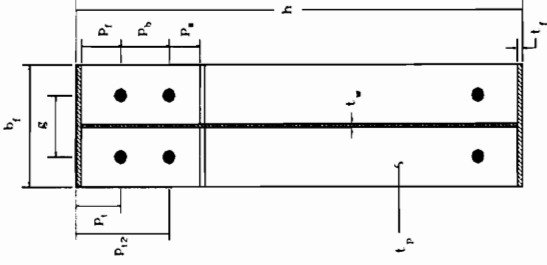
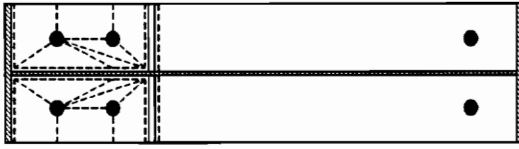
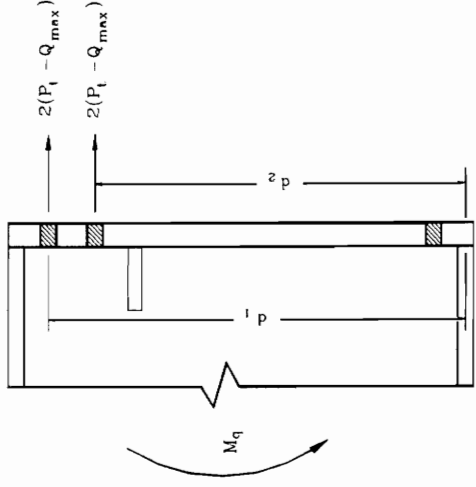
**Table 5.3 Summary of Four-Bolt Flush Unstiffened
Moment End-Plate Analysis**

		
Geometry	Yield-Line Mechanism	Bolt Force Model
<p>End-Plate Yield</p> $\phi M_n = \phi_y M_{pl} = \phi_y F_{yp} t_p^2 \left[\frac{b_f}{2} \left(\frac{h - p_t}{p_f} + \frac{h - p_t 2}{u} \right) + 2(p_f + p_b + u) \left(\frac{h - p_t}{g} \right) \right]$ $u = \frac{1}{2} \sqrt{b_f g \left(\frac{h - p_t 2}{h - p_t} \right)} \quad \phi_y = 0.90$		
<p>Bolt Rupture w/ Prying Action</p> $\phi M_n = \phi_r M_{q, \max} = \frac{\phi_r}{\max} \left[\frac{2(P_t - Q_{\max})(d_1 + d_2)}{2(T_b)(d_1 + d_2)} \right] \quad \phi_r = 0.75$		
<p>Bolt Rupture No Prying Action</p> $\phi M_n = \phi_r M_{np} = \phi_r [2(P_t)(d_1 + d_2)] \quad \phi_r = 0.75$		

**Table 5.4 Summary of Four-Bolt Flush Stiffened
Moment End-Plate Analysis -- Stiffened
Between the Tension Bolt Rows**

		
Geometry	Yield-Line Mechanism	Bolt Force Model
<p>End-Plate Yield</p> $\phi M_n = \phi_y M_{pl} = \phi_y F_{py} t_p^2 \left\{ (h - p_t) \left[\frac{b_f}{2} \left(\frac{1}{p_f} + \frac{1}{p_s} \right) + \frac{2}{g} (p_f + p_s) \right] + (h - p_{t2}) \left[\frac{b_f}{2} \left(\frac{1}{p_s} + \frac{1}{g} \right) + \frac{2}{g} (p_s + s) \right] \right\}$ $s = \frac{1}{2} \sqrt{b_f g} \quad \phi_y = 0.90$		
<p>Bolt Rupture w/ Prying Action</p> $\phi M_n = \phi_r M_{nq} = \max \left[\phi_r \frac{2(P_t - Q_{max})(d_1 + d_2)}{2}, \phi_r \frac{2(T_b)(d_1 + d_2)}{2} \right]$ $\phi_r = 0.75$		
<p>Bolt Rupture No Prying Action</p> $\phi M_n = \phi_r M_{np} = \phi_r \left[2(P_t)(d_1 + d_2) \right]$ $\phi_r = 0.75$		

**Table 5.5 Summary of Four-Bolt Flush Stiffened
Moment End-Plate Analysis -- Stiffened
Outside the Tension Bolt Rows**

			
Geometry	Yield-Line Mechanism		Bolt Force Model
End-Plate Yield $\phi M_n = \phi_y M_{pd} = \phi_y F_{yp} t_p^2 \left[(h - p_r) \left[\frac{b_f}{2p_f} + \frac{2}{g} (p_f + p_b) \right] + \frac{b_f}{4} + 1.25(h - p_{t2}) \right] + \frac{b_f}{2} \left(\frac{1}{2h_t} + \frac{1}{10p_s} + \frac{g}{2} \left(\frac{p_b}{p_s} + p_s \right) \right)$ $\phi_y = 0.90$			
Bolt Rupture w/ Prying Action $\phi M_n = \phi_r M_{q, \max}$	$\phi_r \left[\frac{2(P_t - Q_{\max})(d_1 + d_2)}{2(T_b)(d_1 + d_2)} \right]$ $\phi_r = 0.75$		
Bolt Rupture No Prying Action $\phi M_n = \phi_r M_{np} = \phi_r [2(P_t)(d_1 + d_2)]$	$\phi_r = 0.75$		

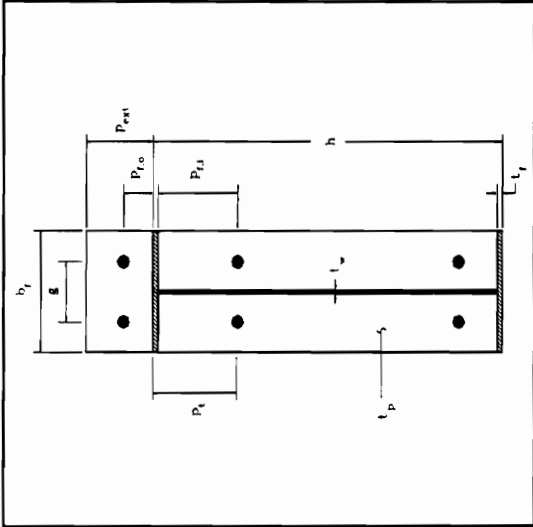
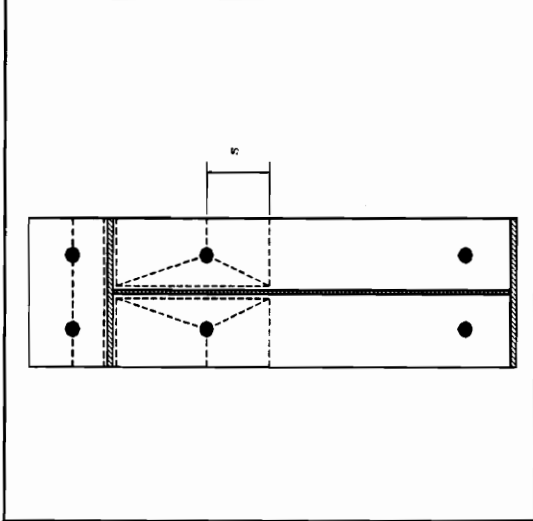
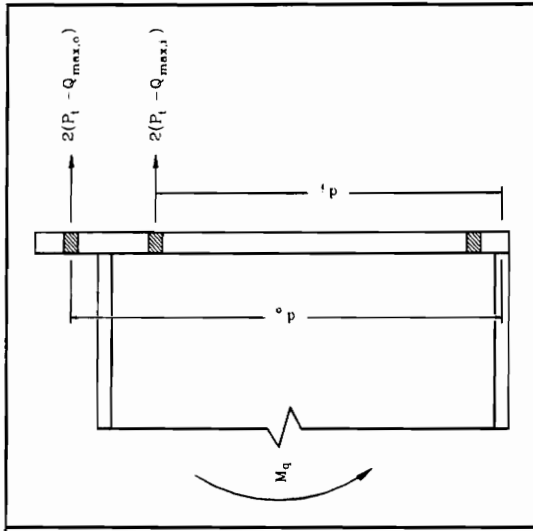
**Table 5.6 Summary of Six-Bolt Flush Unstiffened
Moment End-Plate Analysis**

<p>Geometry</p>	<p>Yield-Line Mechanism I</p>
<p>Bolt Force Model</p>	<p>Yield-Line Mechanism II</p>

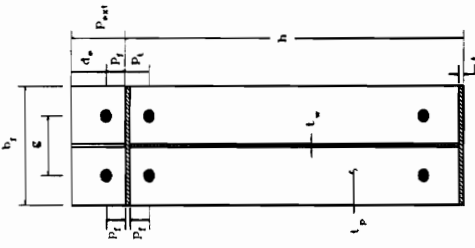
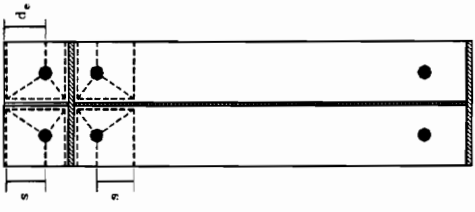
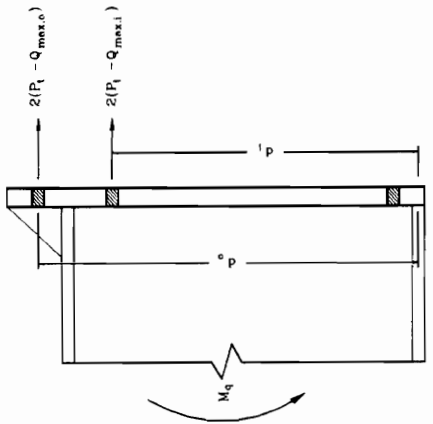
**Table 5.6 Summary of Six-Bolt Flush Unstiffened
Moment End-Plate Analysis (Continued)**

End-Plate Yield	Mech I	$\phi M_n = \phi_y M_{pl} = \phi_y F_{py} t^2 \left[\frac{b_f}{2} \left(\frac{h-p_t}{p_f} + \frac{h-p_{t3}}{u} \right) + 2(p_f + p_{b1,3} + u) \left(\frac{h-p_t}{g} \right) \right]$ $u = \frac{1}{2} \sqrt{b_f g \left(\frac{h-p_{t3}}{h-p_t} \right)} \quad \phi_y = 0.90$
	Mech II	$\phi M_n = \phi_y M_{pl} = \phi_y F_{py} t^2 \left[\frac{b_f}{2} \left(\frac{h-p_t}{p_f} + \frac{h-p_{t3}}{u} \right) + \frac{2}{g} (p_f + p_{b1,3}) (h-t_f) + \frac{2u}{g} (h-p_{t3}) + \frac{g}{2} \right]$ $u = \frac{1}{2} \sqrt{b_f g} \quad \phi_y = 0.90$
Bolt Rupture w/ Prying Action		$\phi M_n = \phi_r M_q = \frac{\phi_r [2(P_t - Q_{\max})(d_1 + d_3) + 2(T_b) d_2]}{\phi_r [2(T_b)(d_1 + d_2 + d_3)]_{\max}} \quad \phi_r = 0.75$
Bolt Rupture No Prying Action		$\phi M_n = \phi_r M_{np} = \phi_r [2(P_t)(d_1 + d_2 + d_3)] \quad \phi_r = 0.75$

Table 5.7 Summary of Four-Bolt Extended Unstiffened Moment End-Plate Analysis

		
Geometry	Yield-Line Mechanism	Bolt Force Model
<p>End-Plate Yield</p>	$\phi M_n = \phi_y M_{pl} = \phi_y F_{py} t_p^2 \left[\left(\frac{b_f}{2} \left(\frac{1}{p_{f,i}} + \frac{1}{s} \right) + (p_{f,i} + s) \left(\frac{2}{g} \right) \right) (h - p_t) + \frac{b_f}{2} \left(\frac{h}{p_{f,o}} + \frac{1}{2} \right) \right]$	
<p>Bolt Rupture w/ Prying Action</p>	$s = \frac{1}{2} \sqrt{b_f g} \quad \phi_y = 0.90$	$\phi_r = 0.75$
<p>Bolt Rupture No Prying Action</p>	$\phi_r \left[2(P_t - Q_{max,o}) d_o + 2(P_t - Q_{max,i}) d_i \right]$ $\phi_r \left[2(P_t - Q_{max,o}) d_o + 2(T_b) (d_i) \right]$ $\phi_r \left[2(P_t - Q_{max,i}) d_i + 2(T_b) (d_o) \right]$ $\phi_r \left[2(T_b) (d_o + d_i) \right]$	$\phi_r = 0.75$

**Table 5.8 Summary of Four-Bolt Extended Stiffened
Moment End-Plate Analysis**

	
<p>Geometry</p> 	<p>Yield-Line Mechanism; Case 1 when $s < d_b$</p>
<p>Bolt Force Model</p>	<p>Yield-Line Mechanism; Case 2 when $s > d_b$</p>

**Table 5.8 Summary of Four-Bolt Extended Stiffened
Moment End-Plate Analysis (Continued)**

End-Plate Yield	Case 1 $s < d_o$	$\phi M_n = \phi_y M_{pl} = \phi_y F_{py} t_p^2 \left[\frac{b_f}{2} \left(\frac{1}{p_f} + \frac{1}{s} \right) + (p_f + s) \left(\frac{2}{g} \right) \right] [(h - p_t) + (h + p_f)]$ $s = \frac{1}{2} \sqrt{b_f g} \quad \phi_y = 0.90$
	Case 2 $s > d_o$	$\phi M_n = \phi_y M_{pl} = \phi_y F_{py} t_p^2 \left[\frac{b_f}{2} \left(\frac{1}{p_f} + \frac{1}{2s} \right) + (p_f + d_o) \left(\frac{2}{g} \right) \right] [(h - p_t) + (h + p_f)]$ $s = \frac{1}{2} \sqrt{b_f g} \quad \phi_y = 0.90$
Bolt Rupture w/ Prying Action	$\phi M_n = \phi_r M_q =$ $\frac{\phi_r}{\phi_r} \left[\frac{\phi_r}{\phi_r} \left[2(p_t - Q_{\max,o}) d_o + 2(p_t - Q_{\max,i}) d_i \right] \right]$ $\frac{\phi_r}{\phi_r} \left[2(p_t - Q_{\max,o}) d_o + 2(T_b) (d_i) \right]$ $\frac{\phi_r}{\phi_r} \left[2(p_t - Q_{\max,i}) d_i + 2(T_b) (d_o) \right]$ $\frac{\phi_r}{\phi_r} \left[2(T_b) (d_o + d_i) \right]$	$\phi_r = 0.75$
Bolt Rupture No Prying Action	$\phi M_n = \phi_r M_{np} = \phi_r [2(p_t)(d_o + d_i)]$	$\phi_r = 0.75$

Table 5.9 Summary of Multiple Row Extended Unstiffened 1/2 Moment End-Plate Analysis

<p>Geometry</p>	<p>Yield-Line Mechanism II</p>
<p>Bolt Force Model</p>	<p>Yield-Line Mechanism II</p>

**Table 5.9 Summary of Multiple Row Extended Unstiffened 1/2
Moment End-Plate Analysis (Continued)**

End-Plate Yield	Mech I	$\phi M_n = \phi_y M_{pl} = \phi_y F_{py} t_p^2 \left[\frac{b_f}{2} \left(\frac{1}{2} + \frac{h}{p_f} + \frac{h - p_t}{p_f} + \frac{h - p_{t2}}{u} \right) + 2(p_f + p_b + u) \left(\frac{h - p_t}{g} \right) \right]$ $u = \frac{1}{2} \sqrt{b_f g \left(\frac{h - p_{t2}}{h - p_t} \right)} \quad \phi_y = 0.90$
	Mech II	$\phi M_n = \phi_y M_{pl} = \phi_y F_{py} t_p^2 \left[\frac{b_f}{2} \left(\frac{1}{2} + \frac{h}{p_f} + \frac{h - p_t}{p_f} + \frac{h - p_{t2}}{u} \right) + \frac{2}{g} (p_f + p_b) (h - t_f) + \frac{2u}{g} (h - p_{t2}) + \frac{g}{2} \right]$ $u = \frac{1}{2} \sqrt{b_f g} \quad \phi_y = 0.90$
Bolt Rupture w/ Prying Action	$\phi M_n = \phi_r M_q =$ $\phi_r \left[\frac{2(p_t - Q_{max,o}) d_1 + 2(p_t - Q_{max,i}) d_2 + 2(T_b) d_3}{2(p_t - Q_{max,o}) d_1 + 2(T_b) (d_2 + d_3)} \right]$ $\phi_r \left[\frac{2(p_t - Q_{max,i}) d_2 + 2(T_b) (d_1 + d_3)}{2(T_b) (d_1 + d_2 + d_3)} \right]$ $\phi_r \left[\frac{2(T_b) (d_1 + d_2 + d_3)}{2(T_b) (d_1 + d_2 + d_3)} \right]$	$\phi_r = 0.75$
Bolt Rupture No Prying Action	$\phi M_n = \phi_r M_{np} = \phi_r [2(p_t) (d_1 + d_2 + d_3)]$	$\phi_r = 0.75$

Table 5.10 Summary of Multiple Row Extended Unstiffened 1/3 Moment End-Plate Analysis

<p>Geometry</p> <p>Bolt Force Model</p>	<p>Yield-Line Mechanism I</p> <p>Yield-Line Mechanism II</p>

**Table 5.10 Summary of Multiple Row Extended Unstiffened 1/3
Moment End-Plate Analysis (Continued)**

End-Plate Yield	Mech I	$\phi M_u = \phi_y M_{pl} = \phi_y F_{yp} t^2 \left[\frac{b_f}{2} \left(\frac{1}{2} + \frac{h}{p_{f,o}} + \frac{h - p_t}{u} + \frac{h - p_{t3}}{p_{f,i}} \right) + 2(p_{f,i} + p_{b1,3} + u) \left(\frac{h - p_t}{g} \right) \right]$ $u = \frac{1}{2} \sqrt{\frac{b_f g (h - p_{t3})}{h - p_t}} \quad \phi_y = 0.90$
	Mech II	$\phi M_n = \phi_y M_{pl} = \phi_y F_{yp} t^2 \left[\frac{b_f}{2} \left(\frac{1}{2} + \frac{h}{p_{f,o}} + \frac{h - p_t}{u} + \frac{h - p_{t3}}{p_{f,i}} \right) + \frac{2}{g} (p_{f,i} + p_{b1,3}) (h - t_f) + \frac{2u}{g} (h - p_{t3}) + \frac{g}{2} \right]$ $u = \frac{1}{2} \sqrt{b_f g} \quad \phi_y = 0.90$
Bolt Rupture w/ Prying Action		$\phi_r \left[2(P_t - Q_{max,o})(d_1) + 2(P_t - Q_{max,i})(d_2 + d_4) + 2(T_b)d_3 \right]$ $\phi_r \left[2(P_t - Q_{max,o})(d_1) + 2(T_b)(d_2 + d_3 + d_4) \right]$ $\phi_r \left[2(P_t - Q_{max,i})(d_2 + d_4) + 2(T_b)(d_1 + d_3) \right]$ $\phi_r \left[2(T_b)(d_1 + d_2 + d_3 + d_4) \right]$ $\phi_r = 0.75$
	Bolt Rupture No Prying Action	$\phi M_n = \phi_r M_{np} = \phi_r \left[2(P_t)(d_1 + d_2 + d_3 + d_4) \right] \quad \phi_r = 0.75$

Table 5.11 Summary of Multiple Row Extended Stiffened 1/3 Moment End-Plate Analysis

<p>Geometry</p>	<p>Yield-Line Mech. I; Case 1 when $s < d_e$</p>	<p>Yield-Line Mech. II; Case 2 when $s > d_e$</p>
<p>Bolt Force Model</p>	<p>Yield-Line Mech. I; Case 2 when $s > d_e$</p>	<p>Yield-Line Mech. II; Case 2 when $s > d_e$</p>

**Table 5.11 Summary of Multiple Row Extended Stiffened 1/3
Moment End-Plate Analysis (Continued)**

End-Plate Yield	Mech I	Case 1 $s < d_o$	$\phi M_n = \phi_y M_{pl} = \phi_y F_{py} t_p^2 \left[\frac{b_f}{2} \left(1 + \frac{h}{p_f} + \frac{h - p_t}{p_f} + \frac{h - p_{t3}}{u} + \frac{h + p_f}{s} \right) + 2(p_f + p_{b1,3} + u) \left(\frac{h - p_t}{g} \right) + \frac{2}{g} (s + p_f)(h + p_f) \right]$ $s = \frac{1}{2} \sqrt{b_f g} \quad u = \frac{1}{2} \sqrt{b_f g \left(\frac{h - p_{t3}}{h - p_t} \right)} \quad \phi_y = 0.90$
		Case 2 $s > d_o$	$\phi M_n = \phi_y M_{pl} = \phi_y F_{py} t_p^2 \left[\frac{b_f}{2} \left(1 + \frac{h}{p_f} + \frac{h - p_t}{p_f} + \frac{h - p_{t3}}{u} + \frac{h + p_f}{2s} \right) + 2(p_f + p_{b1,3} + u) \left(\frac{h - p_t}{g} \right) + \frac{2}{g} (d_o + p_f)(h + p_f) \right]$ $s = \frac{1}{2} \sqrt{b_f g} \quad u = \frac{1}{2} \sqrt{b_f g \left(\frac{h - p_{t3}}{h - p_t} \right)} \quad \phi_y = 0.90$
	Mech II	Case 1 $s < d_o$	$\phi M_n = \phi_y M_{pl} = \phi_y F_{py} t_p^2 \left[\frac{b_f}{2} \left(1 + \frac{h}{p_f} + \frac{h - p_t}{p_f} + \frac{h - p_{t3}}{u} + \frac{h + p_f}{s} \right) + \frac{2}{g} (p_f + p_{b1,3})(h - t_f) + \frac{2u}{g} (h - p_{t3}) + \frac{2}{g} (s + p_f)(h + p_f) + \frac{g}{2} \right]$ $s = \frac{1}{2} \sqrt{b_f g} \quad u = \frac{1}{2} \sqrt{b_f g} \quad \phi_y = 0.90$
		Case 2 $s > d_o$	$\phi M_n = \phi_y M_{pl} = \phi_y F_{py} t_p^2 \left[\frac{b_f}{2} \left(1 + \frac{h}{p_f} + \frac{h - p_t}{p_f} + \frac{h - p_{t3}}{u} + \frac{h + p_f}{2s} \right) + \frac{2}{g} (p_f + p_{b1,3})(h - t_f) + \frac{2u}{g} (h - p_{t3}) + \frac{2}{g} (d_o + p_f)(h + p_f) + \frac{g}{2} \right]$ $s = \frac{1}{2} \sqrt{b_f g} \quad u = \frac{1}{2} \sqrt{b_f g} \quad \phi_y = 0.90$
Bolt Rupture w/ Prying Action			$\phi M_n = \phi_r M_q = \phi_r \left[2(P_t - Q_{max,o})(d_1) + 2(P_t - Q_{max,i})(d_2 + d_4) + 2(T_b)d_3 \right]$ $\phi_r \left[2(P_t - Q_{max,o})(d_1) + 2(T_b)(d_2 + d_3 + d_4) \right]$ $\phi_r \left[2(P_t - Q_{max,i})(d_2 + d_4) + 2(T_b)(d_1 + d_3) \right]$ $\phi_r \left[2(T_b)(d_1 + d_2 + d_3 + d_4) \right]$ <p style="text-align: right;">$\phi_r = 0.75$</p>
			$\phi M_n = \phi_r M_{np} = \phi_r \left[2(P_t)(d_1 + d_2 + d_3 + d_4) \right]$ <p style="text-align: right;">$\phi_r = 0.75$</p>
Bolt Rupture No Prying Action			$\phi M_n = \phi_r M_{np} = \phi_r \left[2(P_t)(d_1 + d_2 + d_3 + d_4) \right]$ <p style="text-align: right;">$\phi_r = 0.75$</p>

5.2 CONCLUSIONS

The major conclusions drawn from this study are:

1.) The threshold for determining whether to use the experimental yield moment, M_y , or the maximum applied moment, M_u , as the experimental failure moment can be designated by the ratio of M_y to M_u . If $M_y/M_u < 0.75$, M_y is designated as the experimental failure moment; if $M_y/M_u > 0.75$, M_u is designated as the experimental failure moment.

2.) The threshold when prying action begins to take place in the bolts is at 90% of the full strength of the plate, or $0.90M_{pl}$. If the applied load is less than this value, the end-plate behaves as a thick plate and prying action can be neglected in the bolts. Once the applied moment crosses the threshold of $0.90M_{pl}$, the plate can be approximated as a thin plate and maximum prying action is incorporated in the bolt analysis.

3.) Of the 52 tests examined in this study, 34 were governed by yielding of the end-plate. The yield-line mechanisms described in Chapter II adequately predict the strength of these end-plate connections. The mean value of the predicted to applied moment ratios for the 34 tests is 1.02, and the standard deviation equal to 12.6%. However, three of the 34 tests had unconservative ratios of predicted to applied moment equal to 1.35, 1.37, and 1.39. The ratio of predicted to applied moment for the other 31 tests varied from 0.85 to 1.11, yielding a mean value equal to 0.99 and a 6.2% standard deviation.

4.) Of the 52 tests examined in this study, 18 were governed by bolt rupture. In eleven tests, the prediction including prying action, M_q , controlled, and in seven tests, the prediction with no prying action, M_{np} , controlled. The simplified Kennedy bolt analysis method described in Chapter III adequately predicted the strength of the end-plate connections examined in this study. The ratio of predicted to applied moment for the cases when prying action was included ranged from 0.80 to 1.12, with an average value equal to 0.91 and a 10.1% standard deviation. The same ratio for the cases when prying action was not included ranged from 0.84 to 1.29, yielding an average equal to 1.01 and a 13.9% standard deviation.

5.3 DESIGN RECOMMENDATIONS

The proposed analytical procedure is appropriate for the design of moment end-plate connections having one of the nine configurations examined in this study. Two LRFD design procedures have been devised depending on the limiting provisions in the design. If it is necessary to limit bolt diameter, Design Procedure 1 is recommended. If it is necessary to limit the thickness of the end-plate, Design Procedure 2 is recommended. Because none of the experimental tests examined in this study used A490 bolts, the two proposed design procedures only allow for the use of A325 bolts.

Design Procedure 1: The following procedure results in a design with a relatively thick end-plate and smaller diameter bolts. The design is governed by bolt rupture when no prying action is included, requiring “thick” plate behavior. The design steps are:

- 1.) Compute the ultimate factored moment, M_u , using the load factors specified in Chapter A, AISC (1986). Set the connection design strength, ϕM_n , equal to the ultimate moment for the most efficient design:

$$\phi M_n = M_u \quad (5.1)$$

Choose one of the nine configurations, and establish values to define the end-plate geometry: b_f , g , p_f , t_f , t_w , h , p_b , p_s , etc. In addition, choose the type of end-plate material.

- 2.) Divide ϕM_n by 0.90 and set it equal to the appropriate equation for the resistance based on end-plate yield, $\phi_y M_{pl}$, from the summary tables:

$$\frac{\phi M_n}{0.90} = \phi_y M_{pl} \quad (5.2)$$

This is to ensure that the plate will be strong enough to cause the connection to fail by bolt rupture with no prying action, thick plate behavior. Solve for the required end-plate thickness, t_p .

- 3.) Set ϕM_n equal to the appropriate expression for the resistance based on bolt rupture with no prying action, $\phi_r M_{np}$, from the summary tables:

$$\phi M_n = \phi_r M_{np} \quad (5.3)$$

Solve for the required bolt proof load, P_t .

- 4.) Solve for the required bolt diameter, d_b , from the expression:

$$P_t = \left(\frac{\pi d_b^2}{4} \right) F_{by} \quad (5.4)$$

where $F_{by} = 90$ ksi, the nominal bolt tensile strength as specified in Table J3.2, AISC (1986).

- 5.) Check that $M_{np} < 0.90 M_{pl}$ for the chosen values of t_p and d_b . If the inequality is true, the design is completed. Otherwise, increase the plate thickness until the inequality stands.

Design Procedure 2: The following procedure results in a design with a relatively thin

end-plate and larger diameter bolts. The design is governed by either the yielding of the end-plate or bolt rupture when prying action is included, “thin” plate behavior.

The design steps are:

- 1.) Compute the ultimate factored moment, M_u , using the load factors specified in Chapter A, AISC (1986). Set the connection resistance, ϕM_n , equal to the ultimate moment for the most efficient design:

$$\phi M_n = M_u \quad (5.5)$$

Choose one of the nine configurations, and establish values to define the end-plate geometry: b_f , g , p_f , t_f , t_w , h , p_b , p_s , etc. In addition, choose the type of end-plate material.

- 2.) Set ϕM_n equal to the appropriate equation for the resistance based on end-plate yield, $\phi_y M_{pl}$, from the summary tables:

$$\phi M_n = \phi_y M_{pl} \quad (5.6)$$

Solve for the required end-plate thickness, t_p .

- 3.) Select a trial bolt diameter, d_b , and calculate the connection resistance for the limit state of bolt rupture with prying action, $\phi_r M_q$, using the appropriate equation in the summary tables.
- 4.) Make sure $\phi_r M_q > M_u$. If necessary, adjust the bolt diameter until ϕM_q is slightly larger than M_u .

5.4 DESIGN EXAMPLES

5.4.1 Two-Bolt Flush Unstiffened Moment End-Plate Connection

Determine the required end-plate thickness and bolt diameter for an end-plate connection with the geometry shown in Figure 5.1 and an ultimate factored moment of 540 k-in. The end-plate material is A572 Gr 50 and the bolts are A325.

Design Procedure 1:

1.) M_u was given as 540 k-in. Therefore:

$$\phi M_n = M_u = 540 \text{ k-in}$$

2.) Divide ϕM_n by 0.90 and set it equal to $\phi_y M_{pl}$ from Table 5.2:

$$\frac{\phi M_n}{0.90} = \frac{540}{0.90} = 600 \text{ k-in}$$

$$\phi_y M_{pl} = \phi_y F_{py} t_p^2 (h - p_t) \left[\frac{b_f}{2} \left(\frac{1}{p_f} + \frac{1}{s} \right) + \frac{2}{g} (p_f + s) \right] = 600 \text{ k-in}$$

$$\phi_y = 0.90$$

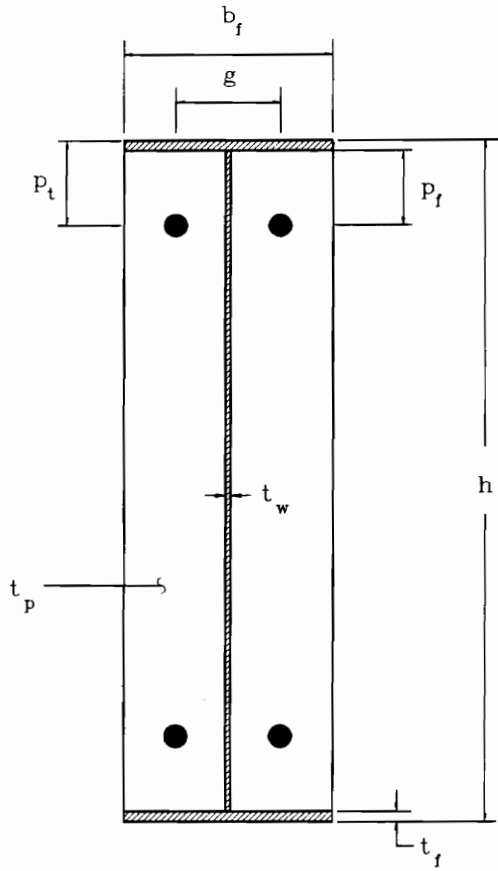
Solve for the required end-plate thickness, t_p :

$$t_p = \left[\frac{600 / (\phi_y F_{py})}{(h - p_t) \left[\frac{b_f}{2} \left(\frac{1}{p_f} + \frac{1}{s} \right) + \frac{2}{g} (p_f + s) \right]} \right]^{1/2}$$

where s and p_t are:

$$s = \frac{1}{2} \sqrt{b_f g} = \frac{1}{2} \sqrt{6(2.75)} = 2.03 \text{ in.}$$

$$p_t = p_f + t_f = 1.375 + 0.25 = 1.625 \text{ in.}$$



Parameter	Value (in.)
h	16
b_f	6
t_f	1/4
t_w	1/4
p_f	1 3/8
g	2 3/4

Figure 5.1 Design Example--Two-Bolt Flush Unstiffened Moment End-Plate Connection

$$t_p = \left[\frac{600/(0.90(50))}{(16 - 1.625) \left[\frac{6}{2} \left(\frac{1}{1.375} + \frac{1}{2.03} \right) + \frac{2}{2.75} (1.375 + 2.03) \right]} \right]^{1/2} = 0.389 \text{ in.}$$

Try $t_p = 7/16$ in.

3.) Compute the required bolt proof load, P_t , by equating ϕM_n to $\phi_r M_{np}$ using

Table 5.2:

$$\phi M_n = \phi_r M_{np} = \phi_r [2(P_t)d_1] = 540 \text{ k-in} \quad \phi_r = 0.75$$

where

$$d_1 = h - p_t - \frac{t_f}{2} = 16 - 1.625 - \frac{0.25}{2} = 14.25 \text{ in.}$$

Solving for P_t results in:

$$P_t = \frac{540}{\phi_r (2)(d_1)} = \frac{540}{0.75(2)(14.25)} = 25.3 \text{ k}$$

4.) Solve for the required bolt diameter, d_b :

$$P_t = \frac{\pi d_b^2}{4} (F_{yb}) = 25.3 \text{ k} \quad F_{yb} = 90 \text{ ksi (AISC, 1986)}$$

$$d_b = \sqrt{\frac{4 P_t}{\pi F_{yb}}} = \sqrt{\frac{4(25.3)}{\pi(90)}} = 0.598 \text{ in.}$$

Try $d_b = 5/8$ in.

5.) Check that $M_{np} < 0.90M_{pl}$ with $t_p = 7/16$ in. and $d_b = 5/8$ in.:

$$M_{np} = 2(P_t)d_1 = 2 \left[\frac{\pi(0.625)^2(90)}{4} \right] (14.25) = 786 \text{ k-in}$$

$$\begin{aligned}
 M_{pl} &= F_{py} t_p^2 (h - p_t) \left[\frac{b_f}{2} \left(\frac{1}{p_f} + \frac{1}{s} \right) + \frac{2}{g} (p_f + s) \right] \\
 &= 50(0.4375)^2 (16 - 1.625) \left[\frac{6}{2} \left(\frac{1}{1.375} + \frac{1}{2.03} \right) + \frac{2}{2.75} (1.375 + 2.03) \right] \\
 &= 844 \text{ k-in}
 \end{aligned}$$

$$0.90 M_{pl} = 0.90(844) = 759 \text{ k-in} < M_{np} = 786 \text{ k-in} \quad \text{NG}$$

It is therefore necessary to increase the plate thickness until $0.90M_{pl} > M_{np}$.

Try $t_p = 1/2$ in.

$$\begin{aligned}
 M_{pl} &= F_{py} t_p^2 (h - p_t) \left[\frac{b_f}{2} \left(\frac{1}{p_f} + \frac{1}{s} \right) + \frac{2}{g} (p_f + s) \right] \\
 &= 50(0.5)^2 (16 - 1.625) \left[\frac{6}{2} \left(\frac{1}{1.375} + \frac{1}{2.03} \right) + \frac{2}{2.75} (1.375 + 2.03) \right] \\
 &= 1102 \text{ k-in}
 \end{aligned}$$

$$0.90 M_{pl} = 0.90(1102) = 992 \text{ k-in} > M_{np} = 786 \text{ k-in} \quad \text{OK}$$

Summary For the given loading, materials and geometry, use 1/2 in. thick A572 Gr. 50 end-plate material, and 5/8 in. diameter A325 bolts.

Design Procedure 2:

1.) M_u was given as 540 k-in. Therefore:

$$\phi M_n = M_u = 540 \text{ k-in}$$

2.) Set ϕM_n equal to $\phi_y M_{pl}$ from Table 5.2:

$$\begin{aligned}
 \phi M_n = \phi_y M_{pl} &= \phi_y F_{py} t_p^2 (h - p_t) \left[\frac{b_f}{2} \left(\frac{1}{p_f} + \frac{1}{s} \right) + \frac{2}{g} (p_f + s) \right] = 540 \text{ k-in} \\
 \phi_y &= 0.90
 \end{aligned}$$

Solve for the required end-plate thickness, t_p :

$$t_p = \left[\frac{540 / (\phi_y F_{py})}{(h - p_t) \left[\frac{b_f}{2} \left(\frac{1}{p_f} + \frac{1}{s} \right) + \frac{2}{g} (p_f + s) \right]} \right]^{1/2}$$

where s and p_t are:

$$s = \frac{1}{2} \sqrt{b_f g} = \frac{1}{2} \sqrt{6(2.75)} = 2.03 \text{ in.}$$

$$p_t = p_f + t_f = 1.375 + 0.25 = 1.625 \text{ in.}$$

$$t_p = \left[\frac{540 / (0.90(50))}{(16 - 1.625) \left[\frac{6}{2} \left(\frac{1}{1.375} + \frac{1}{2.03} \right) + \frac{2}{2.75} (1.375 + 2.03) \right]} \right]^{1/2} = 0.369 \text{ in.}$$

Try $t_p = 3/8$ in.

3.) Try $d_b = 3/4$ in. Calculate $\phi_r M_q$ from Table 5.2:

$$\phi_r M_q = \max \begin{cases} \phi_r [2(P_t - Q_{\max}) d_1] \\ \phi_r [2(T_b) d_1] \end{cases} \quad \phi_r = 0.75$$

where T_b is the pretension load, specified in Table J3.1, AISC (1986), as 28

kips for $3/4$ in. diameter A325 bolts. P_t is:

$$P_t = \frac{\pi d_b^2}{4} (F_{yb}) = \frac{\pi (0.75)^2}{4} (90) = 39.76 \text{ k}$$

and Q_{\max} from Table 5.1 is:

$$Q_{\max} = \frac{w' t_p^2}{4 a} \sqrt{F_{py}^2 - 3 \left(\frac{F'}{w' t_p} \right)^2}$$

where

$$a = 3.682 \left(\frac{t_p}{d_b} \right)^3 - 0.085 = 3.682 \left(\frac{0.375}{0.75} \right)^3 - 0.085 = 0.375 \text{ in.}$$

$$w' = b_f/2 - (d_b + 1/16) = 6.0/2 - (3/4 + 1/16) = 2.1875 \text{ in.}$$

$$\begin{aligned} F' &= \frac{t_p^2 F_{py} (0.85 b_f / 2 + 0.80 w') + \pi d_b^3 F_{yb} / 8}{4 p_f} \\ &= \frac{(0.375)^2 (50) (0.85 (6.0 / 2) + 0.80 (2.1875)) + \pi (0.75)^3 (90) / 8}{4 (1.375)} \\ &= 8.21 \text{ k} \end{aligned}$$

Therefore,

$$Q_{\max} = \frac{(2.1875)(0.375)^2}{4(0.375)} \sqrt{(50)^2 - 3 \left(\frac{8.21}{(2.1875)(0.375)} \right)^2} = 9.62 \text{ k}$$

$$(P_t - Q_{\max}) = 39.76 - 9.62 = \underline{30.14 \text{ k}} > T_b = 28 \text{ k}$$

resulting in:

$$\phi_r M_q = 0.75 [2(39.76 - 9.62)(14.25)] = 644 \text{ k-in}$$

4.) Compare $\phi_r M_q$ with M_u :

$$\phi_r M_q = 644 \text{ k-in} > M_u = 540 \text{ k-in} \quad \underline{\text{OK}}$$

Summary For the given loading, materials and geometry, use 3/8 in. thick A572 Gr. 50 end-plate material, and 3/4 in. diameter A325 bolts.

The final design example summary is as follows:

Final Design Summary

Design Procedure 1

End Plate: A572 Gr 50 $t_p = 1/2$ in.

Bolts: A325 $d_b = 5/8$ in.

Design Procedure 2

End Plate: A572 Gr 50 $t_p = 3/8$ in.

Bolts: A325 $d_b = 3/4$ in.

5.4.2 Multiple Row Extended Unstiffened 1/3 Moment End-Plate Connection

Determine the required end-plate thickness and bolt diameter for an end-plate connection with the geometry shown in Figure 5.2 and an ultimate factored moment of 12,000 k-in. The end-plate material is A572 Gr 50 and the bolts are A325.

Design Procedure 1:

- 1.) M_u was given as 12,000 k-in. Therefore:

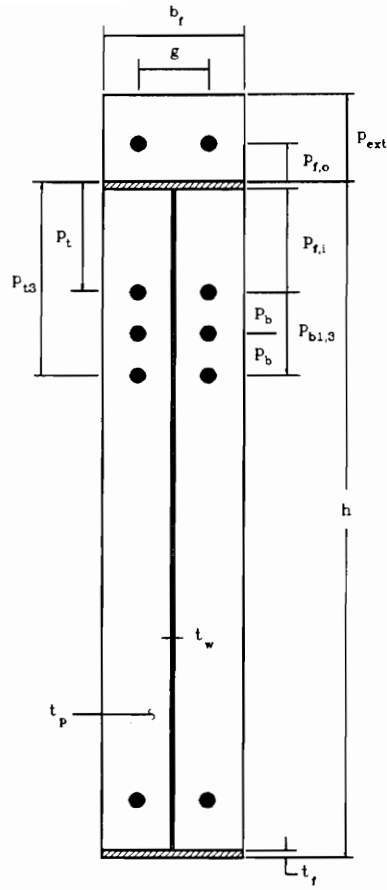
$$\phi M_n = M_u = 12,000 \text{ k-in}$$

- 2.) Divide ϕM_n by 0.90 and set it equal to $\phi_y M_{pl}$ from Table 5.10 for

Mechanisms I and II in the yield-line analysis:

$$\frac{\phi M_n}{0.90} = \frac{12000}{0.90} = 13,333 \text{ k-in}$$

Mechanism I:



Parameter	Value (in.)
h	62
b_f	10
t_f	1
t_w	3/8
$P_{f,i}$	4
$P_{f,o}$	2 3/8
P_{ext}	4 1/4
P_b	3 1/2
g	4 1/2

Figure 5.2 Design Example--Multiple Row Extended Unstiffened 1/3 Moment End-Plate Connection

$$\phi_y M_{pl} = \phi_y F_{py} t_p^2 \left[\frac{b_f}{2} \left(\frac{1}{2} + \frac{h}{p_{f,o}} + \frac{h-p_t}{p_{f,i}} + \frac{h-p_{t3}}{u} \right) + 2(p_{f,i} + p_{b1,3} + u) \left(\frac{h-p_t}{g} \right) \right] = 13,333 \text{ k-in}$$

$$\phi_y = 0.90$$

Solve for the required end-plate thickness, t_p :

$$t_p = \left[\frac{13333 / (\phi_y (50))}{\frac{b_f}{2} \left(\frac{1}{2} + \frac{h}{p_{f,o}} + \frac{h-p_t}{p_{f,i}} + \frac{h-p_{t3}}{u} \right) + 2(p_{f,i} + p_{b1,3} + u) \left(\frac{h-p_t}{g} \right)} \right]^{1/2}$$

where

$$p_t = p_{f,i} + t_f = 4 + 1 = 5 \text{ in.}$$

$$p_{b1,3} = 2p_b = 2(3.5) = 7 \text{ in.}$$

$$p_{t3} = p_t + p_{b1,3} = 5 + 7 = 12 \text{ in.}$$

$$u = \frac{1}{2} \sqrt{b_f g \left(\frac{h-p_{t3}}{h-p_t} \right)} = \frac{1}{2} \sqrt{10(4.5) \left(\frac{62-12}{62-5} \right)} = 3.141 \text{ in.}$$

Substituting into the plate thickness expression:

$$t_p = \left[\frac{13333 / (0.90(50))}{\frac{10}{2} \left(\frac{1}{2} + \frac{62}{2.375} + \frac{62-5}{4} + \frac{62-12}{3.141} \right) + 2(4+7+3.141) \left(\frac{62-5}{4.5} \right)} \right]^{1/2} = 0.679 \text{ in.}$$

Mechanism II:

$$\phi_y M_{pl} = \phi_y F_{py} t_p^2 \left[\frac{b_f}{2} \left(\frac{1}{2} + \frac{h}{p_{f,o}} + \frac{h-p_t}{p_{f,i}} + \frac{h-p_{t3}}{u} \right) + \frac{2}{g} (p_{f,i} + p_{b1,3}) (h-t_f) + \frac{2u}{g} (h-p_{t3}) + \frac{g}{2} \right] = 13,333 \text{ k-in}$$

$$\phi_y = 0.90$$

Solve for the required end-plate thickness, t_p :

$$t_p = \left[\frac{13333/(\phi_y F_{py})}{\frac{b_f}{2} \left(\frac{1}{2} + \frac{h}{p_{f,o}} + \frac{h-p_t}{p_{f,i}} + \frac{h-p_{t3}}{u} \right) + \frac{2}{g} (p_{f,i} + p_{b1,3})(h-t_f) + \frac{2u}{g} (h-p_{t3}) + \frac{g}{2}} \right]^{1/2}$$

where

$$p_t = 5 \text{ in.} \quad p_{b1,3} = 7 \text{ in.} \quad p_{t3} = 12 \text{ in.}$$

calculated earlier, and u is:

$$u = \frac{1}{2} \sqrt{b_f g} = \frac{1}{2} \sqrt{10(4.5)} = 3.354 \text{ in.}$$

Substituting into the plate thickness expression:

$$t_p = \left[\frac{13333/(0.90(50))}{\frac{10}{2} \left(\frac{1}{2} + \frac{62}{2.375} + \frac{62-5}{4} + \frac{62-12}{3.354} \right) + \frac{2}{4.5} (4+7)(62-1) + \frac{2(3.354)}{4.5} (62-12) + \frac{4.5}{2}} \right]^{1/2} = 0.629 \text{ in.}$$

Choose the larger required end-plate thickness calculated from Mechanism I and Mechanism II:

$$t_p = \begin{cases} t_p \text{ Mechanism I} \\ t_p \text{ Mechanism II} \end{cases}_{\max}$$

$$t_p = \begin{cases} 0.679 \text{ in.} \\ 0.629 \text{ in.} \end{cases}_{\max} = 0.679 \text{ in.} \quad (\text{Mechanism I governs})$$

Try $t_p = 11/16 \text{ in.}$

3.) Compute the required bolt proof load, P_t , by equating ϕM_n to $\phi_r M_{np}$ using

Table 5.10:

$$\phi M_n = \phi_r M_{np} = \phi_r [2(P_t)(d_1 + d_2 + d_3 + d_4)] = 12,000 \text{ k-in} \quad \phi_r = 0.75$$

where

$$d_1 = h + p_{f,o} = 62 + 2.375 = 64.375 \text{ in.}$$

$$d_2 = h - p_t - \frac{t_f}{2} = 62 - 5 - \frac{1}{2} = 56.5 \text{ in.}$$

$$d_3 = d_2 - p_b = 56.5 - 3.5 = 53.0 \text{ in.}$$

$$d_4 = d_3 - p_b = 53 - 3.5 = 49.5 \text{ in.}$$

Solving for P_t results in:

$$P_t = \frac{12000}{\phi_T(2)(d_1 + d_2 + d_3 + d_4)} = \frac{12000}{0.75(2)(64.375 + 56.5 + 53.0 + 49.5)} = 35.8 \text{ k}$$

4.) Solve for the required bolt diameter, d_b , by:

$$P_t = \frac{\pi d_b^2}{4} (F_{yb}) = 35.8 \text{ k} \quad F_{yb} = 90 \text{ ksi (AISC, 1986)}$$

$$d_b = \sqrt{\frac{4 P_t}{\pi F_{yb}}} = \sqrt{\frac{4(35.8)}{\pi(90)}} = 0.712 \text{ in.}$$

Try $d_b = 3/4 \text{ in.}$

5.) Check that $M_{np} < 0.90M_{pl}$ with $t_p = 11/16 \text{ in.}$ and $d_b = 3/4 \text{ in.}$:

$$M_{np} = 2(P_t)(d_1 + d_2 + d_3 + d_4)$$

where

$$P_t = \frac{\pi d_b^2}{4} (F_{yb}) = \frac{\pi(0.75)^2}{4} (90) = 39.8 \text{ k}$$

$$M_{np} = 2(39.8)(64.375 + 56.5 + 53.0 + 49.5) = 17,780 \text{ k-in}$$

$$\begin{aligned}
M_{pl} &= F_{py} t_p^2 \left[\frac{b_f}{2} \left(\frac{1}{2} + \frac{h}{p_{f,o}} + \frac{h-p_t}{p_{f,i}} + \frac{h-p_{t3}}{u} \right) + 2(p_{f,i} + p_{b1,3} + u) \left(\frac{h-p_t}{g} \right) \right] \\
&= 50(0.6875)^2 \left[\frac{10}{2} \left(\frac{1}{2} + \frac{62}{2375} + \frac{62-5}{4} + \frac{62-12}{3141} \right) + 2(4+7+3141) \left(\frac{62-5}{45} \right) \right] \\
&= 15,175 \text{ k-in} \quad (\text{Mechanism I})
\end{aligned}$$

$$0.90 M_{pl} = 0.90(15,175) = 13,658 \text{ k-in} < M_{np} = 17,780 \text{ k-in} \quad \text{NG}$$

It is therefore necessary to increase the plate thickness until $0.90M_{pl} > M_{np}$.

Try $t_p = 13/16$ in.

$$\begin{aligned}
M_{pl} &= F_{py} t_p^2 \left[\frac{b_f}{2} \left(\frac{1}{2} + \frac{h}{p_{f,o}} + \frac{h-p_t}{p_{f,i}} + \frac{h-p_{t3}}{u} \right) + 2(p_{f,i} + p_{b1,3} + u) \left(\frac{h-p_t}{g} \right) \right] \\
&= 50(0.8125)^2 \left[\frac{10}{2} \left(\frac{1}{2} + \frac{62}{2375} + \frac{62-5}{4} + \frac{62-12}{3141} \right) + 2(4+7+3141) \left(\frac{62-5}{45} \right) \right] \\
&= 21,195 \text{ k-in} \quad (\text{Mechanism I})
\end{aligned}$$

$$0.90 M_{pl} = 0.90(21,195) = 19,076 \text{ k-in} > M_{np} = 17,780 \text{ k-in} \quad \text{OK}$$

Summary For the given loading, materials and geometry, use 13/16 in. thick A572 Gr. 50 end-plate material, and 3/4 in. diameter A325 bolts.

Design Procedure 2:

1.) M_u was given as 12,000 k-ft. Therefore:

$$\phi M_n = M_u = 12,000 \text{ k-in}$$

2.) Set ϕM_n equal to $\phi_y M_{pl}$ from Table 5.10 for Mechanisms I and II in the yield-line analysis:

Mechanism I:

$$\phi_y M_{pl} = \phi_y F_{py} t_p^2 \left[\frac{b_f}{2} \left(\frac{1}{2} + \frac{h}{p_{f,o}} + \frac{h-p_t}{p_{f,i}} + \frac{h-p_{t3}}{u} \right) + 2(p_{f,i} + p_{b1,3} + u) \left(\frac{h-p_t}{g} \right) \right] = 12,000 \text{ k-in}$$

$$\phi_y = 0.90$$

Solve for the required end-plate thickness, t_p :

$$t_p = \left[\frac{12000 / (\phi_y (50))}{\frac{b_f}{2} \left(\frac{1}{2} + \frac{h}{p_{f,o}} + \frac{h-p_t}{p_{f,i}} + \frac{h-p_{t3}}{u} \right) + 2(p_{f,i} + p_{b1,3} + u) \left(\frac{h-p_t}{g} \right)} \right]^{1/2}$$

where p_t , $p_{b1,3}$, and p_{t3} are the same as for Design Procedure I:

$$p_t = p_{f,i} + t_f = 4 + 1 = 5 \text{ in.}$$

$$p_{b1,3} = 2p_b = 2(3.5) = 7 \text{ in.}$$

$$p_{t3} = p_t + p_{b1,3} = 5 + 7 = 12 \text{ in.}$$

and u is:

$$u = \frac{1}{2} \sqrt{b_f g \left(\frac{h-p_{t3}}{h-p_t} \right)} = \frac{1}{2} \sqrt{10(4.5) \left(\frac{62-12}{62-5} \right)} = 3.141 \text{ in.}$$

$$t_p = \left[\frac{12000 / (0.90(50))}{\frac{10}{2} \left(\frac{1}{2} + \frac{62}{2.375} + \frac{62-5}{4} + \frac{62-12}{3.141} \right) + 2(4+7+3.141) \left(\frac{62-5}{4.5} \right)} \right]^{1/2} = 0.644 \text{ in.}$$

Mechanism II:

$$\phi_y M_{\mu} = \phi_y F_{py} t_p^2 \left[\frac{b_f}{2} \left(\frac{1}{2} + \frac{h}{p_{f,o}} + \frac{h-p_t}{p_{f,i}} + \frac{h-p_{t3}}{u} \right) + \frac{2}{g} (p_{f,i} + p_{b1,3}) (h-t_f) + \frac{2u}{g} (h-p_{t3}) + \frac{g}{2} \right] = 12,000 \text{ k-in}$$

$$\phi_y = 0.90$$

Solve for the required end-plate thickness, t_p :

$$t_p = \left[\frac{12000/(\phi_y F_{py})}{\frac{b_f}{2} \left(\frac{1}{2} + \frac{h}{P_{f,o}} + \frac{h-p_t}{P_{f,i}} + \frac{h-p_{t3}}{u} \right) + \frac{2}{g} (P_{f,i} + P_{b1,3})(h-t_f) + \frac{2u}{g} (h-p_{t3}) + \frac{g}{2}} \right]^{1/2}$$

where u is:

$$u = \frac{1}{2} \sqrt{b_f g} = \frac{1}{2} \sqrt{10(4.5)} = 3.354 \text{ in.}$$

$$t_p = \left[\frac{12000/(0.90(50))}{\frac{10}{2} \left(\frac{1}{2} + \frac{62}{2.375} + \frac{62-5}{4} + \frac{62-12}{3.354} \right) + \frac{2}{4.5} (4+7)(62-1) + \frac{2(3.354)}{4.5} (62-12) + \frac{4.5}{2}} \right]^{1/2} = 0.598 \text{ in.}$$

Choose the larger required end-plate thickness calculated from Mechanism I and Mechanism II:

$$t_p = \begin{cases} t_p \text{ Mechanism I} \\ t_p \text{ Mechanism II} \end{cases}_{\max}$$

$$t_p = \begin{cases} 0.644 \text{ in.} \\ 0.598 \text{ in.} \end{cases}_{\max} = 0.644 \text{ in.} \quad (\text{Mechanism I governs})$$

Try $t_p = 11/16$ in.

3.) Try $d_b = 7/8$ in. Calculate $\phi_r M_q$ from Table 5.10:

$$\phi_r M_q = \begin{cases} \phi_r [2(P_t - Q_{\max,o})(d_1) + 2(P_t - Q_{\max,i})(d_2 + d_4) + 2(T_b) d_3] \\ \phi_r [2(P_t - Q_{\max,o})(d_1) + 2(T_b)(d_2 + d_3 + d_4)] \\ \phi_r [2(P_t - Q_{\max,i})(d_2 + d_4) + 2(T_b)(d_1 + d_3)] \\ \phi_r [2(T_b)(d_1 + d_2 + d_3 + d_4)] \end{cases}_{\max}$$

$$\phi_r = 0.75$$

where T_b is the pretension load, specified in Table J3.1, AISC (1986), as 39

kips for 7/8 inch diameter A325 bolts, and P_t is calculated as:

$$P_t = \frac{\pi d_b^2}{4} (F_{yb}) = \frac{\pi(0.875)^2}{4} (90) = 54.1 \text{ k}$$

The inner prying force, $Q_{\max,i}$, is calculated from Table 5.10:

$$Q_{\max,i} = \frac{w' t_p^2}{4 a_i} \sqrt{F_{py}^2 - 3 \left(\frac{F_i'}{w' t_p} \right)^2}$$

where

$$a_i = 3.682 \left(\frac{t_p}{d_b} \right)^3 - 0.085 = 3.682 \left(\frac{0.6875}{0.875} \right)^3 - 0.085 = 1.701 \text{ in.}$$

$$w' = b_f/2 - (d_b + 1/16) = 10/2 - (7/8 + 1/16) = 4.0625 \text{ in.}$$

$$\begin{aligned} F_i' &= \frac{t_p^2 F_{py} (0.85 b_f / 2 + 0.80 w') + \pi d_b^3 F_{yb} / 8}{4 p_{f,i}} \\ &= \frac{(0.6875)^2 (50) (0.85 (10 / 2) + 0.80 (4.0625)) + \pi (0.875)^3 (90) / 8}{4(4)} \\ &= 12.56 \text{ k} \end{aligned}$$

Therefore,

$$Q_{\max,i} = \frac{(4.0625)(0.6875)^2}{4(1.701)} \sqrt{(50)^2 - 3 \left(\frac{12.56}{(4.0625)(0.6875)} \right)^2} = 13.94 \text{ k}$$

$$(P_t - Q_{\max,i}) = (54.1 - 13.94) = \underline{40.18 \text{ k}} > T_b = 39 \text{ k}$$

The outer prying force, $Q_{\max,o}$, is calculated from Table 5.10:

$$Q_{\max,o} = \frac{w' t_p^2}{4 a_o} \sqrt{F_{py}^2 - 3 \left(\frac{F_o'}{w' t_p} \right)^2}$$

where

$$a_o = \left| \begin{array}{l} 3.682 \left(\frac{t_p}{d_b} \right)^3 - 0.085 = 3.682 \left(\frac{0.6875}{0.875} \right)^3 - 0.085 = 1.701 \text{ in.} \\ \min P_{\text{ext}} - P_{f,o} = 4.25 - 2.375 = 1.875 \text{ in.} \end{array} \right| = 1.701 \text{ in.}$$

$$\begin{aligned} F_o' &= \frac{t_p^2 F_{py} (0.85 b_f / 2 + 0.80 w') + \pi d_b^3 F_{yb} / 8}{4 P_{f,o}} \\ &= \frac{(0.6875)^2 (50)(0.85(10/2) + 0.80(4.0625)) + \pi(0.875)^3(90) / 8}{4(2.375)} \\ &= 2115 \text{ k} \end{aligned}$$

Therefore,

$$Q_{\text{max},o} = \frac{(4.0625)(0.6875)^2}{4(1.701)} \sqrt{(50)^2 - 3 \left(\frac{2115}{(4.0625)(0.6875)} \right)^2} = 13.62 \text{ k}$$

$$(P_t - Q_{\text{max},o}) = (54.1 - 13.62) = \underline{40.50 \text{ k}} > T_b = 39 \text{ k}$$

The calculation of $\phi_r M_q$ is therefore:

$$\begin{aligned} \phi_r M_q &= \phi_r [2(P_t - Q_{\text{max},o})(d_1) + 2(P_t - Q_{\text{max},i})(d_2 + d_4) + 2(T_b)d_3] \\ &= 0.75 [2(54.1 - 13.62)(64.375) + 2(54.1 - 13.94)(56.5 + 49.5) + 2(39)(53.0)] \\ &= 13,400 \text{ k-in} \end{aligned}$$

4.) Compare $\phi_r M_q$ with M_u :

$$\phi_r M_q = 13,400 \text{ k-in} > M_u = 12,000 \text{ k-in} \quad \underline{\text{OK}}$$

Summary For the given loading, materials and geometry, use 11/16 in. thick A572 Gr. 50 end-plate material, and 7/8 in. diameter A325 bolts.

The final design example summary is as follows:

Final Design Summary

Design Procedure 1

End Plate: A572 Gr 50 $t_p = 13/16$ in.

Bolts: A325 $d_b = 3/4$ in.

Design Procedure 2

End Plate: A572 Gr 50 $t_p = 11/16$ in.

Bolts: A325 $d_b = 7/8$ in.

REFERENCES

- Abel, M. S. and T. M. Murray (1992a), "Multiple Row, Extended Unstiffened End-Plate Connection Tests," Research Report CE/VPI-ST-92/04, Department of Civil Engineering, Virginia Polytechnic Institute and State University, Blacksburg, VA, August 1992.
- Abel, M. S. and T. M. Murray (1992b), "Analytical and Experimental Investigation of the Extended Unstiffened Moment End-Plate Connection with Four Bolts at the Beam Tension Flange," Research Report CE/VPI-ST-93/08, Department of Civil Engineering, Virginia Polytechnic Institute and State University, Blacksburg, VA, December 1992, Revised October 1994.
- AISC (1986), "Load and Resistance Factor Design Specification for Structural Steel Buildings," First Edition, American Institute of Steel Construction, Chicago, IL, 1986.
- AISC (1989), "Specification for Structural Steel Buildings," Ninth Edition, American Institute of Steel Construction, Chicago, IL, 1989.
- Bond, D. E. and T. M. Murray (1989), "Analytical and Experimental Investigation of a Flush Moment End-Plate Connection with Six Bolts at the Tension Flange," Research Report CE/VPI-ST-89/10, Department of Civil Engineering, Virginia Polytechnic Institute and State University, Blacksburg, VA, December 1989.
- Borgsmiller, J. T., E. A. Sumner and T. M. Murray (1995), "Tests of Extended Moment End-Plate Connections Having Large Inner Pitch Distances," Research Report CE/VPI-ST-95/01, Department of Civil Engineering, Virginia Polytechnic Institute and State University, Blacksburg, VA, March 1995.
- Hendrick, D., A. R. Kukreti and T. M. Murray (1984), "Analytical and Experimental Investigation of Stiffened Flush End-Plate Connections with Four Bolts at the Tension Flange," Research Report FSEL/MBMA 84-02, Fears Structural Engineering Laboratory, University of Oklahoma, Norman, OK, September 1984.
- Hendrick, D., A. R. Kukreti and T. M. Murray (1985), "Unification of Flush End-Plate Design Procedures," Research Report FSEL/MBMA 85-01, Fears Structural Engineering Laboratory, University of Oklahoma, Norman, OK, March 1985.

- Kennedy, N. A., S. Vinnakota and A. N. Sherbourne (1981), "The Split-Tee Analogy in Bolted Splices and Beam-Column Connections," *Joints in Structural Steelwork*, John Wiley & Sons, London-Toronto, 1981, pp. 2.138-2.157.
- Morrison, S. J., A. Astaneh-Asl and T. M. Murray (1985), "Analytical and Experimental Investigation of the Extended Stiffened Moment End-Plate Connection with Four Bolts at the Beam Tension Flange," Research Report FSEL/MBMA 85-05, Fears Structural Engineering Laboratory, University of Oklahoma, Norman, OK, December 1985.
- Morrison, S. J., A. Astaneh-Asl and T. M. Murray (1986), "Analytical and Experimental Investigation of the Multiple Row Extended Moment End-Plate Connection with Eight Bolts at the Beam Tension Flange," Research Report FSEL/MBMA 86-01, Fears Structural Engineering Laboratory, University of Oklahoma, Norman, OK, May 1986.
- Rodkey, R. W. and T. M. Murray (1993), "Eight-Bolt Extended Unstiffened End-Plate Connection Test," Research Report CE/VPI-ST-93/10, Department of Civil Engineering, Virginia Polytechnic Institute and State University, Blacksburg, VA, December 1993.
- SEI (1984), "Multiple Row, Extended End-Plate Connection Tests," Research Report, Structural Engineers, Inc., Norman, OK, December 1984.
- Srouji, R., A. R. Kukreti and T. M. Murray (1983a), "Strength of Two Tension Bolt Flush End-Plate Connections," Research Report FSEL/MBMA 83-03, Fears Structural Engineering Laboratory, University of Oklahoma, Norman, OK, July 1983.
- Srouji, R., A. R. Kukreti and T. M. Murray (1983b), "Yield-Line Analysis of End-Plate Connections with Bolt Force Predictions," Research Report FSEL/MBMA 83-05, Fears Structural Engineering Laboratory, University of Oklahoma, Norman, OK, December 1983.
- Srouji, R., A. R. Kukreti and T. M. Murray (1984), "Yield-Line Analysis of End-Plate Connections with Bolt Force Predictions -- Addendum," Research Report FSEL/MBMA 83-05A, Fears Structural Engineering Laboratory, University of Oklahoma, Norman, OK, August 1984.

APPENDIX A

NOMENCLATURE

NOMENCLATURE

A_b	=	nominal bolt area
a	=	distance from the bolt centerline to the prying force
a_i	=	distance from the interior bolt centerline to the inner prying force
a_o	=	distance from the outer bolt centerline to the outer prying force
B	=	bolt force
B_1	=	exterior bolt force in multiple row extended end-plate configurations
B_2	=	first interior bolt force in multiple row extended end-plate configurations
B_3	=	second interior bolt force in multiple row extended end-plate configurations
B_4	=	third interior bolt force in multiple row extended end-plate configurations
b_f	=	beam flange width
d	=	distance from a bolt line to the center of the beam compression flange
d_b	=	nominal bolt diameter
d_e	=	end-plate extension beyond the exterior bolt centerline
	=	$p_{ext} - p_{f,o}$
d_i	=	distance from the interior bolt centerline to the center of the beam compression flange in four-bolt extended end-plate configurations
d_o	=	distance from the outer bolt centerline to the center of the beam compression flange in four-bolt extended end-plate configurations
d_1	=	distance from the center of the beam compression flange to the farthest load-carrying bolt line
d_2	=	distance from the center of the beam compression flange to the second farthest load-carrying bolt line

d_3	=	distance from the center of the beam compression flange to the third farthest load-carrying bolt line
d_4	=	distance from the center of the beam compression flange to the fourth farthest load-carrying bolt line
F	=	applied force
F_f	=	beam flange force
F_{py}	=	end-plate material yield stress
F_{yb}	=	nominal tensile strength for A325 bolts (Table J3.2; AISC, 1986)
	=	90 ksi
F'	=	flange force per bolt at the thin plate limit
F'_i	=	flange force per bolt at the thin plate limit when calculating $Q_{max,i}$ for end-plate configurations with large inner pitch distances
F'_o	=	flange force per bolt at the thin plate limit when calculating $Q_{max,o}$ for end-plate configurations with large inner pitch distances
g	=	bolt gage
h	=	total beam depth
h_t	=	distance from the inner edge of the stiffener to outer edge of the compression flange in four-bolt flush configurations stiffened outside the tension bolt rows
	=	$h - p_{t2} - p_s$
L_n	=	length of yield line n
L_{nx}	=	x-component of the length of yield line n
L_{ny}	=	y-component of the length of yield line n
M	=	applied moment
M_b	=	bolt moment capacity
M_{fail}	=	connection failure moment
	=	M_u or M_y
M_n	=	nominal connection resistance

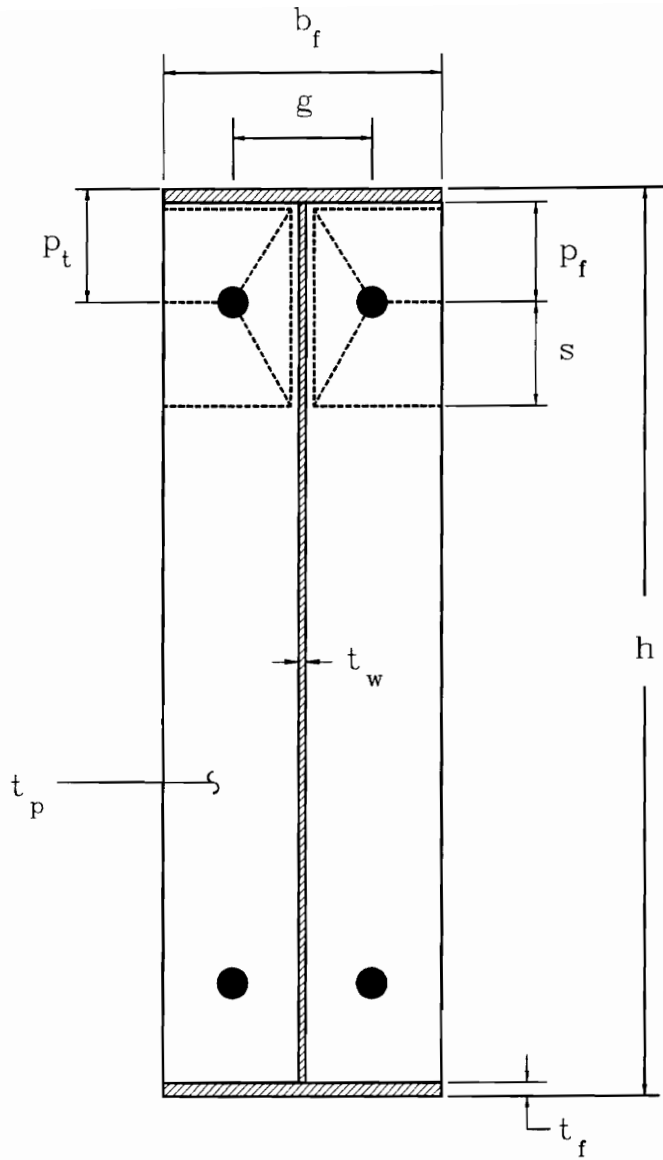
M_{np}	=	connection strength for the limit state of bolt fracture with no prying action
M_{pl}	=	connection strength for the limit state of end-plate yielding
M_{pred}	=	predicted strength of the connection
M_q	=	connection strength for the limit state of bolt fracture with prying action
M_u	=	maximum applied moment in laboratory test
	=	required strength of the connection, AISC (1986)
$M_{u,bolt}$	=	moment at which bolt force reaches its proof load, P_t
M_w	=	working moment
M_y	=	experimental yield moment, obtained from the plot of end-plate separation vs. applied moment via two intersecting lines
M_1	=	plastic moment at the first plate hinge line
M_2	=	plastic moment at the second plate hinge line
m_p	=	plastic moment capacity per unit length of the end-plate
	=	$(F_{py}t_p^2)/4$
m_{px}	=	x-component of the plastic moment capacity per unit length of the end-plate
m_{py}	=	y-component of the plastic moment capacity per unit length of the end-plate
N	=	total number of yield lines in a mechanism
	=	total number of bolt rows in the connection
N_i	=	number of load-carrying bolt rows in the connection
N_j	=	number of non-load-carrying bolt rows in the connection
P_t	=	bolt material ultimate tensile load capacity, proof load
	=	A_bF_{yb}
p_b	=	distance from bolt centerline to bolt centerline
$p_{b1,3}$	=	distance from the first interior bolt centerline to the innermost interior bolt centerline in configurations with three interior bolt rows
	=	$2p_b$

p_{ext}	=	end-plate extension beyond the exterior face of the beam tension flange
p_f	=	distance from the bolt centerline adjacent the beam tension flange to the near face of the beam tension flange
$p_{f,i}$	=	distance from the first interior bolt centerline to the inner face of the beam tension flange
$p_{f,o}$	=	distance from the outer bolt centerline to the outer face of the beam tension flange
p_s	=	distance from the bolt centerline to the near face of the stiffener in four-bolt flush stiffened configurations
p_t	=	distance from the first interior bolt centerline to the far face of the beam tension flange
	=	$t_f + p_{f,i}$
p_{t2}	=	distance from the second interior bolt centerline to the far face of the beam tension flange
	=	$p_t + p_b$
p_{t3}	=	distance from the innermost interior bolt centerline to the far face of the beam tension flange
	=	$p_t + p_{b1,3}$
Q	=	prying force
Q_{max}	=	maximum possible prying force
$Q_{max,i}$	=	maximum possible prying force for interior bolts
$Q_{max,o}$	=	maximum possible prying force for outer bolts
s	=	distance from the innermost bolt centerline to the innermost yield line
T_b	=	specified pretension load in high strength bolts, Table J3.1, AISC (1986)
t_f	=	beam flange thickness
t_p	=	end-plate thickness
t_w	=	beam web thickness
t_1	=	Kennedy thick plate limit

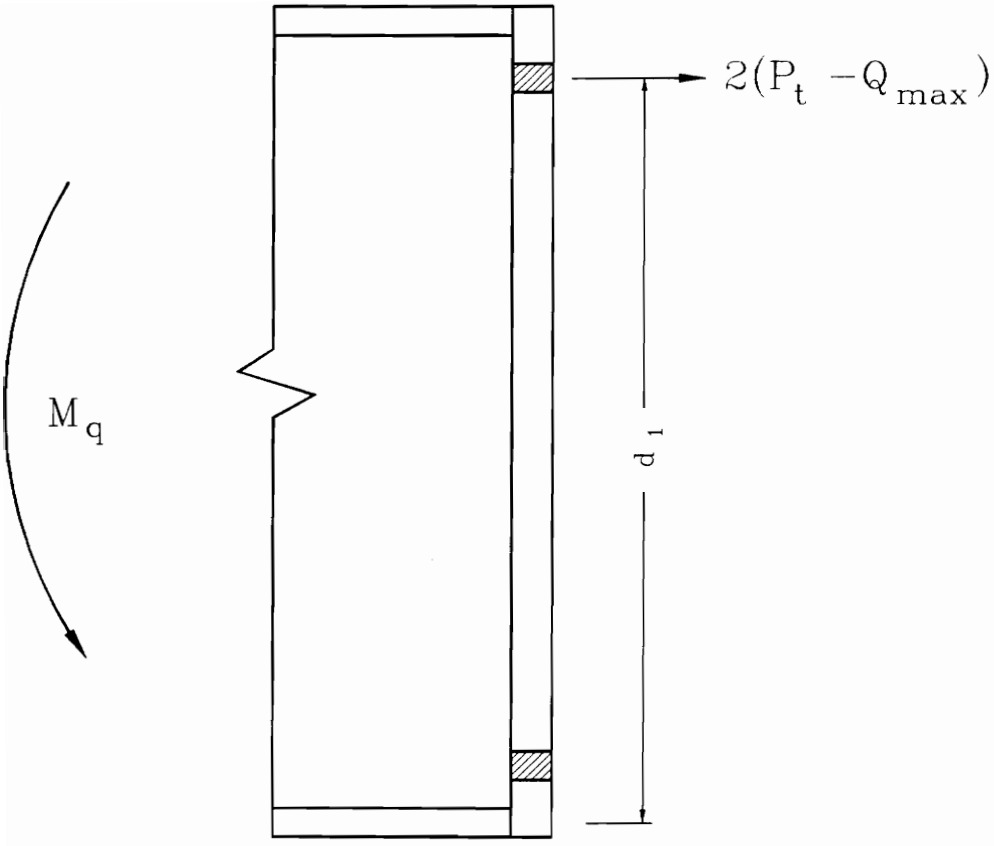
t_{11}	=	Kennedy thin plate limit
u	=	distance from the innermost bolt centerline to the innermost yield line
u_1	=	distance from the innermost bolt centerline to the innermost yield line for Mechanism I
u_2	=	distance from the innermost bolt centerline to the innermost yield line for Mechanism II
W_e	=	external work
	=	$M_u(1/h)$
W_i	=	total internal energy stored in a yield-line mechanism
w_i	=	internal energy stored in a single yield line
w'	=	width of end-plate per bolt minus the bolt hole diameter
	=	$b_f/2 - (d_b + 1/16)$
α	=	outer end-plate factor used in past studies
β	=	inner end-plate factor used in past studies
ϕ	=	resistance factor
ϕ_r	=	resistance factor for bolt rupture
	=	0.75
ϕ_y	=	resistance factor for end-plate yield
	=	0.90
π	=	pi
θ_n	=	relative normal plate rotation on yield-line n
θ_{nx}	=	x-component of the relative normal plate rotation on yield-line n
θ_{ny}	=	y-component of the relative normal plate rotation on yield-line n

APPENDIX B

TWO-BOLT FLUSH UNSTIFFENED MOMENT END-PLATE TEST CALCULATIONS



**Yield-Line Mechanism for Two-Bolt Flush
Unstiffened Moment End-Plates**
(after Srouji *et al.* , 1983b)



**Simplified Bolt Force Model for Two-Bolt Flush
Unstiffened Moment End-Plates**

SROUJI et al. (1983a)
F1-3/4-1/2-16

h = 16 in.
bf = 6 in.
tf = 0.25 in.
tp = 0.505 in.
pf = 1.5 in.
g = 3.5 in.
s = 2.291 in.
F_{py} = 55.48 ksi (measured)
db = 0.75 in.
T_b = 28 kips
P_t = 39.8 kips
F_{yb} = 90.0 ksi (table)

d_l = 14.125 in.
w' = 2.1875 in.

a = 1.039 in.

F = 12.63 kips

Q_{max} = 6.96 kips

M_q = 77.2 k-ft
M_{pl} = 92.0 k-ft
0.90M_{pl} = 82.8 k-ft
M_{np} = 93.6 k-ft

M _{pred} =	77.2 k-ft	M _{pred} /M-
M _y =	75 k-ft	1.03
M _u =	97.5 k-ft	0.79

SROUJI et al. (1983a)
F1-3/4-3/8-16

h = 16 in.
bf = 6 in.
tf = 0.25 in.
tp = 0.383 in.
pf = 1.5 in.
g = 3.5 in.
s = 2.291 in.
F_{py} = 59.45 ksi (measured)
db = 0.75 in.
T_b = 28 kips
P_t = 39.8 kips
F_{yb} = 90.0 ksi (table)

d_l = 14.125 in.
w' = 2.1875 in.

a = 0.405 in.

F = 8.73 kips

Q_{max} = 11.21 kips

M_q = 67.2 k-ft
M_{pl} = 56.7 k-ft
0.90M_{pl} = — k-ft
M_{np} = — k-ft

M _{pred} =	56.7 k-ft	M _{pred} /M-
M _y =	47 k-ft	1.21
M _u =	57 k-ft	0.99

SROUJI et al. (1983a)
F1-5/8-1/2-16

h = 16 in.
bf = 6 in.
tf = 0.25 in.
tp = 0.508 in.
pf = 1.875 in.
g = 3.75 in.
s = 2.372 in.
F_{py} = 53.98 ksi (measured)
db = 0.625 in.
T_b = 19 kips
P_t = 27.6 kips
F_{yb} = 90.0 ksi (table)

d_l = 13.75 in.
w' = 2.3125 in.

a = 1.892 in.

F = 9.32 kips

Q_{max} = 4.12 kips

M_q = 53.8 k-ft
M_{pl} = 82.6 k-ft
0.90M_{pl} = 74.4 k-ft
M_{np} = 63.3 k-ft

M _{pred} =	63.3 k-ft	M _{pred} /M-
M _y =	60 k-ft	1.05
M _u =	75 k-ft	0.84

* — (P_t - Q_{max}) < T_b

SROUJI *et al.* (1983a)
F1-5/8-3/8-16

h = 16 in.
bf = 6 in.
tf = 0.25 in.
tp = 0.385 in.
pf = 1.375 in.
g = 2.75 in.
s = 2.031 in.
Fpy = 56.95 ksi (measured)
db = 0.625 in.
Tb = 19 kips
Pt = 27.6 kips
Fyb = 90.0 ksi (table)

dl = 14.25 in.
w' = 2.3125 in.

a = 0.776 in.

F' = 8.32 kips

Qmax = 6.03 kips

Mq = 51.3 k-ft
Mpl = 62.0 k-ft
0.90Mpl = 55.8 k-ft
Mmp = 65.6 k-ft
> Mq
> 0.90Mpl

Mpred =	51.3 k-ft	Mpred/M-
My =	55 k-ft	0.93
Mu =	63 k-ft	0.81

SROUJI *et al.* (1983a)
F1-5/8-1/2-10

h = 10 in.
bf = 5 in.
tf = 0.25 in.
tp = 0.506 in.
pf = 1.5 in.
g = 3 in.
s = 1.936 in.
Fpy = 55.8 ksi (measured)
db = 0.625 in.
Tb = 19 kips
Pt = 27.6 kips
Fyb = 90.0 ksi (table)

dl = 8.125 in.
w' = 1.8125 in.

a = 1.869 in.

F' = 9.95 kips

Qmax = 3.26 kips

Mq = 33.0 k-ft
Mpl = 51.6 k-ft
0.90Mpl = 46.4 k-ft
Mmp = 37.4 k-ft
> Mq
< 0.90Mpl

Mpred =	37.4 k-ft	Mpred/M-
My =	32 k-ft	1.17
Mu =	39.47 k-ft	0.95

SROUJI *et al.* (1983a)
F1-5/8-3/8-10

h = 10 in.
bf = 5 in.
tf = 0.1875 in.
tp = 0.384 in.
pf = 1.3125 in.
g = 2.25 in.
s = 1.677 in.
Fpy = 51.9 ksi (measured)
db = 0.625 in.
Tb = 19 kips
Pt = 27.6 kips
Fyb = 90.0 ksi (table)

dl = 8.40625 in.
w' = 1.8125 in.

a = 0.769 in.

F' = 6.85 kips

Qmax = 4.26 kips

Mq = 32.7 k-ft
Mpl = 32.8 k-ft
0.90Mpl = 29.5 k-ft
Mmp = 38.7 k-ft
> Mq
> 0.90Mpl

Mpred =	32.7 k-ft	Mpred/M-
My =	25 k-ft	1.31
Mu =	33.92 k-ft	0.96

* - (Pt - Qmax) < Tb

SROUJI *et al.* (1983a)
 F1-3/4-1/2-24A

h = 24 in.
 bf = 6 in.
 tf = 0.25 in.
 tp = 0.504 in.
 pf = 1.75 in.
 g = 3.25 in.
 s = 2.208 in.
 F_{py} = 57.53 ksi (measured)
 db = 0.75 in.
 T_b = 28 kips
 P_t = 39.8 kips
 F_{yb} = 90.0 ksi (table)

d_l = 21.875 in.
 w' = 2.1875 in.
 a = 1.032 in.

F = 11.11 kips

Q_{max} = 7.38 kips

M_q = 118.1 k-ft
 M_{pl} = 147.6 k-ft
 0.90M_{pl} = 132.8 k-ft
 M_{mp} = 145.0 k-ft
 > M_q
 > 0.90M_{pl}

M _{pred} =	118.1 k-ft	M _{pred} /M-
M _y =	110 k-ft	1.07
M _u =	120.25 k-ft	0.98

SROUJI *et al.* (1983a)
 F1-3/4-1/2-24B

h = 24 in.
 bf = 6 in.
 tf = 0.25 in.
 tp = 0.502 in.
 pf = 1.375 in.
 g = 2.75 in.
 s = 2.031 in.
 F_{py} = 57.53 ksi (measured)
 db = 0.75 in.
 T_b = 28 kips
 P_t = 39.8 kips
 F_{yb} = 90.0 ksi (table)

d_l = 22.25 in.
 w' = 2.1875 in.

a = 1.019 in.

F = 14.05 kips

Q_{max} = 7.18 kips

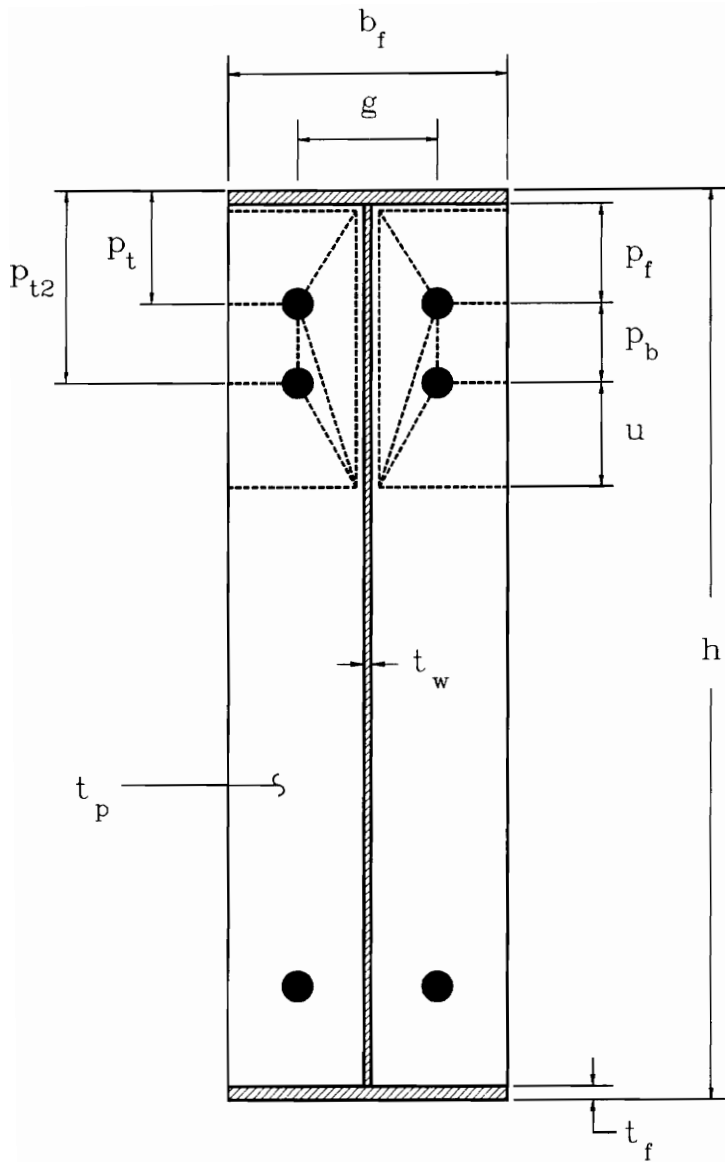
M_q = 120.8 k-ft
 M_{pl} = 165.9 k-ft
 0.90M_{pl} = 149.3 k-ft
 M_{mp} = 147.4 k-ft
 > M_q
 < 0.90M_{pl}

M _{pred} =	147.4 k-ft	M _{pred} /M-
M _y =	125 k-ft	1.18
M _u =	154.2 k-ft	0.96

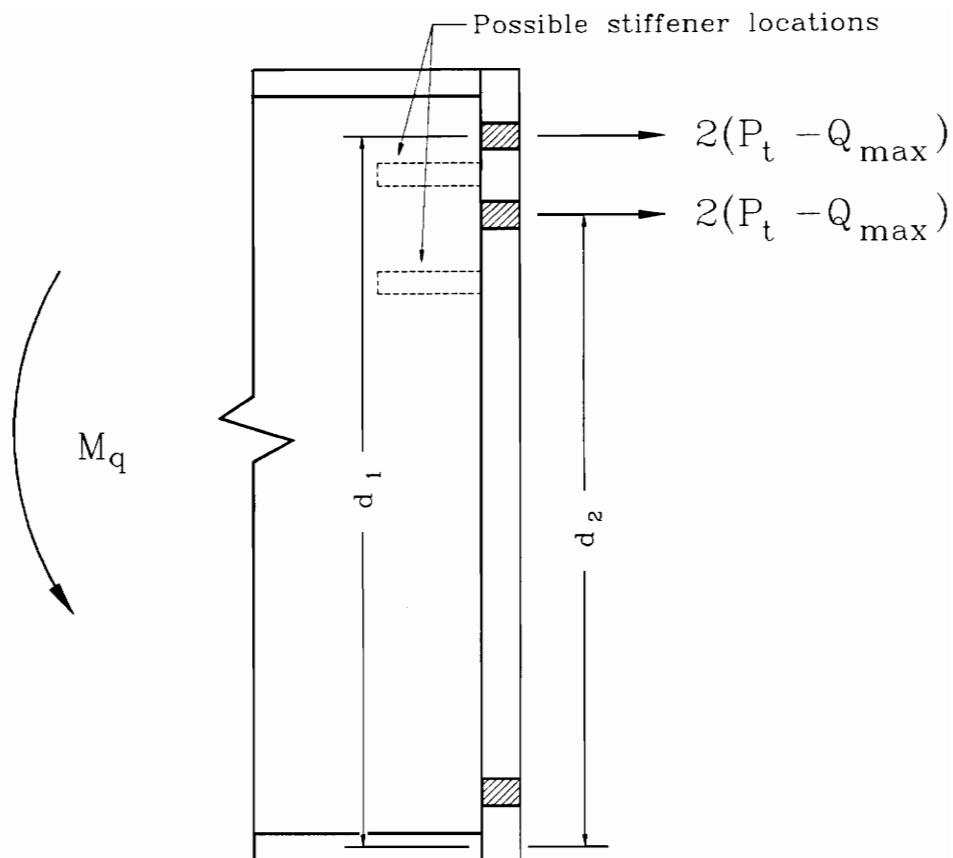
* - (P_t - Q_{max}) < T_b

APPENDIX C

FOUR-BOLT FLUSH UNSTIFFENED MOMENT END-PLATE TEST CALCULATIONS



Yield-Line Mechanism for Four-Bolt Flush
Unstiffened Moment End-Plates
(after Srouji *et al.* , 1983b)



**Simplified Bolt Force Model for Four-Bolt Flush
Unstiffened and Stiffened Moment End-Plates**

SROUJI et al. (1983b, 1984)
F2-5/8-1/2-16

h = 16 in.
bf = 6 in.
tf = 0.25 in.
tp = 0.5 in.
pf = 1.875 in.
g = 2.75 in.
pb = 3 in.
u = 1.798 in.

F_{py} = 58.6 ksi (measured)
db = 0.625 in.
T_b = 19 kips
P_t = 27.6 kips
F_{yb} = 90.0 ksi (table)
d₁ = 13.75 in.
d₂ = 10.75 in.
w' = 2.3125 in.
a = 1.800 in.

F = 9.75 kips
Q_{max} = 4.56 kips

M_q = 94.1 k-ft
M_{pl} = 131.5 k-ft
0.90M_{pl} = 118.3 k-ft
M_{mp} = 112.7 k-ft

M _{pred} =	112.7 k-ft	M _{pred} /M-
M _y =	85 k-ft	1.33
M _u =	108 k-ft	1.04

SROUJI et al. (1983b, 1984)
F2-5/8-3/8-16

h = 16 in.
bf = 6 in.
tf = 0.25 in.
tp = 0.375 in.
pf = 1.375 in.
g = 2.75 in.
pb = 3 in.
u = 1.807 in.

F_{py} = 60.5 ksi (measured)
db = 0.625 in.
T_b = 19 kips
P_t = 27.6 kips
F_{yb} = 90.0 ksi (table)
d₁ = 14.25 in.
d₂ = 11.25 in.
w' = 2.3125 in.
a = 0.710 in.

F = 8.38 kips
Q_{max} = 6.65 kips

M_q = 89.1 k-ft
M_{pl} = 81.4 k-ft
0.90M_{pl} = — k-ft
M_{mp} = — k-ft

M _{pred} =	81.4 k-ft	M _{pred} /M-
M _y =	85 k-ft	0.96
M _u =	85.5 k-ft	0.95

SROUJI et al. (1983b, 1984)
F2-3/4-1/2-24

h = 24 in.
bf = 6 in.
tf = 0.25 in.
tp = 0.5 in.
pf = 1.75 in.
g = 3.25 in.
pb = 3 in.
u = 2.052 in.

F_{py} = 54 ksi (measured)
db = 0.75 in.
T_b = 28 kips
P_t = 39.8 kips
F_{yb} = 90.0 ksi (table)
d₁ = 21.875 in.
d₂ = 18.875 in.
w' = 2.1875 in.
a = 1.006 in.

F = 10.42 kips
Q_{max} = 6.99 kips

M_q = 222.6 k-ft
M_{pl} = 177.3 k-ft
0.90M_{pl} = — k-ft
M_{mp} = — k-ft

M _{pred} =	177.3 k-ft	M _{pred} /M-
M _y =	140 k-ft	1.27
M _u =	171.8 k-ft	1.03

* - (P_t - Q_{max}) < T_b

SROUJI et al. (1983b, 1984)
F2-3/4-3/8-24

h = 24 in.
bf = 6 in.
tf = 0.25 in.
tp = 0.375 in.
pf = 1.375 in.
g = 2.75 in.
pb = 3 in.
u = 1.890 in.

F_{py} = 64.1 ksi (measured)
db = 0.75 in.
T_b = 28 kips
P_t = 39.8 kips
F_{yb} = 90.0 ksi (table)
d₁ = 22.25 in.
d₂ = 19.25 in.
w' = 2.1875 in.
a = 0.375 in.

F = 9.76 kips
Q_{max} = 12.44 kips *

M_q = 193.7 k-ft
M_{pl} = 136.4 k-ft
0.90M_{pl} = — k-ft
M_{np} = — k-ft

M _{pred} =	136.4 k-ft	M _{pred} /M _{pl}
M _y =	110 k-ft	1.24
M _u =	144.7 k-ft	0.94

SROUJI et al. (1983b, 1984)
F2-3/4-1/2-16

h = 16 in.
bf = 6 in.
tf = 0.25 in.
tp = 0.5 in.
pf = 1.5 in.
g = 3.5 in.
pb = 3 in.
u = 2.036 in.

F_{py} = 54.8 ksi (measured)
db = 0.75 in.
T_b = 28 kips
P_t = 39.8 kips
F_{yb} = 90.0 ksi (table)
d₁ = 14.125 in.
d₂ = 11.125 in.
w' = 2.1875 in.
a = 1.006 in.

F = 12.30 kips
Q_{max} = 6.96 kips

M_q = 138.0 k-ft
M_{pl} = 112.2 k-ft
0.90M_{pl} = — k-ft
M_{np} = — k-ft

M _{pred} =	112.2 k-ft	M _{pred} /M _{pl}
M _y =	85 k-ft	1.32
M _u =	115.5 k-ft	0.97

SROUJI et al. (1983b, 1984)
F2-3/4-3/8-16

h = 16 in.
bf = 6 in.
tf = 0.25 in.
tp = 0.375 in.
pf = 1.5 in.
g = 3.5 in.
pb = 3 in.
u = 2.036 in.

F_{py} = 59.7 ksi (measured)
db = 0.75 in.
T_b = 28 kips
P_t = 39.8 kips
F_{yb} = 90.0 ksi (table)
d₁ = 14.125 in.
d₂ = 11.125 in.
w' = 2.1875 in.
a = 0.375 in.

F = 8.50 kips
Q_{max} = 11.67 kips

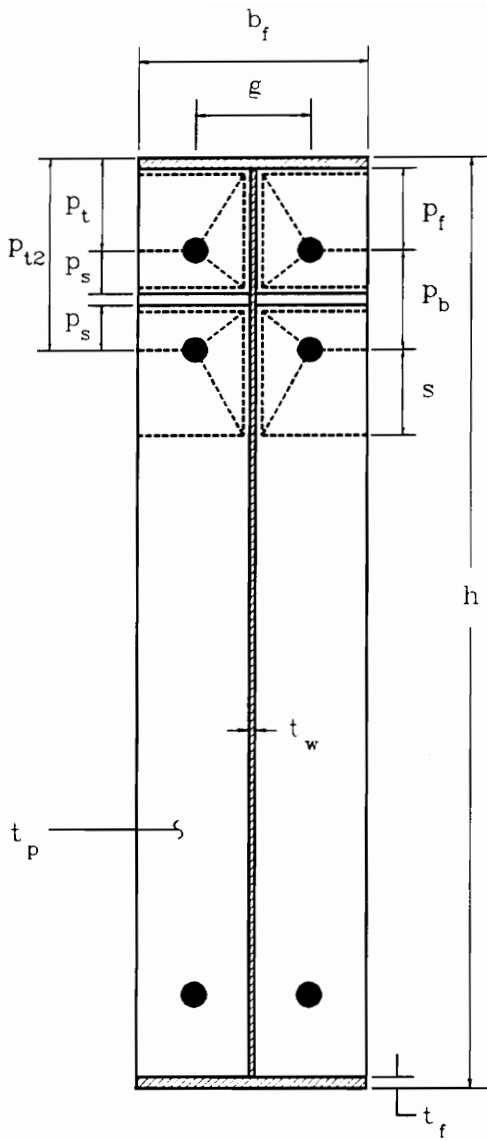
M_q = 118.2 k-ft
M_{pl} = 68.8 k-ft
0.90M_{pl} = — k-ft
M_{np} = — k-ft

M _{pred} =	68.8 k-ft	M _{pred} /M _{pl}
M _y =	62 k-ft	1.11
M _u =	73.2 k-ft	0.94

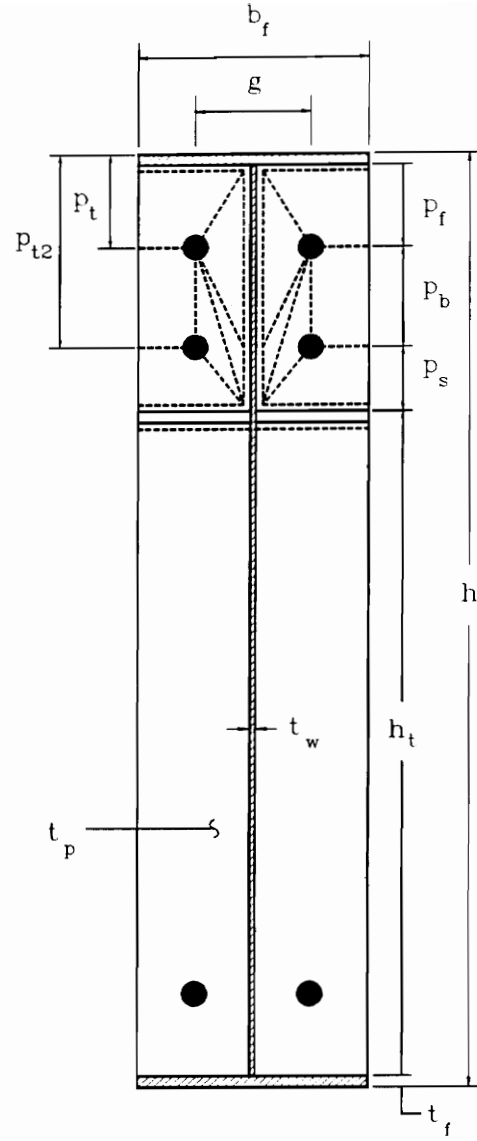
* - (P_t - Q_{max}) < T_b

APPENDIX D

FOUR-BOLT FLUSH STIFFENED MOMENT END-PLATE TEST CALCULATIONS

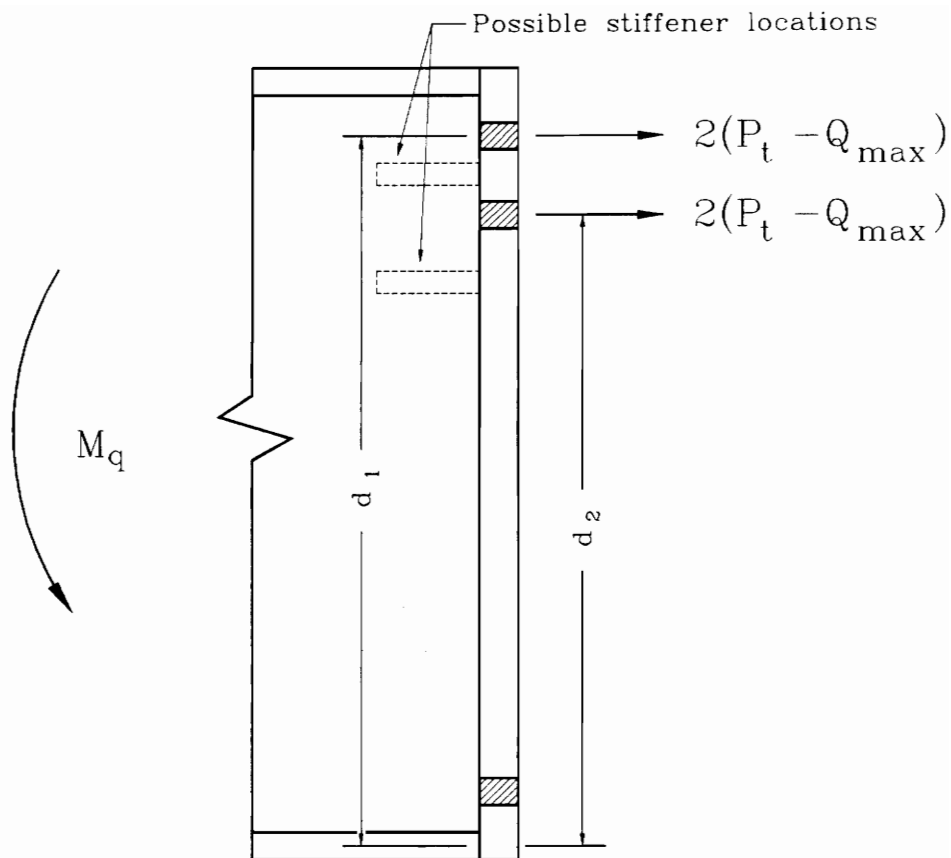


Stiffener Between the
Tension Bolt Rows



Stiffener Outside the
Tension Bolt Rows

**Yield-Line Mechanisms for Four-Bolt Flush
Stiffened Moment End-Plate
(after Hendrick *et al.*, 1985)**



**Simplified Bolt Force Model for Four-Bolt Flush
Unstiffened and Stiffened Moment End-Plates**

HENDRICK *et al.* (1984)
FB2-3/4-3/8-16

h = 16 in.
bf = 6 in.
tf = 0.25 in.
tp = 0.379 in.
ps = 1.375 in.
pf = 1.5 in.
g = 3.5 in.
pb = 3 in.
s = 2.291 in.
F_{py} = 55.48 ksi (measured)
db = 0.75 in.
T_b = 28 kips
P_t = 39.8 kips
F_{yb} = 90.0 ksi (table)
d₁ = 14.125 in.
d₂ = 11.125 in.
w' = 2.1875 in.
a = 0.390 in.
F = 8.20 kips
Q_{max} = 10.63 kips

M_q = 122.6 k-ft
M_{pl} = 96.9 k-ft
0.90M_{pl} = — k-ft
M_{mp} = — k-ft
M_{pred}/M_y = 96.9 k-ft / 85 k-ft = 1.14
M_{pred}/M_u = 96.9 k-ft / 92.8 k-ft = 1.04

M _{pred} =	96.9 k-ft	M _{pred} /M _y =	1.14
M _y =	85 k-ft	M _{pred} /M _u =	1.04
M _u =	92.8 k-ft		

HENDRICK *et al.* (1984)
FO2-3/4-3/8-16

h = 16 in.
bf = 6 in.
tf = 0.25 in.
tp = 0.379 in.
ht = 8.959 in.
pf = 1.5 in.
g = 3.5 in.
pb = 3 in.
ps = 2.291 in.
F_{py} = 55.48 ksi (measured)
db = 0.75 in.
T_b = 28 kips
P_t = 39.8 kips
F_{yb} = 90.0 ksi (table)
d₁ = 14.125 in.
d₂ = 11.125 in.
w' = 2.1875 in.
a = 0.390 in.
F = 8.20 kips
Q_{max} = 10.63 kips

M_q = 122.6 k-ft
M_{pl} = 74.9 k-ft
0.90M_{pl} = — k-ft
M_{mp} = — k-ft
M_{pred}/M_y = 74.9 k-ft / 74 k-ft = 1.01
M_{pred}/M_u = 74.9 k-ft / 74.4 k-ft = 1.01

M _{pred} =	74.9 k-ft	M _{pred} /M _y =	1.01
M _y =	74 k-ft	M _{pred} /M _u =	1.01
M _u =	74.4 k-ft		

HENDRICK *et al.* (1984)
FB2-3/4-3/8-24

h = 24 in.
bf = 6 in.
tf = 0.25 in.
tp = 0.366 in.
ps = 1.375 in.
pf = 1.75 in.
g = 3.25 in.
pb = 3 in.
s = 2.208 in.
F_{py} = 52.82 ksi (measured)
db = 0.75 in.
T_b = 28 kips
P_t = 39.8 kips
F_{yb} = 90.0 ksi (table)
d₁ = 21.875 in.
d₂ = 18.875 in.
w' = 2.1875 in.
a = 0.343 in.
F = 6.48 kips
Q_{max} = 10.88 kips

M_q = 196.1 k-ft
M_{pl} = 139.9 k-ft
0.90M_{pl} = — k-ft
M_{mp} = — k-ft
M_{pred}/M_y = 139.9 k-ft / 146 k-ft = 0.96
M_{pred}/M_u = 139.9 k-ft / 146.2 k-ft = 0.96

M _{pred} =	139.9 k-ft	M _{pred} /M _y =	0.96
M _y =	146 k-ft	M _{pred} /M _u =	0.96
M _u =	146.2 k-ft		

* - (P_t - Q_{max}) < T_b

HENDRICK *et al.* (1984)
FO2-3/4-3/8-24

h = 24 in.
bf = 6 in.
tf = 0.25 in.
tp = 0.366 in.
ht = 16.792 in.
pf = 1.75 in.
g = 3.25 in.
pb = 3 in.
ps = 2.208 in.
Fpy = 52.82 ksi (measured)
db = 0.75 in.
Tb = 28 kips
Pt = 39.8 kips
Fyb = 90.0 ksi (table)
d1 = 21.875 in.
d2 = 18.875 in.
w' = 2.1875 in.
a = 0.343 in.
F = 6.48 kips
Qmax = 10.88 kips

Mq = 196.1 k-ft
Mpl = 107.6 k-ft
0.90Mpl = — k-ft
Mnp = — k-ft
Mpred = 107.6 k-ft
My = 110 k-ft
Mu = 120.2 k-ft

Mpred/M-	Mpred/M-
My	0.98
Mu	0.89

HENDRICK *et al.* (1984)
FB2-5/8-3/8-16

h = 16 in.
bf = 6 in.
tf = 0.25 in.
tp = 0.381 in.
ps = 1.25 in.
pf = 1.375 in.
g = 2.75 in.
pb = 2.75 in.
s = 2.031 in.
Fpy = 55.9 ksi (measured)
db = 0.625 in.
Tb = 19 kips
Pt = 27.6 kips
Fyb = 90.0 ksi (table)
d1 = 14.25 in.
d2 = 11.5 in.
w' = 2.3125 in.
a = 0.749 in.
F = 8.06 kips
Qmax = 6.01 kips

Mq = 92.7 k-ft
Mpl = 112.3 k-ft
0.90Mpl = 101.1 k-ft
Mnp = 118.5 k-ft
Mpred = 92.7 k-ft
My = 108 k-ft
Mu = 108.4 k-ft

Mpred/M-	Mpred/M-
My	0.86
Mu	0.86

HENDRICK *et al.* (1984)
FO2-5/8-3/8-16

h = 16 in.
bf = 6 in.
tf = 0.25 in.
tp = 0.381 in.
ht = 10.469 in.
pf = 1.375 in.
g = 2.75 in.
pb = 1.875 in.
ps = 2.031 in.
Fpy = 55.9 ksi (measured)
db = 0.625 in.
Tb = 19 kips
Pt = 27.6 kips
Fyb = 90.0 ksi (table)
d1 = 14.25 in.
d2 = 12.375 in.
w' = 2.3125 in.
a = 0.749 in.
F = 8.06 kips
Qmax = 6.01 kips

Mq = 95.9 k-ft
Mpl = 82.2 k-ft
0.90Mpl = — k-ft
Mnp = — k-ft
Mpred = 82.2 k-ft
My = 85 k-ft
Mu = 85 k-ft

Mpred/M-	Mpred/M-
My	0.97
Mu	0.97

* - (Pt - Qmax) < Tb

HENDRICK et al. (1984)
 FB2-3/4-1/2-23

$h = 23$ in.
 $bf = 6$ in.
 $tf = 0.375$ in.
 $tp = 0.507$ in.
 $ps = 1.3125$ in.
 $pf = 1.875$ in.
 $g = 3.25$ in.
 $pb = 3$ in.
 $s = 2.208$ in.
 $F_{py} = 50.07$ ksi (measured)
 $db = 0.75$ in.
 $Tb = 28$ kips
 $Pt = 39.8$ kips
 $F_{yb} = 90.0$ ksi (table)
 $d1 = 20.5625$ in.
 $d2 = 17.5625$ in.
 $w' = 2.1875$ in.
 $a = 1.052$ in.
 $F' = 9.37$ kips
 $Q_{max} = 6.40$ kips

$M_q = 212.0$ k-ft
 $M_{pl} = 240.8$ k-ft
 $0.90M_{pl} = 216.7$ k-ft
 $M_{np} = 252.6$ k-ft
 $M_{pred} = 212.0$ k-ft
 $M_v = 250$ k-ft
 $M_{tu} = 254$ k-ft

M_{pred}/M_v	0.85
M_{tu}/M_v	0.83

HENDRICK et al. (1984)
 FO2-3/4-1/2-23

$h = 23$ in.
 $bf = 6$ in.
 $tf = 0.375$ in.
 $tp = 0.507$ in.
 $ht = 15.542$ in.
 $pf = 1.875$ in.
 $g = 3.25$ in.
 $pb = 3$ in.
 $ps = 2.208$ in.
 $F_{py} = 50.07$ ksi (measured)
 $db = 0.75$ in.
 $Tb = 28$ kips
 $Pt = 39.8$ kips
 $F_{yb} = 90.0$ ksi (table)
 $d1 = 20.5625$ in.
 $d2 = 17.5625$ in.
 $w' = 2.1875$ in.
 $a = 1.052$ in.
 $F' = 9.37$ kips
 $Q_{max} = 6.40$ kips

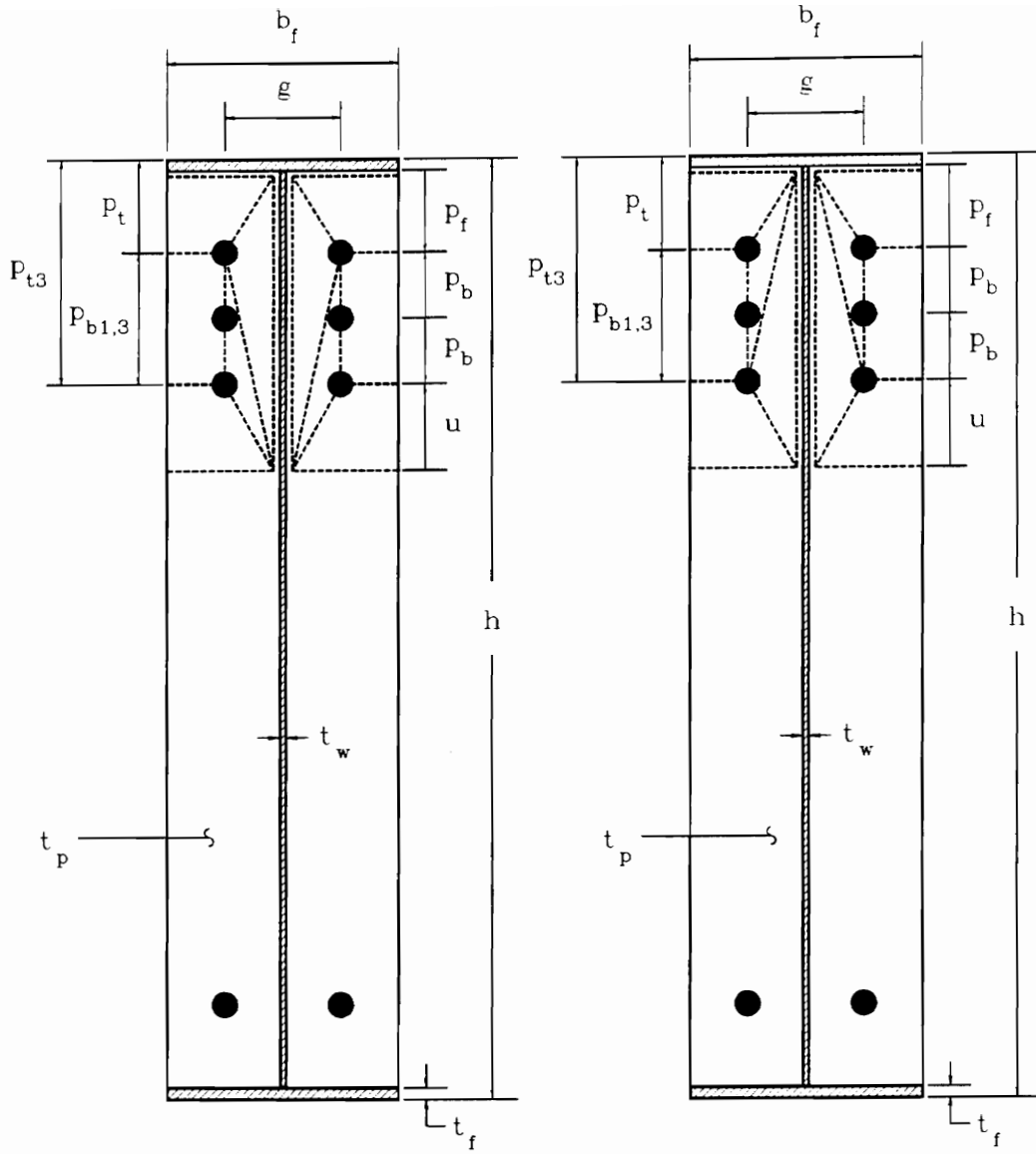
$M_q = 212.0$ k-ft
 $M_{pl} = 183.2$ k-ft
 $0.90M_{pl} = \text{---}$ k-ft
 $M_{np} = \text{---}$ k-ft
 $M_{pred} = 183.2$ k-ft
 $M_v = 200$ k-ft
 $M_{tu} = 207$ k-ft

M_{pred}/M_v	0.92
M_{tu}/M_v	0.89

* - (Pt - Qmax) < Tb

APPENDIX E

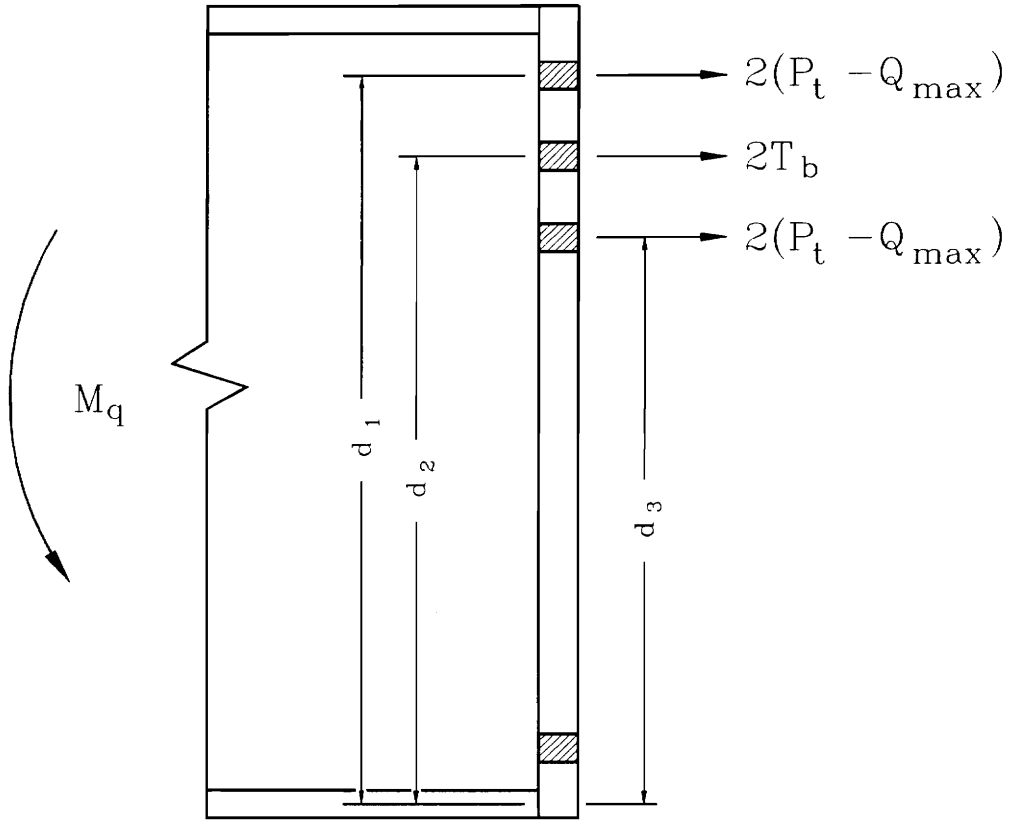
SIX-BOLT FLUSH UNSTIFFENED MOMENT END-PLATE TEST CALCULATIONS



Mechanism I

Mechanism II

**Yield-Line Mechanisms for Six-Bolt Flush
Unstiffened Moment End-Plate
(after Bond and Murray, 1989)**



**Simplified Bolt Force Model for Six-Bolt Flush
Unstiffened Moment End-Plates**

BOND AND MURRAY (1989)
MRF-7/8-3/8-28

$h = 27.91$ in.
 $bf = 10.03$ in.
 $tf = 0.376$ in.
 $tp = 0.373$ in.
 $pf = 1.44$ in.
 $g = 3.49$ in.
 $pb = 2.5$ in.
 $pt3 = 6.816$ in.
 $u1 = 2.660$ in.
 $u2 = 2.958$ in.
 $Fpy = 56.5$ ksi (measured)
 $db = 0.875$ in.
 $Tb = 39$ kips
 $Pt = 54.1$ kips
 $Fyb = 90.0$ ksi (table)
 $d1 = 25.906$ in.
 $d2 = 23.406$ in.
 $d3 = 20.906$ in.
 $w' = 4.0775$ in.
 $a = 0.200$ in.
 $F' = 14.38$ kips
 $Qmax = 38.30$ kips *
 $Mq = 456.4$ k-ft
 $Mpl = 174.1$ k-ft
 $0.90Mpl = \text{---}$ k-ft
 $Mnp = \text{---}$ k-ft
 $Mpred = 174.1$ k-ft
 $M_y = 185$ k-ft
 $M_u = 365$ k-ft
 $Mpred/M_y = 0.94$
 $Mpred/M_u = 0.48$
 $Mq < Mpl$

$Mpred = 174.1$ k-ft	$Mpred/M_y = 0.94$
$M_y = 185$ k-ft	
$M_u = 365$ k-ft	0.48

BOND AND MURRAY (1989)
MRF-1-1/2-28

$h = 28.02$ in.
 $bf = 10$ in.
 $tf = 0.38$ in.
 $tp = 0.502$ in.
 $pf = 1.88$ in.
 $g = 3.98$ in.
 $pb = 2.5$ in.
 $pt3 = 7.26$ in.
 $u1 = 2.832$ in.
 $u2 = 3.154$ in.
 $Fpy = 64$ ksi (measured)
 $db = 1$ in.
 $Tb = 51$ kips
 $Pt = 70.7$ kips
 $Fyb = 90.0$ ksi (table)
 $d1 = 25.57$ in.
 $d2 = 23.07$ in.
 $d3 = 20.57$ in.
 $w' = 3.9375$ in.
 $a = 0.381$ in.
 $F' = 20.57$ kips
 $Qmax = 40.00$ kips *
 $Mq = 588.3$ k-ft
 $Mpl = 310.3$ k-ft
 $0.90Mpl = \text{---}$ k-ft
 $Mnp = \text{---}$ k-ft
 $Mpred = 310.3$ k-ft
 $M_y = 280$ k-ft
 $M_u = 399$ k-ft
 $Mpred/M_y = 1.11$
 $Mpred/M_u = 0.78$
 $Mq < Mpl$

$Mpred = 310.3$ k-ft	$Mpred/M_y = 1.11$
$M_y = 280$ k-ft	
$M_u = 399$ k-ft	0.78

BOND AND MURRAY (1989)
MRF-3/4-3/8-36

$h = 35.96$ in.
 $bf = 6$ in.
 $tf = 0.378$ in.
 $tp = 0.37$ in.
 $pf = 2.06$ in.
 $g = 2.97$ in.
 $pb = 2.48$ in.
 $pt3 = 7.398$ in.
 $u1 = 1.948$ in.
 $u2 = 2.111$ in.
 $Fpy = 62.7$ ksi (measured)
 $db = 0.75$ in.
 $Tb = 28$ kips
 $Pt = 39.8$ kips
 $Fyb = 90.0$ ksi (table)
 $d1 = 33.333$ in.
 $d2 = 30.853$ in.
 $d3 = 28.373$ in.
 $w' = 2.1875$ in.
 $a = 0.357$ in.
 $F' = 6.29$ kips
 $Qmax = 12.84$ kips *
 $Mq = 431.9$ k-ft
 $Mpl = 211.2$ k-ft
 $0.90Mpl = \text{---}$ k-ft
 $Mnp = \text{---}$ k-ft
 $Mpred = 211.2$ k-ft
 $M_y = 220$ k-ft
 $M_u = 365$ k-ft
 $Mpred/M_y = 0.96$
 $Mpred/M_u = 0.58$
 $Mq < Mpl$

$Mpred = 211.2$ k-ft	$Mpred/M_y = 0.96$
$M_y = 220$ k-ft	
$M_u = 365$ k-ft	0.58

* - $(Pt - Qmax) < Tb$

BOND AND MURRAY (1989)
MRF-7/8-1/2-36

$h = 35.99$ in.
 $bf = 6$ in.
 $tf = 0.381$ in.
 $tp = 0.508$ in.
 $pf = 1.52$ in.
 $g = 3.45$ in.
 $pb = 2.5$ in.
 $pt3 = 6.901$ in.
 $u1 = 2.101$ in.
 $u2 = 2.275$ in.
 $F_{py} = 60.4$ ksi (measured)
 $db = 0.875$ in.
 $Tb = 39$ kips
 $Pt = 54.1$ kips
 $F_{yb} = 90.0$ ksi (table)
 $d1 = 33.8985$ in.
 $d2 = 31.3985$ in.
 $d3 = 28.8985$ in.
 $w' = 2.0625$ in.
 $a = 0.636$ in.
 $F' = 14.66$ kips
 $Q_{max} = 11.58$ kips

$M_q = 649.3$ k-ft
 $M_{pl} = 362.6$ k-ft
 $0.90M_{pl} = \text{---}$ k-ft
 $M_{mp} = \text{---}$ k-ft
 $< M_q$

$M_{pred} =$	362.6 k-ft	$M_{pred}/M_{pl} =$	1.02
$M_y =$	355 k-ft		
$M_u =$	459 k-ft		0.79

BOND AND MURRAY (1989)
MRF-7/8-1/2-36B

$h = 35.97$ in.
 $bf = 5.97$ in.
 $tf = 0.379$ in.
 $tp = 0.499$ in.
 $pf = 1.55$ in.
 $g = 3.48$ in.
 $pb = 2.5$ in.
 $pt3 = 6.929$ in.
 $u1 = 2.105$ in.
 $u2 = 2.279$ in.
 $F_{py} = 62.5$ ksi (measured)
 $db = 0.875$ in.
 $Tb = 39$ kips
 $Pt = 54.1$ kips
 $F_{yb} = 90.0$ ksi (table)
 $d1 = 33.8515$ in.
 $d2 = 31.3515$ in.
 $d3 = 28.8515$ in.
 $w' = 2.0475$ in.
 $a = 0.598$ in.
 $F' = 14.30$ kips
 $Q_{max} = 12.28$ kips

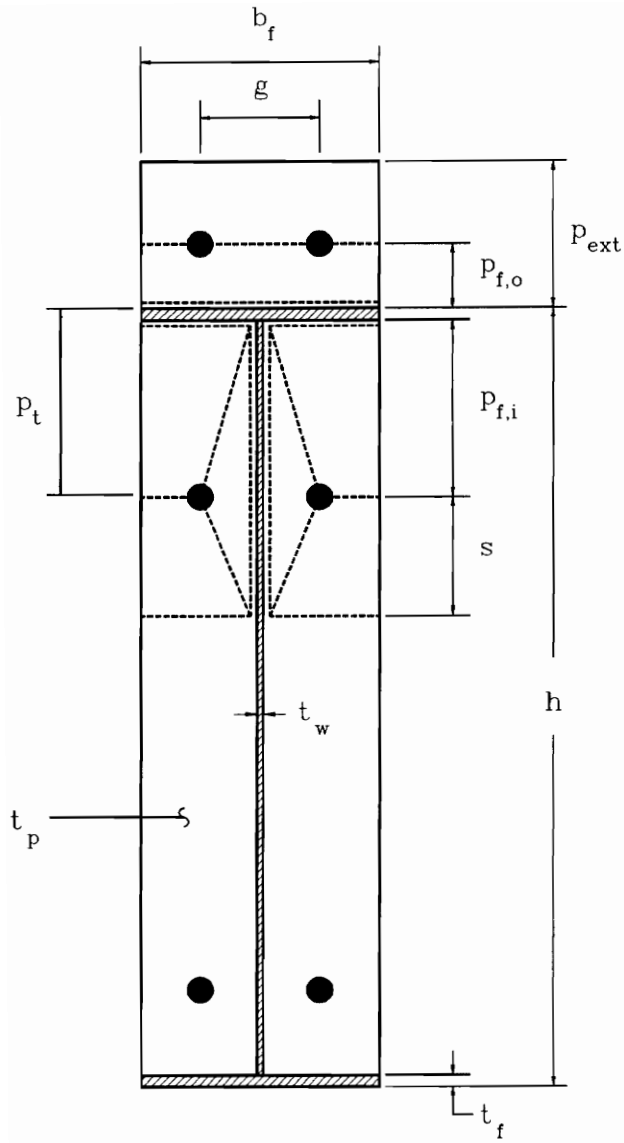
$M_q = 641.0$ k-ft
 $M_{pl} = 358.0$ k-ft
 $0.90M_{pl} = \text{---}$ k-ft
 $M_{mp} = \text{---}$ k-ft
 $< M_q$

$M_{pred} =$	358.0 k-ft	$M_{pred}/M_{pl} =$	1.01
$M_y =$	355 k-ft		
$M_u =$	379 k-ft		0.94

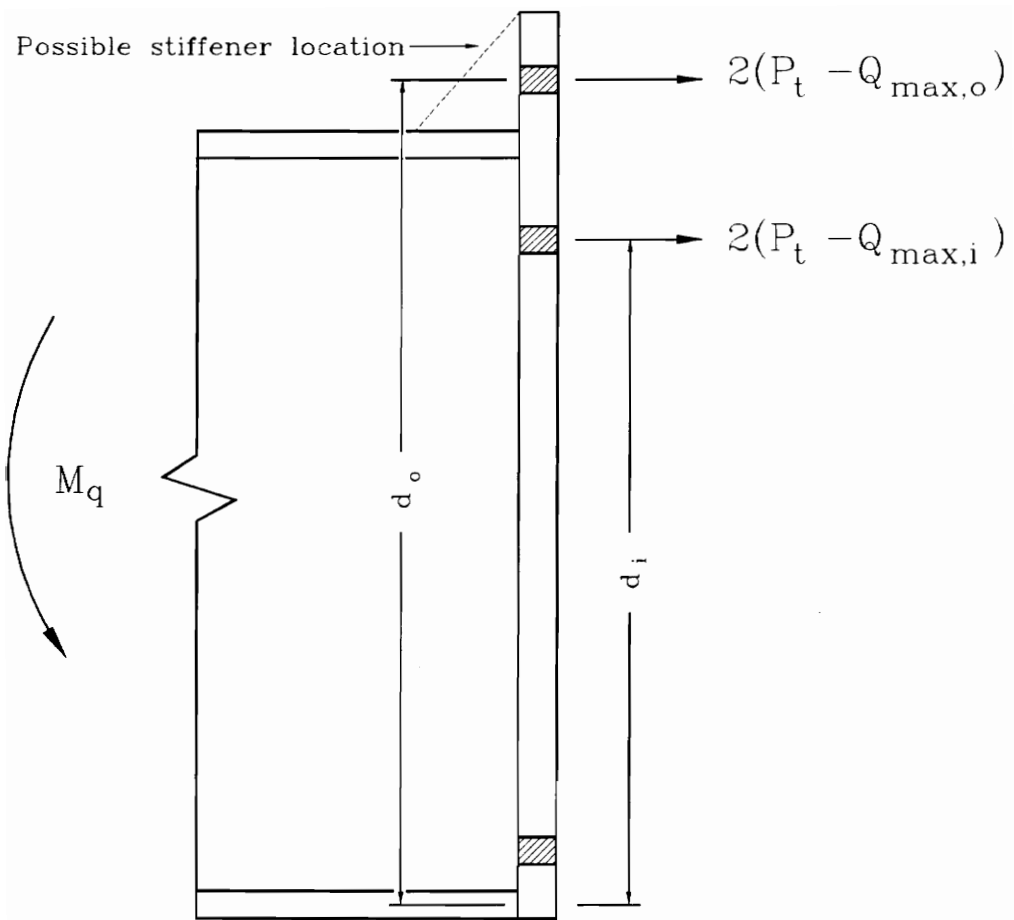
* - $(P_t - Q_{max}) < T_b$

APPENDIX F

FOUR-BOLT EXTENDED UNSTIFFENED MOMENT END-PLATE TEST CALCULATIONS



**Yield-Line Mechanism for Four-Bolt Extended
Unstiffened Moment End-Plates
(after Srouji *et al.*, 1983b)**



**Simplified Bolt Force Model for Four-Bolt Extended
Unstiffened and Stiffened Moment End-Plates**

ABEL AND MURRAY (1992b)
E50-3/4-5/8-18

h = 18 in.
 bf = 8 in.
 tf = 0.512 in.
 tp = 0.633 in.
 pext = 2.438 in.
 pfi = 1.25 in.
 pfo = 1.25 in.
 g = 2.986 in.
 Fpy = 66.9 ksi (measured)
 db = 0.75 in.
 Tb = 28 kips
 Pt = 45.9 kips (measured)
 Fyb = 103.9 ksi
 do = 18.994 in.
 di = 15.982 in.
 w' = 3.1875 in.
 ai = 2.129 in.
 ao = 1.188 in.
 Fi = 35.34 kips
 Fo = 35.34 kips
 Qmax,i = 8.94 kips
 Qmax,o = 16.03 kips

Mq = 193.0 k-ft
 Mpl = 398.3 k-ft
 0.90Mpl = 358.5 k-ft
 Mmp = 267.6 k-ft
 > Mq
 < 0.90Mpl

Mpred =	267.6 k-ft	Mpred/M-
My =	250 k-ft	1.07
Mu =	259.7 k-ft	1.03

ABEL AND MURRAY (1992b)
E50-3/4-3/4-18

h = 18 in.
 bf = 8 in.
 tf = 0.512 in.
 tp = 0.788 in.
 pext = 2.5 in.
 pfi = 1.25 in.
 pfo = 1.25 in.
 g = 2.991 in.
 Fpy = 57.4 ksi (measured)
 db = 0.75 in.
 Tb = 28 kips
 Pt = 45.9 kips (measured)
 Fyb = 103.9 ksi
 do = 18.994 in.
 di = 15.982 in.
 w' = 3.1875 in.
 ai = 4.185 in.
 ao = 1.25 in.
 Fi = 45.86 kips
 Fo = 45.86 kips
 Qmax,i = 5.66 kips
 Qmax,o = 18.96 kips *

Mq = 195.8 k-ft
 Mpl = 529.4 k-ft
 0.90Mpl = 476.5 k-ft
 Mmp = 267.6 k-ft
 > Mq
 < 0.90Mpl

Mpred =	267.6 k-ft	Mpred/M-
My =	275 k-ft	0.97
Mu =	275.1 k-ft	0.97

ABEL AND MURRAY (1992b)
E36-1 1/8-7/8-16

h = 16.21 in.
 bf = 10.25 in.
 tf = 0.657 in.
 tp = 0.886 in.
 pext = 4 in.
 pfi = 2.5 in.
 pfo = 2.5 in.
 g = 7 in.
 Fpy = 46.5 ksi (measured)
 db = 1.125 in.
 Tb = 56 kips
 Pt = 99.1 kips (measured)
 Fyb = 99.7 ksi
 do = 18.3815 in.
 di = 12.7245 in.
 w' = 3.9375 in.
 ai = 1.714 in.
 ao = 1.5 in.
 Fi = 32.97 kips
 Fo = 32.97 kips
 Qmax,i = 19.63 kips
 Qmax,o = 22.42 kips

Mq = 403.5 k-ft
 Mpl = 314.7 k-ft
 0.90Mpl = — k-ft
 Mmp = — k-ft
 < Mq

Mpred =	314.7 k-ft	Mpred/M-
My =	230 k-ft	1.37
Mu =	337.8 k-ft	0.93

* - (Pt - Qmax) < Tb

ABEL AND MURRAY (1992b)
E36-1 1/4-7/8-16

$h = 16.21$ in.
 $bf = 10.25$ in.
 $tf = 0.657$ in.
 $tp = 0.886$ in.
 $pext = 3.375$ in.
 $pfi = 2$ in.
 $pfo = 2$ in.
 $g = 6$ in.
 $F_{py} = 46.5$ ksi (measured)
 $db = 1.25$ in.
 $Tb = 71$ kips
 $Pt = 124.6$ kips (measured)
 $F_{yb} = 101.5$ ksi
 $do = 17.8815$ in.
 $di = 13.2245$ in.
 $w' = 3.8125$ in.
 $ai = 1.226$ in.
 $ao = 1.2261576$ in.
 $Fi = 43.53$ kips
 $F'o = 43.53$ kips
 $Q_{max,i} = 24.89$ kips
 $Q_{max,o} = 24.89$ kips
 $Mq = 516.9$ k-ft
 $Mpl = 375.0$ k-ft
 $0.90Mpl = \text{---}$ k-ft
 $Mmp = \text{---}$ k-ft
 $Mq < Mpl$

$M_{pred} =$	375.0 k-ft	$M_{pred}/M-$
$M_y =$	350 k-ft	1.07
$M_u =$	503 k-ft	0.75

BORGSMILLER et al. (1995)
E55-1/2-3/8-16 1/2

$h = 16.5$ in.
 $bf = 5$ in.
 $tf = 0.252$ in.
 $tp = 0.378$ in.
 $pext = 3.0625$ in.
 $pfi = 3.75$ in.
 $pfo = 1.3125$ in.
 $g = 2.5$ in.
 $F_{py} = 59.2$ ksi (measured)
 $db = 0.5$ in.
 $Tb = 12$ kips
 $Pt = 17.7$ kips
 $F_{yb} = 90.0$ ksi (table)
 $do = 17.6865$ in.
 $di = 12.372$ in.
 $w' = 1.9375$ in.
 $ai = 1.506$ in.
 $ao = 1.506$ in.
 $Fi = 2.37$ kips
 $F'o = 6.76$ kips
 $Q_{max,i} = 2.71$ kips
 $Q_{max,o} = 2.62$ kips
 $Mq = 75.2$ k-ft
 $Mpl = 80.3$ k-ft
 $0.90Mpl = 72.2$ k-ft
 $Mmp = 88.5$ k-ft
 $Mq > Mpl$

$M_{pred} =$	75.2 k-ft	$M_{pred}/M-$
$M_y =$	70 k-ft	1.07
$M_u =$	84.9 k-ft	0.89

BORGSMILLER et al. (1995)
E55-1-3/4-64

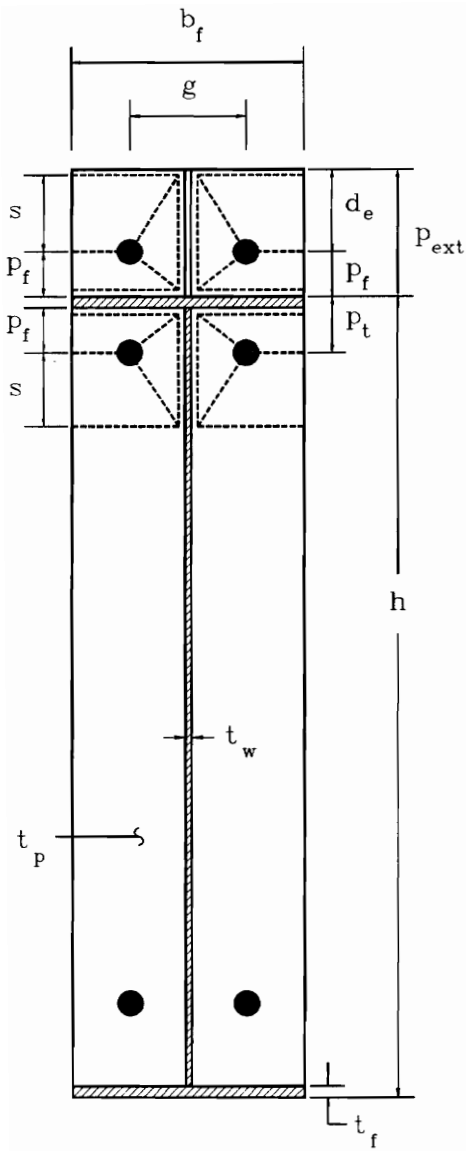
$h = 63.875$ in.
 $bf = 8.0625$ in.
 $tf = 1.006$ in.
 $tp = 0.76$ in.
 $pext = 3.125$ in.
 $pfi = 4$ in.
 $pfo = 1.375$ in.
 $g = 5$ in.
 $F_{py} = 59.3$ ksi (measured)
 $db = 1$ in.
 $Tb = 51$ kips
 $Pt = 70.7$ kips
 $F_{yb} = 90.0$ ksi (table)
 $do = 64.747$ in.
 $di = 58.366$ in.
 $w' = 2.96875$ in.
 $ai = 1.531$ in.
 $ao = 1.531$ in.
 $Fi = 14.63$ kips
 $F'o = 42.56$ kips
 $Q_{max,i} = 16.30$ kips
 $Q_{max,o} = 13.85$ kips
 $Mq = 1142.3$ k-ft
 $Mpl = 1405.2$ k-ft
 $0.90Mpl = 1264.7$ k-ft
 $Mmp = 1450.4$ k-ft
 $Mq > Mpl$

$M_{pred} =$	1142.3 k-ft	$M_{pred}/M-$
$M_y =$	1350 k-ft	0.85
$M_u =$	1423 k-ft	0.80

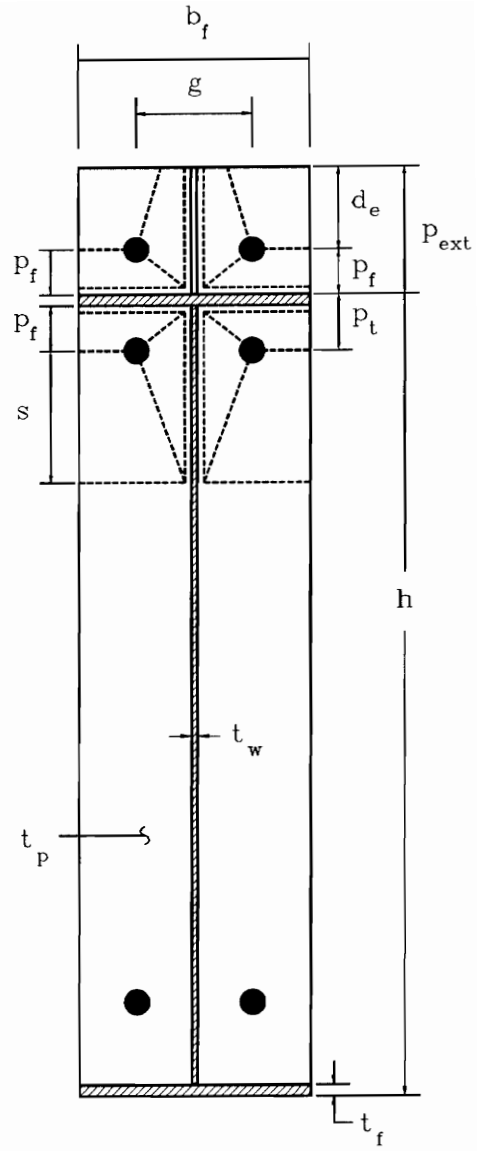
* - ($Pt - Q_{max}$) < Tb

APPENDIX G

FOUR-BOLT EXTENDED STIFFENED MOMENT END-PLATE TEST CALCULATIONS

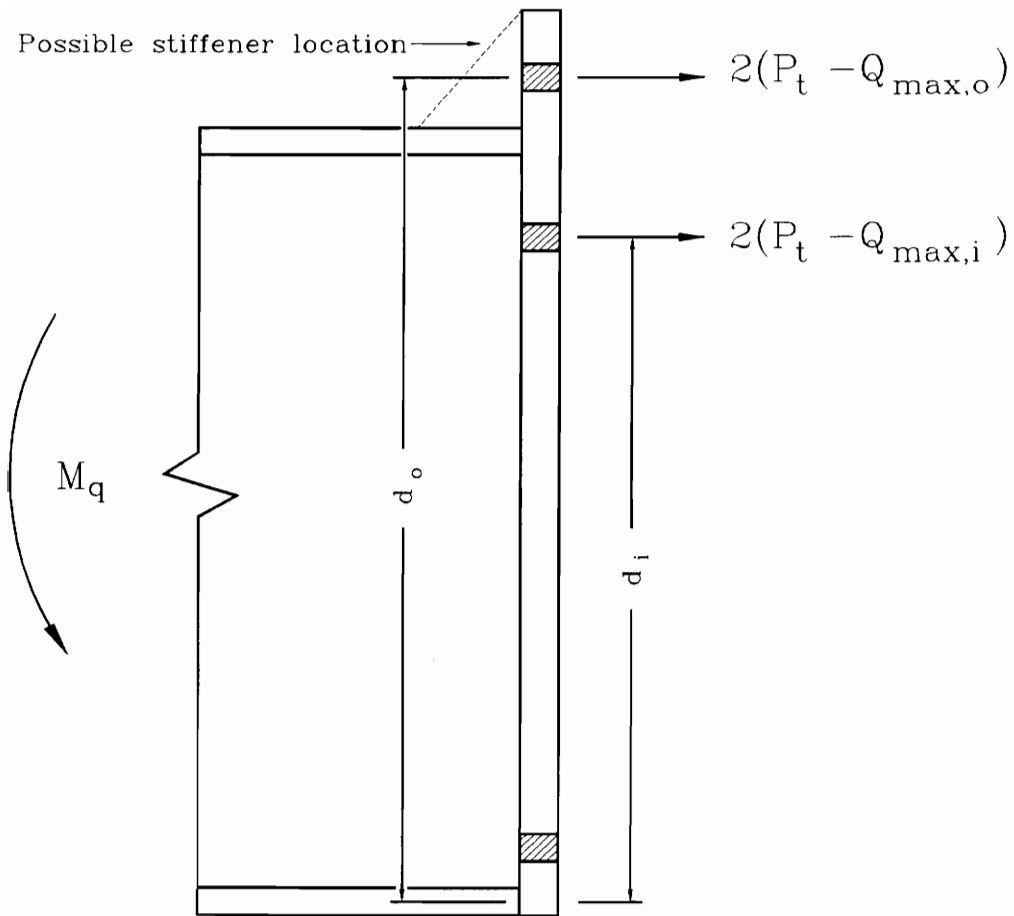


Case 1, when $s < d_e$



Case 2, when $s > d_e$

**Yield-Line Mechanisms for Four-Bolt Extended
Stiffened Moment End-Plates
(after Srouji *et al.*, 1983b)**



**Simplified Bolt Force Model for Four-Bolt Extended
Unstiffened and Stiffened Moment End-Plates**

MORRISON *et al.*. (1985)
ES-5/8-3/8-16

$h = 15.907$ in.
 $bf = 6$ in.
 $tf = 0.38$ in.
 $tp = 0.375$ in.
 $pext = 2.469$ in.
 $pfi = 1.089$ in.
 $pfo = 1.089$ in.
 $g = 2.734$ in.
 $s = 2.025$ in.
 $de = 1.38$ in.
 $F_{py} = 55.5$ ksi (measured)
 $db = 0.625$ in.
 $T_b = 19$ kips
 $P_t = 27.6$ kips
 $F_{yb} = 90.0$ ksi (table)
 $do = 16.806$ in.
 $di = 14.248$ in.
 $w' = 2.3125$ in.
 $ai = 0.710$ in.
 $ao = 0.710$ in.
 $F'_i = 9.86$ kips
 $F_o = 9.86$ kips
 $Q_{max,i} = 5.94$ kips
 $Q_{max,o} = 5.94$ kips
 $M_q = 112.2$ k-ft
 $M_{pl} = 108.4$ k-ft
 $0.90M_{pl} = \text{---}$ k-ft
 $M_{mp} = \text{---}$ k-ft
 $M_{pred} = 108.4$ k-ft
 $M_y = 80$ k-ft
 $M_u = 114.9$ k-ft
 $M_{pred}/M_u < M_q$
 $M_{pred}/M_u = 1.35$
 $M_{pred}/M_u = 0.94$

$M_{pred} =$	108.4 k-ft	$M_{pred}/M_u =$	1.35
$M_y =$	80 k-ft		
$M_u =$	114.9 k-ft		0.94

MORRISON *et al.*. (1985)
ES-3/4-1/2-16

$h = 15.75$ in.
 $bf = 6$ in.
 $tf = 0.38$ in.
 $tp = 0.481$ in.
 $pext = 3.125$ in.
 $pfi = 1.12$ in.
 $pfo = 1.12$ in.
 $g = 3.282$ in.
 $s = 2.219$ in.
 $de = 2.005$ in.
 $F_{py} = 53.2$ ksi (measured)
 $db = 0.75$ in.
 $T_b = 28$ kips
 $P_t = 39.8$ kips
 $F_{yb} = 90.0$ ksi (table)
 $do = 16.68$ in.
 $di = 14.06$ in.
 $w' = 2.1875$ in.
 $ai = 0.886$ in.
 $ao = 0.886$ in.
 $F'_i = 15.14$ kips
 $F_o = 15.14$ kips
 $Q_{max,i} = 6.71$ kips
 $Q_{max,o} = 6.71$ kips
 $M_q = 169.3$ k-ft
 $M_{pl} = 167.9$ k-ft
 $0.90M_{pl} = \text{---}$ k-ft
 $M_{mp} = \text{---}$ k-ft
 $M_{pred} = 167.9$ k-ft
 $M_y = 130$ k-ft
 $M_u = 163.4$ k-ft
 $M_{pred}/M_u < M_q$
 $M_{pred}/M_u = 1.29$
 $M_{pred}/M_u = 1.03$

$M_{pred} =$	167.9 k-ft	$M_{pred}/M_u =$	1.29
$M_y =$	130 k-ft		
$M_u =$	163.4 k-ft		1.03

MORRISON *et al.*. (1985)
ES-3/4-7/16-20

$h = 19.938$ in.
 $bf = 6.094$ in.
 $tf = 0.479$ in.
 $tp = 0.434$ in.
 $pext = 2.625$ in.
 $pfi = 1.037$ in.
 $pfo = 1.037$ in.
 $g = 2.766$ in.
 $s = 2.053$ in.
 $de = 1.588$ in.
 $F_{py} = 60.5$ ksi (measured)
 $db = 0.75$ in.
 $T_b = 28$ kips
 $P_t = 39.8$ kips
 $F_{yb} = 90.0$ ksi (table)
 $do = 20.7355$ in.
 $di = 18.1825$ in.
 $w' = 2.2345$ in.
 $ai = 0.628$ in.
 $ao = 0.628$ in.
 $F'_i = 15.62$ kips
 $F_o = 15.62$ kips
 $Q_{max,i} = 8.99$ kips
 $Q_{max,o} = 8.99$ kips
 $M_q = 199.6$ k-ft
 $M_{pl} = 208.7$ k-ft
 $0.90M_{pl} = 187.8$ k-ft
 $M_{mp} = 257.9$ k-ft
 $M_{pred} = 199.6$ k-ft
 $M_y = 180$ k-ft
 $M_u = 235.1$ k-ft
 $M_{pred}/M_u > M_q$
 $M_{pred}/M_u = 0.90M_{pl}$
 $M_{pred}/M_u > 0.90M_{pl}$

$M_{pred} =$	199.6 k-ft	$M_{pred}/M_u =$	1.11
$M_y =$	180 k-ft		
$M_u =$	235.1 k-ft		0.85

* - ($P_t - Q_{max}$) < T_b

MORRISON *et al.* (1985)
ES-3/4-1/2-20

h =	19.669 in.
bf =	6 in.
tf =	0.483 in.
tp =	0.476 in.
pext =	2.937 in.
pfi =	1.58 in.
pfo =	1.58 in.
g =	3.5 in.
s =	2.291 in.
de =	1.357 in.
Fpy =	51.8 ksi (measured)
db =	0.75 in.
Tb =	28 kips
Pt =	39.8 kips
Fyb =	90.0 ksi (table)
do =	21.3075 in.
di =	17.6645 in.
w' =	2.1875 in.
ai =	0.856 in.
ao =	0.856 in.
Fi =	10.34 kips
F'o =	10.34 kips
Qmax,i =	7.07 kips
Qmax,o =	7.07 kips
Mq =	212.3 k-ft
Mpl =	163.3 k-ft
0.90Mpl =	— k-ft
Mmp =	— k-ft

Mpred =	163.3 k-ft	Mpred/M-
My =	150 k-ft	1.09
Mu =	203 k-ft	0.80

MORRISON *et al.* (1985)
ES-1-1/2-24

h =	24.063 in.
bf =	8.031 in.
tf =	0.496 in.
tp =	0.486 in.
pext =	3.218 in.
pfi =	1.692 in.
pfo =	1.692 in.
g =	3.218 in.
s =	2.542 in.
de =	1.526 in.
Fpy =	51.6 ksi (measured)
db =	1 in.
Tb =	51 kips
Pt =	70.7 kips
Fyb =	90.0 ksi (table)
do =	25.507 in.
di =	21.627 in.
w' =	2.953 in.
ai =	0.338 in.
ao =	0.338 in.
Fi =	15.62 kips
F'o =	15.62 kips
Qmax,i =	24.80 kips *
Qmax,o =	24.80 kips *
Mq =	400.6 k-ft
Mpl =	249.8 k-ft
0.90Mpl =	— k-ft
Mmp =	— k-ft

Mpred =	249.8 k-ft	Mpred/M-
My =	260 k-ft	0.96
Mu =	349.5 k-ft	0.71

MORRISON *et al.* (1985)
ES-1-5/8-24

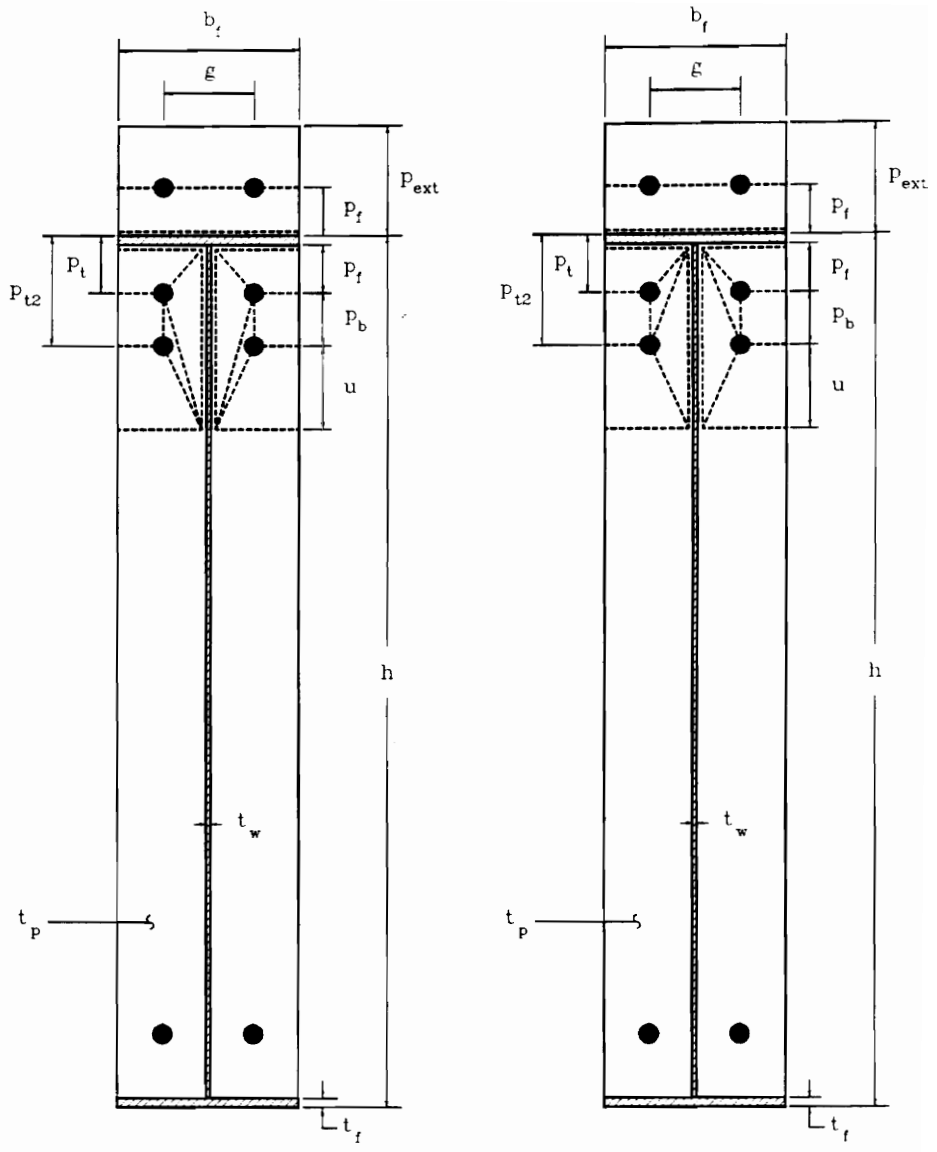
h =	23.938 in.
bf =	8 in.
tf =	0.496 in.
tp =	0.62 in.
pext =	3.531 in.
pfi =	1.723 in.
pfo =	1.723 in.
g =	4.5 in.
s =	3.000 in.
de =	1.808 in.
Fpy =	52.7 ksi (measured)
db =	1 in.
Tb =	51 kips
Pt =	70.7 kips
Fyb =	90.0 ksi (table)
do =	25.413 in.
di =	21.471 in.
w' =	2.9375 in.
ai =	0.793 in.
ao =	0.793 in.
Fi =	22.03 kips
F'o =	22.03 kips
Qmax,i =	17.22 kips
Qmax,o =	17.22 kips
Mq =	417.7 k-ft
Mpl =	364.5 k-ft
0.90Mpl =	— k-ft
Mmp =	— k-ft

Mpred =	364.5 k-ft	Mpred/M-
My =	280 k-ft	1.30
Mu =	379.4 k-ft	0.96

* - (Pt - Qmax) < Tb

APPENDIX H

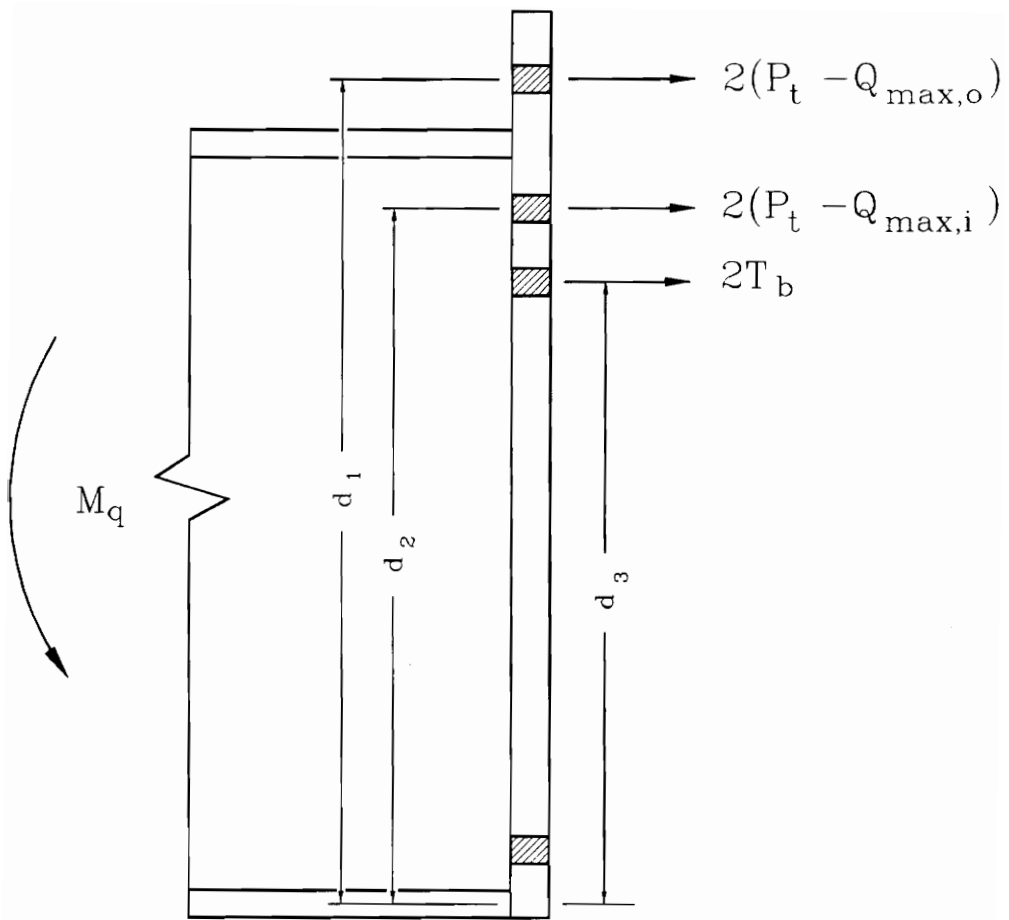
MULTIPLE ROW EXTENDED UNSTIFFENED 1/2 MOMENT END-PLATE TEST CALCULATIONS



Mechanism I

Mechanism II

Yield-Line Mechanisms for Multiple Row Extended Unstiffened 1/2 Moment End-Plate



Simplified Bolt Force Model for Multiple Row Extended Unstiffened 1/2 Moment End-Plates

ABEL AND MURRAY (1992a)

MRE1/2-3/4-3/4-26

h = 25.906 in.
 bf = 6 in.
 tf = 0.44 in.
 tp = 0.749 in.
 pext = 2.5 in.
 pfi = 1.25 in.
 pfo = 1.25 in.
 g = 3.003 in.
 Fpy = 61.4 ksi (measured)
 db = 0.75 in.
 Tb = 28 kips
 Pt = 39.8 kips
 Fyb = 90.0 ksi (table)
 d1 = 26.936 in.
 d2 = 23.996 in.
 d3 = 21.746 in.
 w' = 2.1875 in.
 ai = 3.582 in.
 ao = 1.250 in.
 Fi = 32.61 kips
 Fo = 32.61 kips
 Qmax,i = 4.35 kips
 Qmax,o = 12.47 kips *

Mq = 368.8 k-ft
 Mpl = 803 k-ft
 0.90Mpl = 722.7 k-ft
 Mmp = 481.6 k-ft

Mpred = 481.6 k-ft

My = 370 k-ft

Mu = 372.1 k-ft

Mpred/M- = 1.30

Mu = 372.1 k-ft

Mu = 372.1 k-ft

Mu = 372.1 k-ft

Mu = 372.1 k-ft

Mu = 372.1 k-ft

Mu = 372.1 k-ft

Mu = 372.1 k-ft

Mu = 372.1 k-ft

Mu = 372.1 k-ft

Mu = 372.1 k-ft

Mu = 372.1 k-ft

Mu = 372.1 k-ft

Mu = 372.1 k-ft

Mu = 372.1 k-ft

Mu = 372.1 k-ft

Mu = 372.1 k-ft

Mu = 372.1 k-ft

Mu = 372.1 k-ft

Mu = 372.1 k-ft

Mu = 372.1 k-ft

Mu = 372.1 k-ft

Mu = 372.1 k-ft

Mu = 372.1 k-ft

Mu = 372.1 k-ft

Mu = 372.1 k-ft

Mu = 372.1 k-ft

Mu = 372.1 k-ft

Mu = 372.1 k-ft

* - (Pt - Qmax) < Tb

ABEL AND MURRAY (1992a)

MRE1/2-3/4-3/8-26

h = 25.906 in.
 bf = 6 in.
 tf = 0.44 in.
 tp = 0.372 in.
 pext = 2.5 in.
 pfi = 1.25 in.
 pfo = 1.25 in.
 g = 2.994 in.
 Fpy = 55.4 ksi (measured)
 db = 0.75 in.
 Tb = 28 kips
 Pt = 39.8 kips
 Fyb = 90.0 ksi (table)
 d1 = 26.936 in.
 d2 = 23.996 in.
 d3 = 21.746 in.
 w' = 2.1875 in.
 ai = 0.364 in.
 ao = 0.364 in.
 Fi = 9.58 kips
 Fo = 9.58 kips
 Qmax,i = 10.70 kips
 Qmax,o = 10.70 kips

Mq = 348.2 k-ft
 Mpl = 179 k-ft
 0.90Mpl = — k-ft
 Mmp = — k-ft

Mpred = 179.0 k-ft

My = 210 k-ft

Mu = 309.2 k-ft

Mpred/M- = 0.85

Mu = 309.2 k-ft

Mu = 309.2 k-ft

Mu = 309.2 k-ft

Mu = 309.2 k-ft

Mu = 309.2 k-ft

Mu = 309.2 k-ft

Mu = 309.2 k-ft

Mu = 309.2 k-ft

Mu = 309.2 k-ft

Mu = 309.2 k-ft

Mu = 309.2 k-ft

Mu = 309.2 k-ft

Mu = 309.2 k-ft

Mu = 309.2 k-ft

Mu = 309.2 k-ft

Mu = 309.2 k-ft

Mu = 309.2 k-ft

Mu = 309.2 k-ft

Mu = 309.2 k-ft

Mu = 309.2 k-ft

Mu = 309.2 k-ft

Mu = 309.2 k-ft

Mu = 309.2 k-ft

Mu = 309.2 k-ft

Mu = 309.2 k-ft

Mu = 309.2 k-ft

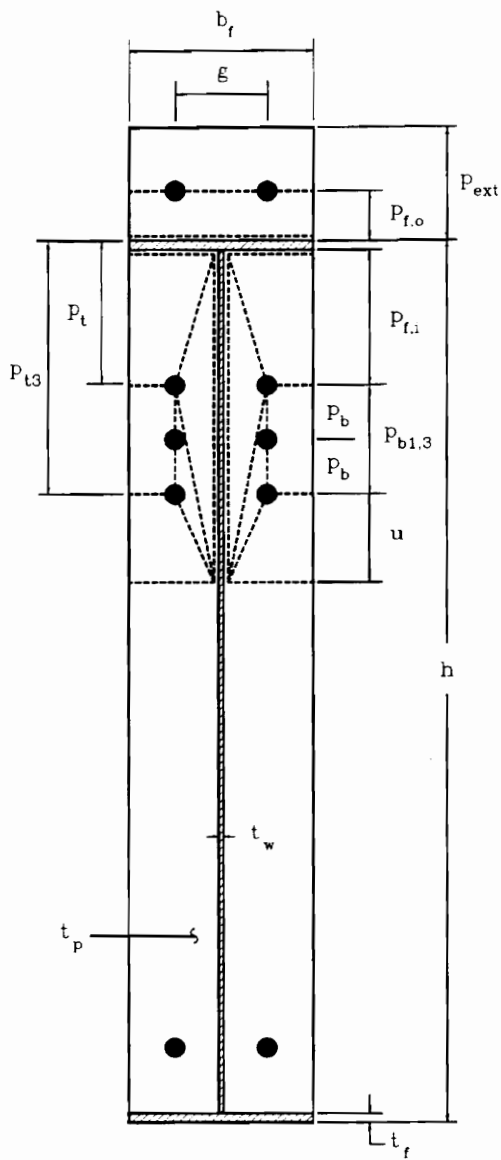
Mu = 309.2 k-ft

Mu = 309.2 k-ft

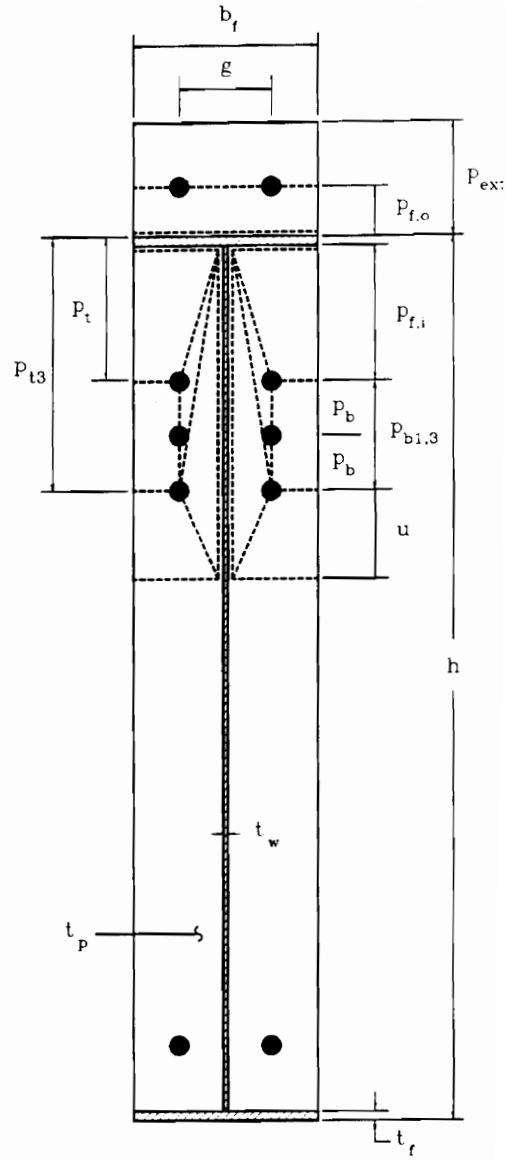
* - (Pt - Qmax) < Tb

APPENDIX I

MULTIPLE ROW EXTENDED UNSTIFFENED 1/3 MOMENT END-PLATE TEST CALCULATIONS

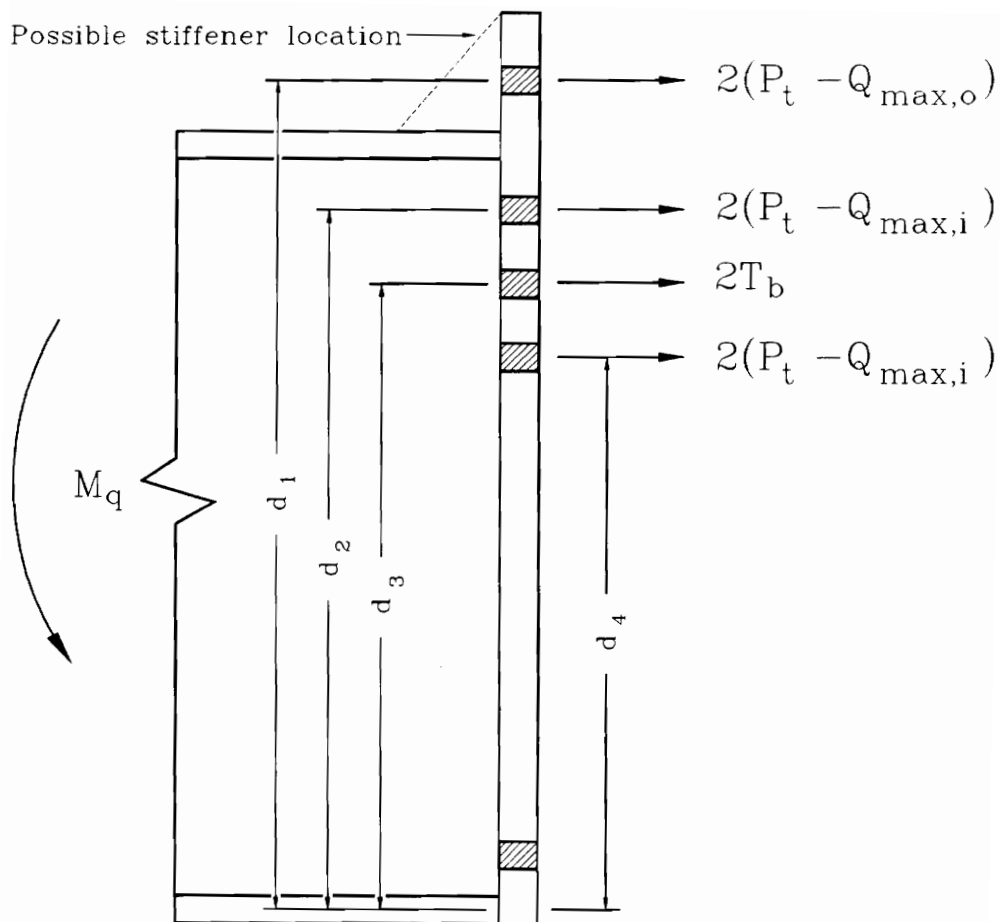


Mechanism I



Mechanism II

Yield-Line Mechanisms for Multiple Row Extended
Unstiffened 1/3 Moment End-Plate
(after SEI, 1984)



**Simplified Bolt Force Model for Multiple Row Extended
Unstiffened and Stiffened 1/3 Moment End-Plates**

BORGSMILLER *et al.* (1995)
MRE1/3-1-3/4-64

$h = 63.875$ in.
 $bf = 8$ in.
 $tf = 1.006$ in.
 $tp = 0.76$ in.
 $pext = 3.125$ in.
 $pfi = 4$ in.
 $pfo = 1.375$ in.
 $g = 5$ in.
 $F_{py} = 62$ ksi (meas.)
 $db = 1$ in.
 $T_b = 51$ kips
 $P_t = 70.7$ kips
 $F_{yb} = 90.0$ ksi (table)
 $d1 = 64.747$ in.
 $d2 = 58.366$ in.
 $w' = 2.9375$ in.
 $ai = 1.531$ in.
 $ao = 1.531$ in.
 $F'_i = 15.08$ kips
 $F_o = 43.86$ kips
 $Q_{max,i} = 16.87$ kips
 $Q_{max,o} = 14.36$ kips
 $M_q = 2081.7$ k-ft
 $M_{p1} = 1810.4$ k-ft
 $0.90M_{p1} = \text{---}$ k-ft
 $M_{np} = \text{---}$ k-ft
 $M_{pred} = 1810.4$ k-ft
 $M_y = 1870$ k-ft
 $M_u = 1870$ k-ft
 $M_{pred}/M_y = 0.97$
 $M_{pred}/M_u = 0.97$

* - (P_t - Q_{max}) < T_b

MORRISON *et al.* (1986)
MRE1/3-3/4-3/8-30

$h = 29.813$ in.
 $bf = 8$ in.
 $tf = 0.377$ in.
 $tp = 0.377$ in.
 $pext = 2.688$ in.
 $pfi = 1.105$ in.
 $pfo = 1.105$ in.
 $g = 2.72$ in.
 $F_{py} = 52.3$ ksi (meas.)
 $db = 0.75$ in.
 $T_b = 28$ kips
 $P_t = 39.8$ kips
 $F_{yb} = 90.0$ ksi (table)
 $d1 = 30.7295$ in.
 $d2 = 28.1425$ in.
 $w' = 3.1875$ in.
 $ai = 0.383$ in.
 $ao = 0.383$ in.
 $F'_i = 13.38$ kips
 $F_o = 13.38$ kips
 $Q_{max,i} = 14.39$ kips *
 $Q_{max,o} = 14.39$ kips *
 $M_q = 505.5$ k-ft
 $M_{p1} = 258.9$ k-ft
 $0.90M_{p1} = \text{---}$ k-ft
 $M_{np} = \text{---}$ k-ft
 $M_{pred} = 258.9$ k-ft
 $M_y = 270$ k-ft
 $M_u = 404.9$ k-ft
 $M_{pred}/M_y = 0.96$
 $M_{pred}/M_u = 0.64$

MORRISON *et al.* (1986)
MRE1/3-1-1/2-30

$h = 30.003$ in.
 $bf = 8.063$ in.
 $tf = 0.377$ in.
 $tp = 0.501$ in.
 $pext = 3.404$ in.
 $pfi = 1.567$ in.
 $pfo = 1.567$ in.
 $g = 4.574$ in.
 $Fpy = 50.1$ ksi (meas.)
 $db = 1$ in.
 $Tb = 51$ kips
 $Pt = 70.7$ kips
 $Fyb = 90.0$ ksi (table)
 $d1 = 31.3815$ in.
 $d2 = 27.8705$ in.
 $w' = 2.969$ in.
 $ai = 0.378$ in.
 $ao = 0.378$ in.
 $Fi = 17.28$ kips
 $Fo = 17.28$ kips
 $Qmax,i = 22.61$ kips *
 $Qmax,o = 22.61$ kips *
 $Mq = 900.5$ k-ft
 $Mpl = 325.6$ k-ft
 $0.90Mpl = \text{---}$ k-ft
 $Mnp = \text{---}$ k-ft
 $Mpred = 325.6$ k-ft
 $My = 300$ k-ft
 $Mu = 425.1$ k-ft
 $Mpred/M- = 1.09$
 $Mu = 0.77$

* - (Pt - Qmax) < Tb

MORRISON *et al.* (1986)
MRE1/3-7/8-7/16-46

$h = 45.994$ in.
 $bf = 8.112$ in.
 $tf = 0.495$ in.
 $tp = 0.445$ in.
 $pext = 2.894$ in.
 $pfi = 1.435$ in.
 $pfo = 1.435$ in.
 $g = 3.253$ in.
 $Fpy = 62.1$ ksi (meas.)
 $db = 0.875$ in.
 $Tb = 39$ kips
 $Pt = 54.1$ kips
 $Fyb = 90.0$ ksi (table)
 $d1 = 47.1815$ in.
 $d2 = 43.8165$ in.
 $w' = 3.1185$ in.
 $ai = 0.399$ in.
 $ao = 0.399$ in.
 $Fi = 16.86$ kips
 $Fo = 16.86$ kips
 $Qmax,i = 22.59$ kips *
 $Qmax,o = 22.59$ kips *
 $Mq = 1114.5$ k-ft
 $Mpl = 570.0$ k-ft
 $0.90Mpl = \text{---}$ k-ft
 $Mnp = \text{---}$ k-ft
 $Mpred = 570.0$ k-ft
 $My = 520$ k-ft
 $Mu = 866.1$ k-ft
 $Mpred/M- = 1.10$
 $Mu = 0.66$

MORRISON et al. (1986)
MRE1/3-1 1/2-3/4-62

$h = 61.945$ in.
 $bf = 9.926$ in.
 $tf = 1.005$ in.
 $tp = 0.753$ in.
 $pext = 5.13$ in.
 $pfi = 2.584$ in.
 $pfo = 2.584$ in.
 $g = 5.559$ in.
 $F_{py} = 54.6$ ksi (meas.)
 $db = 1.5$ in.
 $Tb = 103$ kips
 $Pt = 159.0$ kips
 $F_{yb} = 90.0$ ksi (table)
 $d1 = 64.027$ in.
 $d2 = 57.854$ in.
 $w' = 3.4005$ in.
 $ai = 0.381$ in.
 $ao = 0.381$ in.
 $Fi = 32.32$ kips
 $Fo = 32.32$ kips
 $Q_{max,i} = 63.33$ kips *
 $Q_{max,o} = 63.33$ kips *
 $Mq = 3846.0$ k-ft
 $Mpl = 1601.6$ k-ft
 $0.90Mpl = \text{---}$ k-ft
 $Mtp = \text{---}$ k-ft
 $Mpred = 1601.6$ k-ft
 $M_y = 1600$ k-ft
 $M_u = 2329.6$ k-ft
 $Mpred/M_y = 1.00$
 $M_u/M_y = 0.69$

* - (Pt - Qmax) < Tb

RODKEY AND MURRAY (1993b)
MRE1/3-3/4-5/8-33 1/4

$h = 33.25$ in.
 $bf = 7.96875$ in.
 $tf = 0.624$ in.
 $tp = 0.622$ in.
 $pext = 2.35$ in.
 $pfi = 1.25$ in.
 $pfo = 1.125$ in.
 $g = 3.06$ in.
 $F_{py} = 51.5$ ksi (meas.)
 $db = 0.75$ in.
 $Tb = 28$ kips
 $Pt = 39.8$ kips
 $F_{yb} = 90.0$ ksi (table)
 $d1 = 34.063$ in.
 $d2 = 31.064$ in.
 $w' = 3.171875$ in.
 $ai = 2.015$ in.
 $ao = 1.225$ in.
 $Fi = 26.59$ kips
 $Fo = 29.54$ kips
 $Q_{max,i} = 6.99$ kips
 $Q_{max,o} = 11.14$ kips
 $Mq = 600.0$ k-ft
 $Mpl = 760.1$ k-ft
 $0.90Mpl = 684.1$ k-ft
 $Mtp = 783.7$ k-ft
 $Mpred = 600.0$ k-ft
 $M_y = 690$ k-ft
 $M_u = 692.5$ k-ft
 $Mpred/M_y = 0.87$
 $M_u/M_y = 0.87$
 $> Mq$
 $> 0.90Mpl$

SEI (1984)
MRE1/3-3/4-1/2-62

h =	62 in.
bf =	10 in.
tf =	1 in.
tp =	0.5 in.
pext =	2.625 in.
pfi =	1.375 in.
pfo =	1.375 in.
g =	3.5 in.
Fpy =	52.9 ksi (meas.)
db =	0.75 in.
Tb =	28 kips
Pt =	39.8 kips
Fyb =	90.0 ksi (table)
d1 =	62.875 in.
d2 =	59.125 in.
w' =	4.1875 in.
ai =	1.006 in.
ao =	1.006 in.
Fi =	20.99 kips
Fo =	20.99 kips
Qmax,i =	13.00 kips *
Qmax,o =	13.00 kips *
Mq =	1089.7 k-ft
Mpl =	923.2 k-ft
0.90Mpl =	— k-ft
Mmp =	— k-ft
Mpred =	923.2 k-ft
Mv =	750 k-ft
Mu =	929 k-ft
Mpred/Mv =	1.23
Mu/Mv =	0.99

Mpred =	923.2 k-ft	Mpred/Mv =
Mv =	750 k-ft	1.23
Mu =	929 k-ft	0.99

SEI (1984)
MRE1/3-1-3/4-62

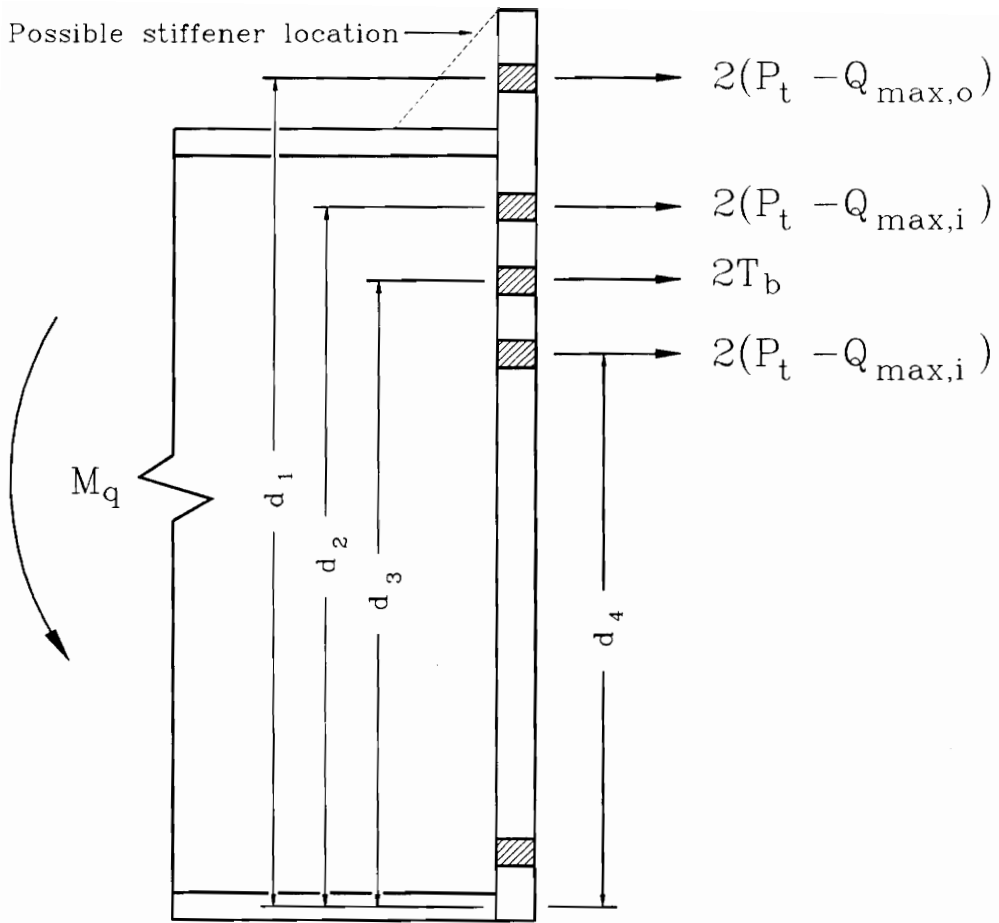
h =	62 in.
bf =	10 in.
tf =	1 in.
tp =	0.75 in.
pext =	3.375 in.
pfi =	1.625 in.
pfo =	1.625 in.
g =	3.5 in.
Fpy =	49.1 ksi (meas.)
db =	1 in.
Tb =	51 kips
Pt =	70.7 kips
Fyb =	90.0 ksi (table)
d1 =	63.125 in.
d2 =	58.875 in.
w =	3.9375 in.
ai =	1.468 in.
ao =	1.468 in.
Fi =	36.88 kips
Fo =	36.88 kips
Qmax,i =	16.62 kips
Qmax,o =	16.62 kips
Mq =	2050.7 k-ft
Mpl =	1896.3 k-ft
0.90Mpl =	— k-ft
Mmp =	— k-ft
Mpred =	1896.3 k-ft
Mv =	1250 k-ft
Mu =	1364 k-ft
Mpred/Mv =	1.52
Mu/Mv =	1.39

Mpred =	1896.3 k-ft	Mpred/Mv =
Mv =	1250 k-ft	1.52
Mu =	1364 k-ft	1.39

* - (Pt - Qmax) < Tb

APPENDIX J

MULTIPLE ROW EXTENDED STIFFENED 1/3 MOMENT END-PLATE TEST CALCULATIONS



Simplified Bolt Force Model for Multiple Row Extended Unstiffened and Stiffened 1/3 Moment End-Plates

SEI (1984)

MRES1/3-1-3/4-62

h = 62 in.
bf = 10 in.
tf = 1 in.
tp = 0.75 in.
pext = 3.375 in.
pfi = 1.625 in. pb = 3 in.
pfo = 1.625 in. pt3 = 8.625 in.
g = 3.5 in.
Fpy = 49.1 ksi (measured)
db = 1 in.
Tb = 51 kips
Pt = 70.7 kips
Fyb = 90.0 ksi (table)
d1 = 63.125 in. d3 = 55.875 in.
d2 = 58.875 in. d4 = 52.875 in.
w' = 3.9375 in.
ai = 1.468 in.
ao = 1.468 in.
F'i = 36.88 kips
F'o = 36.88 kips
Qmax,i = 16.62 kips
Qmax,o = 16.62 kips

Mq = 2050.7 k-ft
Mpl = 2311.0 k-ft > Mq
0.90Mpl = 2079.9 k-ft
Mnp = 2718.5 k-ft > 0.90Mpl

Mpred =	2050.7 k-ft	Mpred/M-
My =	1600 k-ft	1.28
Mu =	1834 k-ft	1.12

* -- (Pt - Qmax) < Tb

VITA

Jeffrey Thomas Borgsmiller was born in Albuquerque, New Mexico on August 8, 1971. He was raised in Denver, Colorado where he graduated from Northglenn High School. In May of 1993, he received his Bachelor of Science degree in Civil Engineering from the University of Colorado at Boulder. He entered the structures graduate program at Virginia Polytechnic Institute and State University in the Fall of 1993 to pursue a Master of Science degree in Civil Engineering.

A handwritten signature in black ink, reading "Jeff Borgsmiller". The signature is written in a cursive style with a large initial "J" and a long horizontal stroke at the end.